



**Politecnico  
di Torino**



**KTH ROYAL INSTITUTE  
OF TECHNOLOGY**

**Politecnico di Torino**

**KTH Royal Institute of  
Technology**

Corso di Laurea Magistrale  
In Ingegneria Energetica E Nucleare

Degree Project in Energy Technology  
Second Cycle, 30 Credits

# **Puerto Rico Renewable Energy Oasis**

Enhancing Disaster Relief and Recovery Efforts Through a  
Renewable Energy Microgrid in the University of Puerto Rico's  
Mayagüez Campus

Relatori:

Prof. Massimo Santarelli  
Prof. Francisco Beltran

Candidati:

Jacob Mason  
Arturo Garcia Palou

July 2023

## Abstract

With the global rise in temperatures fueling an increase in Severe Weather Events (SWE) such as hurricanes, many islands around the world who lie in their path are seeking alternatives to their frequently outdated grid systems. These are often composed of dated infrastructure prone to damage during such events that leaves the dependent population without power for extended periods of time. In parallel to this increasingly common problem is the growing transition from centralized grids towards decentralized microgrids largely powered by Renewable Energy Sources (RES). This thesis researches a potential RES microgrid for the University of Puerto Rico's Mayagüez campus and analyzes its potential impact on disaster relief and recovery efforts for the surrounding community. The study is divided into two sections. First, a microgrid design suitable for the campus in Puerto Rico is proposed using only RES available within the campus boundaries. The recommended design is selected based on its ability to minimize the campus's dependence on the island's grid using the lowest cost and most sustainable design. And secondly, using the selected system, the study further analyzes the potential for this microgrid to enhance disaster relief and recovery efforts for the surrounding community after SWEs by operating as an Energy Oasis (EO). This impact is measured by estimating the population size served and for how long the system can support these relief efforts. The services focused on for the Oasis operation are medical services, water purification, meal preparation, and telecommunications. Additionally, a unique measurement of a microgrid's effectiveness as an EO is proposed within the study to provide comparison between microgrids operating in a similar fashion in any location around the world. The selected microgrid consists of 2.6-MW of PV panels, 3-MW of onshore wind turbines, and a 750-kW vanadium redox flow battery (VRFB) system. The system achieves a renewable fraction of 90.8% at a levelized cost of electricity (LCOE) of 0.053 \$/kWh over a 20-year period, under 20% of the current cost of electricity from the island grid. A variety of other designs consistently yield renewable fractions over 88% at similar costs. Using a tiered system of strategic load shedding across the campus during Oasis operation, the recommended microgrid can serve between 1,556 to 4,558 people depending on the load shedding profile and the service provided every day it is in operation. The results and subsequent analyses indicate that investment into a microgrid system can significantly reduce dependence on the Puerto Rican grid and provide significant savings in utilities over the course of the project. From a social perspective, the inclusion of a microgrid into a community can significantly improve the quantity and effectiveness of disaster relief efforts. In this case the Oasis Scores range between 3.32 and 5.84. Further analysis and field trials of microgrids operated as Energy Oases will yield invaluable information on how disaster relief and recovery can be positively influenced.

## Distribution of Work

### *Arturo Garcia Palou*

- UPRM Data Acquisition, Scheduling & Point of Contact
- Methodology Development
- Microgrid Design Support
- Campus buildings Load Profile
- Energy Oasis System Design Lead
- Microgrid Analysis
- Oasis Modeling and Analysis
- Report Writing & Editing

### *Jacob Mason*

- UPRM Data Acquisition
- Methodology Development
- Microgrid Design Lead
- Resource Availability & Component Design
- HOMER Pro Simulation
- Energy Oasis System Design Support
- Microgrid Analysis
- Energy Oasis Analysis
- Report Writing & Editing

# Table of Contents

Abstract.....	2
Distribution of Work.....	3
Figures.....	6
Tables.....	8
Acronyms.....	10
1 Introduction.....	12
1.1 Background.....	12
1.2 Objectives.....	13
1.3 Scope.....	13
1.4 Overview.....	14
2 Literature Review.....	15
2.1 Puerto Rico’s Energy Situation.....	15
2.1.1 PR100.....	15
2.1.2 Energy Access & Injustice.....	15
2.2 Micro-Grids.....	15
2.2.1 Definition & Impacts.....	15
2.2.2 Energy Storage Systems.....	15
2.2.3 Regulations & Standards.....	16
2.2.4 Around the World.....	16
2.2.5 At Home.....	17
2.2.6 Resilience.....	17
2.3 Energy Oasis.....	17
2.3.1 Definition.....	17
2.3.2 Oasis Trigger Events.....	19
2.3.3 Sandia National Labs.....	19
2.3.4 FEMA.....	19
3 Scientific Approach.....	20
3.1 Microgrid Design.....	21
3.1.1 Input Data Inventory.....	21
3.1.2 Microgrid KPIs.....	22
3.1.3 Results Analysis.....	23
3.1.4 Design Recommendation.....	23
3.2 Energy Oasis.....	23
3.2.1 Building Loads.....	24
3.2.2 Oasis Services.....	24
3.2.3 Scenario Simulation.....	25
3.2.4 Oasis KPIs.....	26



3.3	Sustainability Analysis.....	27
4	Methods.....	29
4.1	Microgrid Design.....	29
4.1.1	System Demand .....	29
4.1.2	Input Data Inventory .....	30
4.2	Energy Oasis .....	53
4.2.1	Building Loads.....	53
4.2.2	Oasis Services .....	56
4.2.3	Scenario Simulation .....	59
5	Results & Discussion.....	61
5.1	Microgrid Results Analysis.....	61
5.1.1	Sensitivity Analysis.....	64
5.2	Oasis Results .....	69
5.2.1	Scenario Simulation Results .....	70
5.2.2	Oasis KPI's .....	71
5.3	Sustainability Impacts .....	75
5.3.1	Land .....	77
5.3.2	Energy.....	78
5.3.3	Food.....	78
5.3.4	Water.....	78
5.3.5	Social .....	79
6	Conclusion.....	80
7	The Road Ahead.....	81
7.1	Recommendations & Limitations.....	81
7.2	Future Work.....	82
	Bibliography .....	83
	Appendix A. UPRM Electricity Consumption Data.....	92
	Appendix B. ReNCAT .....	93
	Appendix C. PV Model Datasheet [77] .....	95
	Appendix D. IceWind RW500 Datasheet [87].....	97
	Appendix E. Redox Flow Battery Datasheet [123].....	99
	Appendix F. Hydrogen Tank Costs .....	102
	Appendix G. HOMER Inputs .....	103
	Appendix H. Measured Energy Loads .....	111
	Appendix I. Building Load Estimates and Categories .....	112
	Appendix J. Building Loads Based on MID and Priority Level .....	113
	Appendix K. Current Accounts Settings and Inputs .....	116
	Appendix L. Microgrid Component Cost Sensitivity Results .....	119

# Figures

Figure 1: Study boundaries and the energy flows of people/energy.....14

Figure 2: Flowchart outlining the methodological approach used in this study. ....20

Figure 3: Diagram of the relationship between the different scenarios simulated for the Oasis performance. ....26

Figure 4: Location of UPRM campus.....29

Figure 5: Monthly consumption (red line - left axis) and cost (blue line - right axis) for UPRM between July 2020 and September 2022.....30

Figure 6: Climate Classification map of Puerto Rico and the northern part of the Caribbean showing that Miami and Mayagüez share the same classification. Images were captured from Google Earth with Climate Classifications overlaid using data provided by Vienna University. [70], [71].....30

Figure 7: Average monthly GHI for Mayagüez, generated using data from the NSRDB [73].....31

Figure 8: Average daily GHI for each month of the year in Mayagüez, generated using data from the NSRDB [73]. ....32

Figure 9: Cumulative annual time that the PV system produces at a power level, shown as a percentage of the maximum power produced for the system.....34

Figure 10: Amount of time throughout the year that clipping occurs (red) and the amount of power that is clipped (blue) for different inverter ratios at UPRM.....34

Figure 11: Sollega Inc.'s ballasted roof mounts installed into a PV system [81]. ....35

Figure 12: Extrapolated values for expected OPEX costs expressed as percentages of the projected CAPEX for the same year [84].....37

Figure 13: Cumulative wind speeds by hour for UPRM in 2017. Data provided by NASA's POWER database [74].....39

Figure 14: The IceWind RW500 ground mounted (image courtesy of IceWind Inc.) [88]. The RW500 is the predecessor to the new RW600 that is used in this study.....39

Figure 15: Power curves for the IceWind RW600 and the Homer Pro Generic 1.5 MW wind turbines. ....40

Figure 16: Comparison for projected CAPEX costs of a large scale wind turbine for three different levels of market growth between 2020 and 2050 [90].....41

Figure 17: Labeled diagram of temporary and permanent land use requirements for a wind farm. Image courtesy of the NREL [91]. ....42

Figure 18: Map of the UPRM campus. The two selected sites for the 1.5 MW turbines are labeled as red dots. ....43

Figure 19: Heat map of wave energy potential around Puerto Rico and the US Virgin Islands in 2015 [105], the color gradient is measured in kW/m. The approximate location of UPRM is given by a red dot. ....45

Figure 20: Heat map of the mean annual rainfall for Puerto Rico and the U.S. Virgin Islands. Image courtesy of the U.S. National Oceanic and Atmospheric Administration [110].....46

Figure 21: Watershed map of western Puerto Rico surrounding Mayagüez [112]. ....47

Figure 22: Ragone chart of difference energy storage devices [114].....48

Figure 23: Comparison graph of discharge times and power rating for energy storage devices [114].....49

Figure 24: Rendering showing the setup of the CellCube FB 250-2000 system [122].....50

Figure 25: Excess electrical generation by a 1 MW solar PV system, 1.5 MW turbine, and one 250 kW VRFB on the campus for a random 10-day period throughout the year, as simulated by HOMER Pro.....51

Figure 26: H<sub>2</sub> tank CAPEX as a function of tank size for three market scenarios [64].....53

Figure 27: Electrical Energy Breakdown for Campus Buildings for each MID and Priority. ....56

Figure 28: Microgrid design with minimized LCOE.....61

Figure 29: Total annual energy generation by source for the optimized microgrid design.....	61
Figure 30: Baseline system for techno-economic comparison of microgrid designs.....	62
Figure 31: System design optimized for the Forced Hydrogen microgrid.....	62
Figure 32: System design for the Forced VRFB microgrid.....	63
Figure 33: LCOE and CAPEX of the microgrid as a function of the renewable fraction for three different configurations.....	64
Figure 34: Energy generation system for the microgrid in a conservative market.....	66
Figure 35: Discounted payback time for different design configurations from the three cost scenarios: advanced, moderate, conservative. The conservative systems marked by * indicate the system design is forced to match the design for the advanced and moderate markets.....	66
Figure 36: Projected growth in the cost of electricity (per kWh) from the PR grid based on current data trends.....	67
Figure 37: ROI and IRR for different costs of electricity from the grid.....	67
Figure 38: Discounted payback period for the optimal microgrid with an energy storage system: 23,652-kW PV, two 1.5-MW wind turbine, and three 250-kW/8-hr VRFB.....	68
Figure 39: Variations in NPC for the selected design in a moderate scenario as buyback rate for energy sold to the grid increases.....	68
Figure 40: Annual campus demand across the different scenarios.....	69
Figure 41: Breakdown of the flow of energy into the campus, the Oasis, or curtailed during hurricane season in the different scenarios.....	70
Figure 42: Maximum access time as a function of the population served for each service within the P4 Scenario.....	71
Figure 43: Energy supply to each Oasis service for every scenario.....	72
Figure 44: Correlation between number of people served and the access time for each service in the Oasis with the new energy service distribution for P4.....	73
Figure 45: Comparison of energy distribution into the Oasis services between the original and the adjusted systems.....	74
Figure 46: Overall schematic of the microgrid in HOMER.....	103
Figure 47: System load inputs and profile.....	103
Figure 48: Solar GHI profile for the UPRM campus.....	104
Figure 49: Wind availability at 50m above ground for UPRM.....	104
Figure 50: Biomass production capabilities within the campus grounds.....	105
Figure 51: Temperature profile for the region.....	105
Figure 52: Large generic converter input values.....	106
Figure 53: Solar PV cost structure and size constraint input values.....	106
Figure 54: Generic 1.5-MW wind turbine cost structure and size constraint inputs.....	107
Figure 55: IceWind RW600 turbine cost structure and size constraints.....	107
Figure 56: Biogas genset cost and efficiency inputs.....	108
Figure 57: Grid energy purchase and buyback rates used. Specific constraint criteria are displayed on the pop-out. No information is behind the pop-out.....	108
Figure 58: Electrolyzer cost, size and conversion efficiency input values.....	109
Figure 59: Hydrogen tank price scaling (as defined in Appendix F) and initial size options.....	109
Figure 60: Hydrogen fuel cell cost inputs.....	110

## Tables

Table 1: Recovery Core Capabilities by Mission Area according to FEMA's Natural Disaster Recovery Framework [56].	18
Table 2: Order of criticality of the Oasis services utilized in this study.	25
Table 3: Disaster relief multipliers for the different services included in the Oasis.	28
Table 4: Decision matrix table for the three PV modules.	32
Table 5: Relevant simulation input variables for the LA Solar Group LS55BL PV module [77].	33
Table 6: CAPEX breakdown for PV system [82].	36
Table 7: Replacement cost breakdown for PV system.	36
Table 8: OPEX values (low, medium, and high) used for the solar PV design.	37
Table 9: The maximum capacity (kW) and the maximum number of panels that are estimated utilizing building rooftops and parking lots across the UPRM campus.	38
Table 10: Standard pricing values used to simulate the generic 1.5 MW and the IceWind RW600 turbines.	41
Table 11: Component costs for the two wind turbine models in each of the three market scenarios.	41
Table 12: Carbon contents and mass flow rates for each source of biomass studied on the UPRM campus.	44
Table 13: Cost values for the biogas generation system [103]. The OPEX value will be adjusted to an accurate value for the size of the system through iteration.	44
Table 14: Costs, both per kW and per unit, for the BESS in all three sensitivity scenarios used in the model [119].	51
Table 15: Typical operating conditions of AE, PEM, and SOEC [124].	52
Table 16: Costs for the electrolyzer [64].	52
Table 17: Costs ranges for the fuel cell [64], [127].	52
Table 18: Sample building loads and classifications. Courtesy of Dr. Yuly Garcia [41].	54
Table 19: MID Energy Consumption and Building Count.	55
Table 20 Academic Institution Prioritization Scheme.	55
Table 21: Estimated Oasis services and their corresponding daily energy consumption per capita.	57
Table 22: Medical service load in the energy Oasis.	57
Table 23: Water service energy load and water demand per person.	57
Table 24: Cafeteria service load variables as provided by the UPRM cafeteria manager.	58
Table 25: Telecommunications service load and cell tower on wheels.	59
Table 26: Input considerations for each scenario; Y includes the variable whereas N excludes the variable.	59
Table 27: Economic assessment results of the optimal system design by component.	62
Table 28: KPI comparison between microgrid designs with the optimal LCOE, forced hydrogen, and forced VRFB.	63
Table 29: Values for sensitivity analysis on component costs within the system.	65
Table 30: Minimum buyback rates that allow the Forced Battery system to be profitable in all three market scenarios.	69
Table 31: Energy supplies for campus and Oasis including seasonal daily average.	70
Table 32: Maximum number of people served based on the available energy for each service in each load shedding scenario.	71

Table 33: Relationship between constants for redistribution of energy within the Oasis.....	72
Table 34: The maximum number of people served in a single day with adjusted energy distribution to Oasis services and the addition of curtailed energy. ....	73
Table 35: Adjusted energy values per service for each scenario including the addition of curtailed energy. ....	73
Table 36: Disaster Relief Fraction for each scenario as a function of Oasis duration. ....	75
Table 37: Oasis Score calculated for each of the load shedding scenarios with the current campus load as well as for the P4 load shedding with PR100 efficiency improvements.....	75
Table 38: The Oasis Score using the recalculated distribution of energy to the services. ....	76
Table 39: Maximum people served in each service per scenario compared to only using only the curtailed energy of the microgrid. ....	76
Table 40: Adjusted Oasis Score results with the inclusion of the curtailed energy in each scenario. ....	77
Table 41: Input considerations for each scenario including Baratex; Y includes the variable whereas N excludes the variable. ....	82

## Acronyms

AEC/FC	Alkaline Electrolyzer Cell/Fuel Cell
AEE	Autoridad de Energía Eléctrica
ATB	Annual Technology Baseline
BAU	Business-As-Usual
BESS	Battery Energy Storage System
BTM	Behind The Meter
CAOSE	Center for Applied Ocean Science and Engineering
CAPEX	Capital Expenditure
DBG	Department of Buildings and Grounds
DoD	Depth of Discharge
DOE	Department of Energy
DRM	Disaster Relief Multiplier
EC	Electrolyzer Cell
EIA	Energy Information Administration
ESS	Energy Storage System
FC	Fuel Cell
FEMA	Federal Emergency Management Agency
FW	Food Waste
GHG	Green House Gas
GHI	Global Horizontal Irradiance
HOMER	Hybrid Optimization of Multiple Energy Resources
IEEE	Institute of Electrical and Electronics Engineers
IRENA	International Renewable Energy Agency
IRR	Internal Rate of Return
ISO	International Standards Organization
KPI	Key Performance Indicator
LCA	Life Cycle Assessment
LCOE	Levelized Cost of Electricity
LHV	Lower Heating Value
LEAP	Low Emissions Analysis Platform
MID	Microgrid Interconnection Device
MSW	Municipal Solid Waste
NASA	National Aeronautics and Space Administration

NG	Natural Gas
NOAA	National Oceanic and Atmospheric Administration
NOCT	Nominal Operating Cell Temperature
NPC	Net Present Cost
NPV	Net Present Value
NREL	National Renewable Energy Laboratory
NRSD	National Solar Renewable Database
OPEX	Operational Expenditure
OAS	Organization of American States
OF	Organic Fraction
OS	Oasis Score
OSHA	Occupational Safety and Health Administration
PEMEC/FC	Proton Exchange Membrane Electrolyzer Cell/Fuel Cell
PoC	Point of Connection
PCC	Point of Common Coupling
PR	Puerto Rico
PREPA	Puerto Rico Electric Power Authority
PRREO	Puerto Rico Renewable Energy Oasis
PURPA	Public Utility Regulatory Policies Act
PV	Photovoltaic
PWER	Prediction of Worldwide Energy Resource
ReNCAT	Resilient Note Cluster Analysis Tool
RES	Renewable Energy Source
RF	Renewable Fraction
RFB	Redox Flow Battery
ROI	Return on Investment
SOEC/FC	Solid Oxide Electrolyzer Cell/Fuel Cell
STC	Standard Testing Conditions
SWE	Severe Weather Event
UPRM	University of Puerto Rico Mayagüez
VRFB	Vanadium Redox Flow Battery
YD	Yard Waste

# 1 Introduction

## 1.1 Background

On September 21 of 2017 the inhabitants of Puerto Rico (PR) prepared for the eventual landfall of Hurricane Maria, but there was not much commotion as it was expected to be another standard storm. The following morning, September 22, 2017, life had changed completely for the residents of the island as power lines were broken, tree branches had fallen, and no power was coming from the grid. This category 5 (Cat5) hurricane decimated the electrical grid and caused island-wide blackouts in 2017 that would take well over a year and a half to restore. Unfortunately, the repairs that were completed by 2019 were not meant to be permanent and would suffer further damage from subsequent storms, like Fiona in 2022.

While grid outages are a severe problem in isolation, they are exacerbated by a high dependence on imported fossil fuels. The Energy Information Administration (EIA) reports Puerto Rico generated 97% of its electricity by burning fossil fuels in 2021 [1]. According to the same report, 44% of the electricity comes from natural gas-fired power plants, 36.3% comes from petroleum-fired power plants, 17% from a single coal-fired power plant, and only 2.7% from renewables. This reliance on fossil fuels causes severe bottlenecks in the energy supply pipeline during natural disasters as experienced post-Maria (2017-2018) [2].

The fossil fuel reliance is strongly coupled to a privatized electrical grid with a history of instability and slow response times by the governing agency [3], Puerto Rico Electric Power Authority (PREPA). In 2021 LUMA energy, a joint Canadian-Texan venture took over the management of Puerto Rico's grid following PREPA's bankruptcy. In a short time span, the company has increased the electrical rates seven times over, while also failing to restore electrical services in a timely manner following hurricane Fiona's landfall in 2022 [4]. The effects of privatization are not exclusive to Puerto Rico, they have also caused many Texans to face instability in the grid and soaring electrical prices following extreme weather events [5]. In both cases, the privatization of the grid exacerbated energy injustices while also imparting the burden on customers. These problems have driven many islanders to seek self-sufficiency by installing solar photovoltaic (PV) and battery energy storage systems (BESS). One of the earliest communities to take such action is called Casa Pueblo, located in the small town of Adjuntas. Within this community, a house is powered by 25 panels and 12 batteries for storage purposes [6]. Other communities have similar projects running, such as in Caguas where the Mutual Support Center has 6 kW of solar panels installed and 30 kWh of BESS [7]. Following Hurricane Maria's devastation, the organizers of Casa Pueblo coined the term "Energy Oasis" as a microgrid system that provides continuity to services otherwise unavailable in the event of a blackout.

These examples of decentralized microgrids are becoming more prevalent and are expected to be larger in scale in the coming years. An ideal case for the next evolution in the energy system meets the following criteria: it serves a large portion of a community, has large area availability, and has strong infrastructure. This makes a large facility such as the University of Puerto Rico's Mayagüez campus (UPRM) an ideal candidate for research. A study of this topic will serve the added benefit of filling in the gaps of existing renewable resource literature with regards to the overall design and disaster relief potential achievable by larger microgrids. This is confirmed through background research and firsthand accounts in a communication with Dr. Ruben Diaz, Director of the Mechanical Engineering Department at UPRM.

A study conducted in 2008 by multiple researchers from the Universidad de Puerto Rico network have estimated the theoretical potential for various energy systems across the island [8], [9]. The intensive study indicated that the island of Puerto Rico has an abundance of renewable energy resources. If only 10% of all resources are utilized across the island to produce electricity, then 3.9 TWh of solar energy could be produced via photovoltaics, 3.0 TWh of wind energy (~90% via large offshore installations), 16.9 TWh of oceanic energy from tidal or wave energy along the coastlines, and 2.1 TWh from agricultural and municipal waste biomass (26.1 TWh if microalgae potential is considered). This totals to over 300% of the 15.68 TWh of electricity demanded across the island in 2022 [10].

The PR 100 energy targets, proposed by local legislation and the National Renewable Energy Laboratory (NREL), aim to reach 100% renewable energy generation on the island by 2035. To achieve this, large communal buildings must be converted to renewable-based energy sources as the available real-estate for large solar and/or wind farms throughout the island is limited [11].

The years 2002, 2017, 2022, each marks a historical occurrence of significant infrastructural damages on the island of Puerto Rico due to hurricanes. The National Oceanic and Atmospheric Association (NOAA) reports suggest an increase in severity and frequency of these events in the coming years due to



anthropogenic climate change. The 2017 events served as a catalyst for the renewable energy movement on the island, which eventually led to the declaration of the PR100 targets.

During hurricane Maria in 2017, the entire population saw a collapse in the electrical grid, and an extreme case of fossil fuel import dependence due to the nature of gasoline/diesel-based backup generators being brought online to maintain a baseline standard of living and survival. At that time, and to this day, approximately 97% of all power generated on the island relies on imported fossil fuels despite the high approval rate of renewables on the island. This discrepancy can be explained by the overall energy budget of the island, and the indebted national grid which has historically been operated by a single entity.

McMahon and the UN state that a large percentage of the population at risk of natural disasters are also those closest to and below the poverty line [12]. This brings up the question of how to set up modern energy generation entities that are not only resilient, but also serve to provide families in need of assistance with easy access to energy.

This joint thesis aims to define a techno-economic pathway to shift the UPRM campus energy supply from the grid to a renewable energy-powered microgrid. Furthermore, the study aims to fill in gaps in literature related to decentralized energy systems and their effects on natural disaster recovery. The study will also define and characterize, in an exploratory manner, the expanded concept of an Energy Oasis capable of providing electrical energy for the community of Mayagüez, Puerto Rico during disaster recovery efforts.

## 1.2 Objectives

This study aims to develop a framework for converting the University of Puerto Rico's Mayaguez campus into a self-supporting renewable energy-based microgrid with the capability of serving the greater Mayaguez community as an Energy Oasis during the natural disaster occurrence, response, and recovery periods. This study defines an Energy Oasis as an islanded renewable energy microgrid with a dedicated portion of energy temporarily supplying a neighboring community during the aftermath of a severe weather event (SWE). The following research questions outline the focuses of this study:

- Using renewable energy resources available within the campus boundaries, what is the ideal system design for a microgrid that is optimized to reduce costs and maximize energy independence?
- How much would such a system cost at present and over a 20-year period?
- How effective is such a system at operating as an Energy Oasis? What adjustments can be made to improve its efficacy?
- What is the scale of impact of this Energy Oasis in terms of time, population, and services provided?
- What effects does the UPRM Energy Oasis have on the disaster relief for the Mayaguez community through the services it can maintain?

## 1.3 Scope

The Oasis is designed for a 25-year lifetime based on historical climatic data for the previous 25 years, thereby accounting for the variation in energy usage per capita, equipment age, and frequency of natural disasters. The study will focus on the geographical boundary of the UPRM campus to source renewable energy resources while allowing energy imports and exports from the Autoridad de Energía Eléctrica (AEE) grid. During the Oasis operational season, the geographical boundary allows inflows of people from the neighboring Mayagüez community. Disruptions to basic services in the Mayagüez community are expected to occur following a natural disaster (SWE). Therefore, the continuation of these services will be provided within the campus boundary and extended to the community during disaster response and recovery periods as depicted in Figure 1.

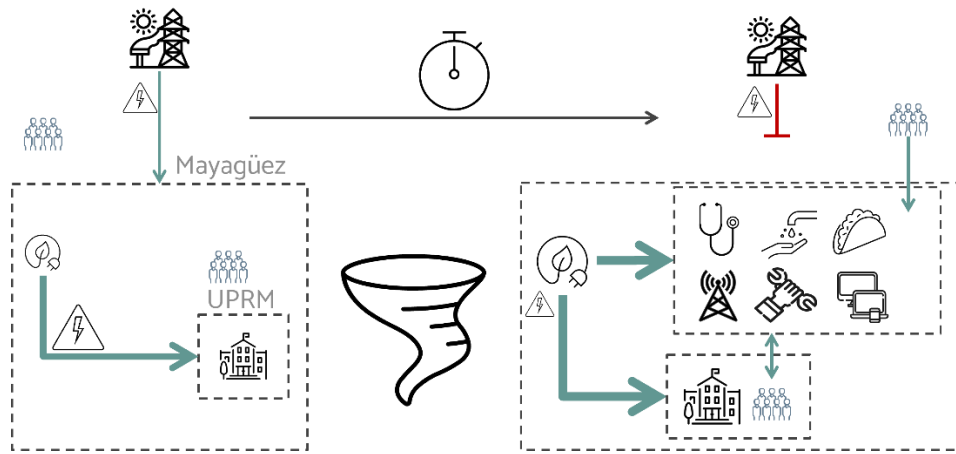


*Figure 1: Study boundaries and the energy flows of people/energy.*

The primary focus of the study is the application and impact of the Oasis on the community during disaster relief efforts. As such, the purpose of the microgrid design is to support these efforts and provide baseline values for further simulations. This implies the development of the microgrid will not provide an exhaustive list of technologies for consideration in the techno-economic analysis. Instead, it will serve to meet the UPRM demand at the cheapest cost with a system optimized for resilience and durability. The techno-economic model for the microgrid will provide the baseline energy supplies needed for the evaluation of the Energy Oasis operation. The Oasis will then be assessed in terms of access to services provided, the quantity of people who receive access, and the effectiveness of the system in preserving quality of life in the Mayaguez community.

## 1.4 Overview

The study follows a conventional structure where each main section is sub-divided to address the Microgrid and Energy Oasis independently. Section 2 provides a literature review where key concepts are defined, and their current states of research and applications are analyzed. Section 3 outlines the methodology that will be used to develop a microgrid design as well as the capacity and impacts of this grid when operated in Oasis mode. Section 4.1 defines the inputs and boundary conditions of the simulated microgrid and its components, Section 4.2 defines the load shedding of the selected microgrid(s) when in Oasis mode and offers key performance indicators for disaster recovery and disaster relief provided by the system. Section 5 provides the results of the simulations and discusses the findings, while Section 5.3 analyzes the sustainability impacts of the results. Finally, Sections 6 and 7 outline the conclusion and elaborate on future work.

## 2 Literature Review

### 2.1 Puerto Rico's Energy Situation

#### 2.1.1 PR100

The US Department of Energy (DOE) launched the PR100 [13]–[15] study in 2020 to determine the grid resilience and transitions to 100% renewable energy on the island with a transition to 40%, 60%, and 100% renewable energy supplies by 2025, 2040, and 2050 respectively. Several partnering agencies, such as the Federal Emergency Management Agency (FEMA), the NREL, Oak Ridge National Lab, and other research institutes are working to increase renewable resource knowledge in conjunction with providing detailed outlooks for the energy balances on the island up to 2050. The 2023 progress report [16] depicts a phaseout of coal-fired generation by 2028 and increased energy efficiency for all usage of 30% by 2040 as mandated by Act 17 [17], the Puerto Rico Energy Public Policy Act of 2019. The NREL progress report also mentions how smaller distributed renewable energy resources can recover power much faster than the current centralized electric generation systems. The report predicts rooftop-mounted solar PV will have a significant increase to local reliability and resilience, however this aspect is not investigated in the study.

#### 2.1.2 Energy Access & Injustice

The issue of energy injustice arises from the disproportionate distribution of energy in society. According to the World Bank, there is a direct relationship between energy poverty and financial poverty [18]. Likewise National Geographic denotes there is a longer gap to bridge between primitive energy sources to reliable energy resources [19] for these communities. Moreover, there is an even greater disproportion in the impact of natural disasters on poor communities in comparison to rich communities, as these have no means of escape or emergency funds [12].

A growing number of communities around the world have endeavored to overcome the energy injustices depicted. These include Puerto Rican examples such as the well-known Casa Pueblo community [20] and the Centro de Apoyo Mutuo in San Juan [7] to name a few.

## 2.2 Micro-Grids

### 2.2.1 Definition & Impacts

The NREL defines a microgrid as “a group of interconnected loads and distributed energy resources that acts as a single controllable entity with respect to the grid” [21]. In the modern era of decarbonization and decentralized electricity grids, microgrids are an essential component to the energy transition, energy access, and energy equality. Recently, in regards to decarbonization, Life Cycle Assessments (LCAs) have been performed on microgrids around the world comparing a new design to the existing grid connection or an existing microgrid [22], [23].

Gandiglio et al. compared an existing diesel-based grid to a microgrid for the small village of Ginostra in southern Italy. The microgrid consisted of a smaller diesel generator than the base grid and a PV system in conjunction with a hydrogen-battery energy storage system (ESS). Compared to the baseline, the microgrid resulted in a small reduction, only below -10% from the baseline energy consumption, in many impact categories (climate change, ozone depletion, acidification, etc.) but had an 89% reduction in greenhouse gas (GHG) emissions [22].

A comparative LCA was performed for a microgrid system at an ammonia plant in the central Inner Mongolia region of China. In the study, they compared a natural gas-based grid to two microgrids: one with the maximum number of renewables necessary to meet the demand and another optimized to minimize greenhouse gas (GHG) emissions and energy consumption across the life cycle of the microgrid from cradle to grave. The study concluded that, compared to the baseline natural gas (NG)-based grid, the optimized microgrid had little reduction in energy consumption and emissions. However, the maximized renewable microgrid was able to cut energy from fossil fuels by 56.9% and had a 66.3% reduction in GHG emissions [23].

### 2.2.2 Energy Storage Systems

Additionally, many recent studies have performed techno-economic analyses, which are less broad than LCAs, to understand the impacts that integrating hydrogen-battery ESSs has on renewable microgrids.

These focus on a range of topics from sizing ESSs for real microgrid applications to utilizing H<sub>2</sub> storage systems to capture curtailed energy from offshore wind farms [24], [25].

The Department of Energy at the Politecnico di Torino in Turin, Italy has studied the incorporation of hydrogen storage systems in different microgrid scenarios. In optimized off-grid hybrid renewable microgrids, the inclusion of hydrogen storage (via electrolyzers and fuel cells) resulted in a 35% drop in the levelized cost of energy (LCOE) compared to the battery-only microgrid [26].

An earlier study was performed as a part of the European REMOTE project focusing on hydrogen storage system integration in Europe. In it the addition of hydrogen storage into micro- or off-grid systems is studied in four remote locations: Rye/Froan (Norway), Ambornetti (Italy), Ginostra (Italy), and Agkistro (Greece). In each case, incorporating hydrogen storage significantly cut down or eliminated altogether dependence on fossil-fuel generation. Each system also saw a projected reduction in LCOE within 15 to 20 years for Ginostra and within 5 years for the other three locations [27].

Another study compared ESSs on 21 French islands that would reduce the amount of imported diesel currently used to compensate for the intermittency of the renewable generation systems. The storage systems compared were battery-only, electrolyzer-only, and combined hydrogen-battery. Like the previously discussed studies, the results indicate that incorporating both hydrogen and battery technology into the storage systems is more economical and environmentally friendly than either alone or the baseline case without storage [28].

### 2.2.3 Regulations & Standards

Taking a step back from the economics and benefits of different storage technologies, the designing of microgrids has also been researched and developed extensively. Currently, there are many international standards that provide guidelines and limitations to microgrids. Chief among them is those proposed by the International Standards Organization (ISO) develops and maintains guidelines for industrial and commercial use and certification across many fields of application. The ones most relevant to microgrid and renewable energy system design are ISO 50001-4, ISO 50006-7, ISO 50015, ISO 50047, and ISO 17741-3 [29].

Locally, Puerto Rico maintains regulations for grid connected generation units, among other regulations, under the Public Utility Regulatory Policies Act (PURPA) [30]. As a U.S. territory, Puerto Rico also abides by Occupational Safety and Health Administration (OSHA) standards such as those for the proper storage of flammable liquids and gas, like hydrogen [31].

Puerto Rico also faces challenges internally from PREPA with expanding distributed energy resource (DER) generation across the island [32]. For example, PREPA requires any generation provided by photovoltaics to not exceed a ramp rate, increase or decrease, of more than 10% of its total capacity per minute; a limit that exceeded by most PV systems more than 45 times on the average day in Mayagüez [33].

### 2.2.4 Around the World

These facilities can be found in a plethora of locations and can be designed to operate as a substitute or auxiliary to local grids. On the Greek island of Crete, the environmental and economic benefits of equipping the local campus of the Hellenic Mediterranean University was analyzed [34]. The results indicated that integrating renewable microgrids into university campuses can reduce environmental impacts and grid dependence, and still be economically viable.

Some communities have taken the concept further as a means of gaining energy independence from the grid, thereby increasing local resilience. Examples of this include the Babcock Ranch in Florida (74.5 MW solar PV) [35] which serves a total of 3148 people [36], Adjuntas Pueblo Solar in Puerto Rico (220 kW solar PV, 1 MW second Life BESS) [20] which serves a total of approximately 18,000 people [37].

A 2018 study developed a microgrid design tool that incorporated renewable energy incentives, tax benefits, and grid ancillary services into the design optimization for a microgrid in Seoul National University, South Korea [38]. The results indicate that failure to include these incentives and benefits can negatively impact both the optimal size and the economic feasibility of microgrids.

Another study in 2021 researched how incorporating adequate energy storage into urban energy systems can provide the flexibility necessary to adapt to extreme weather events, a feature that is a necessity for any Puerto Rican system [39]. The study offers a glimpse into extreme weather events and their effects on energy access for the region of Xiamen, China while investigating the potential for securing energy resources. The demands are classified as critical and non-critical, where the critical loads must always be supplied with

energy. The findings of the study suggest demand side management can reduce the size of energy storage systems.

### 2.2.5 At Home

In Puerto Rico, specifically, the concept of incorporating renewable energy has been a point of focus since well before the island-wide damages of the late 2010's. In 2008, a study conducted by UPRM estimated the total generation capacity of renewable sources (such as solar, wind, ocean, and biomass) across the island with the findings indicating that even 10% of many resources would be sufficient to supply the entire island's demand [9].

A noticeable increase in studies that focus on the potential impacts and implementations of renewable energy resources, DERs, and microgrids has occurred after the effects of Hurricane Maria in 2017. Research topics focusing on microgrids have ranged from high level analysis to technology- or resource-specific designs. In the nearby town of Adjuntas, a student team from the University of Michigan's School for Environment and Sustainability worked with Casa Pueblo to expand its existing solar and battery system to include a biomass gasifier system [40].

In the local academics of Puerto Rico, many graduate theses focus on infrastructure improvements and microgrid implementation across the island. One thesis submitted at UPRM developed a methodology of how to develop, size, and implement a microgrid design, in this case the campus was used as a case study [41]. A senior design course for undergraduates at the University took this one step further by looking into how renewable energy technology could be implemented into communities, with an emphasis on engagement and understanding by the community members [42]. Another thesis project identified technological components of a microgrid within the UPRM that are essential to prevent or reduce negative impacts of power outages [43].

The design and implementation of an off- or microgrid system is not an easy task. However, given Puerto Rico's abundance of renewable resources and need for improved infrastructure, the effort required to design and overcome the hurdles of implementing microgrid systems is well worth it.

### 2.2.6 Resilience

The resilience of a system increases as the components within it become more durable against physical damage. Damages can come in the form of external events such as high winds and debris strikes, or corrosion due to environmental conditions and ageing. The NREL and FEMA designed a Solar PV preparation guideline for survivability of equipment, with information on common failures and measures to avoid them [44]. The document serves as a supplementary guide for selecting generation and storage system components.

Technological advances focusing on system resiliency and generation flexibility are occurring in all sectors of renewable energy. Research is focusing on wind turbine durability, both in a general context [45], [46] and in relation to their ability to withstand hurricane-force winds [47]. New studies into hydrogen generation via electrolysis reveal methods to utilize normal seawater as a source of hydrogen, removing the requirement for high purity water [48], [49].

Within PR, a number of developments and initiatives addressing system resiliency and durable engineering are being instigated [50]. Innovative ballasted mounting racks for PV panels have allowed a PV system on the roof of the Veteran's Affairs hospital in San Juan, PR to survive two hurricanes with no loss of productivity [51]. Researchers are focusing on technology fragility to understand the conditions that lead to catastrophic failures within systems, arguing in favor of distributed energy systems over the classical centralized model [52].

## 2.3 Energy Oasis

### 2.3.1 Definition

The term "Energy Oasis" was first coined by Arturo Massol Deya, the director of Casa Pueblo in Adjuntas after Hurricane Maria in 2017. An Energy Oasis, defined for the context of this study, is a renewable energy microgrid capable of meeting the entirety of a sector's load (in this case the UPRM campus) with the capability of performing demand-side load curtailment, thereby diverting the energy towards natural disaster relief or large-scale emergency response efforts. This novel concept borrows from existing practices observed in the Casa Pueblo Microgrid community and expands upon the operating principles [20].

The main objective of the Energy Oasis is to provide an energy access point where members of the community can gather for uninterrupted services in the event a natural disaster wreaks havoc on the local electrical grid [53]–[55]. The oasis operates by load shedding some of the primary loads (ie. Buildings and services), thereby freeing up the consumption for response and recovery activities as defined by the FEMA National Disaster Recovery Framework. To appropriately measure the amount of support provided by the Oasis, it is necessary to have a thorough understanding of the Baseline Loads and the expected Recovery Loads by taking into account: Additional pumping requirements, personal use loads, medical equipment loads, cafeteria and cooking services, communications, vehicle charging, heavy machinery charging, etc.

A baseline load prioritization scheme is of utmost importance to ensure no critical systems are blacked out during the Oasis operation. In the case of universities, this may include: Running experiments and laboratory work, communication services, Campus Police, Building and grounds services, IT, Library A/C systems to name a few.

*Table 1: Recovery Core Capabilities by Mission Area according to FEMA's Natural Disaster Recovery Framework [56]*

Prevention	Protection	Mitigation	Response	Recovery
Planning				
Public Information and Warning				
Operational Coordination				
Intelligence and Information Sharing		Community Resilience	Infrastructure Systems	
Interdiction and Disruption		Long-term Vulnerability Reduction	Critical Transportation	Economic Recovery
Screening, Search, and Detection		Risk and Disaster Resilience Assessment	Environmental Response/Health and Safety	Health and Social Services
		Threats and Hazards Identification	Fatality Management Services	Housing
Forensics and Attribution		Access Control and Identity Verification	Fire Management and Suppression	Natural and Cultural Resources
			Logistics and Supply Chain Management	
Forensics and Attribution		Cybersecurity	Mass Care Services	
		Physical Protective Measures	Mass Search and Rescue Operations	
Forensics and Attribution		Risk Management for Protection Programs and Activities	On-scene Security, Protection, and Law Enforcement	
		Supply Chain Integrity and Security	Operational Communications	
Forensics and Attribution			Public Health, Healthcare, and Emergency Medical Services	
			Situational Assessment	

\*Planning, Public Information and Warning, and Operational Coordination are common to all mission areas.



### 2.3.2 Oasis Trigger Events

The Oasis mode is intended for recovery and relief scenarios; therefore, it will only come online when there is a severe disruption to the local grid. Although the island has experienced earthquakes and there is a potential for tsunamis and wildfires [57], especially as the effects of climate change worsen, the primary disruptor for Puerto Rico has been hurricanes. As a result, this study will focus on the impacts and responses to hurricanes by an Oasis system.

One study identified an increase in frequency of severe tropical storms due to increasing ocean temperatures and reports a 25% increase per decade for the Northern Atlantic [58]. The study highlights an increased frequency for Cat3-Cat5 events, which can range from 185.2 km/h to above 254 km/h. The most recent storms, namely Hurricane Maria, produced around \$90B in damages, and caused around 4645 deaths on the island of Puerto Rico alone [59].

### 2.3.3 Sandia National Labs

As part of the collaborative efforts in the PR100 study, Sandia National Laboratory has developed the Resilient Note Cluster Analysis tool (ReNCAT). The software suggests microgrid portfolios to reduce the impact of large-scale disruptions to power. It provides candidate microgrids to bring online to the virtual power plant pool by leveraging tradeoffs between operating cost and service availability [60]. Another valuable tool from the software is the Social Burden calculator, which can provide data regarding the reduction in social burdens during grid outages.

A workshop hosted by the Sandia National Labs' Resiliency and Microgrids Team offers a resiliency scorecard. It aims to provide a method of comparison between resiliency solutions in reference to an established benchmark [61]. The workshop provides an example where the mitigation scorecard is used to assess the impacts of a defined hazard. The equations and tutorials used in the document are depicted in ReNCAT.

### 2.3.4 FEMA

FEMA has been supporting Puerto Rico's recovery efforts since Hurricane Maria made landfall in 2017[56]. Funding, logistical support, and recovery toolkits have been distributed and developed for these scenarios. In the Lifelines toolkit [62] they outline the emergency response protocols for state-level disruptions and natural disasters, with the goal of providing community support for safety, food, medical, energy, communications, transportation, and handling of hazardous materials. These different services are made up of critical functions that must be operational for community support. These sectors and their associated components are useful for establishing the performance of an Energy Oasis system as described in this work. The document also offers a colored status system to depict the condition of each component, these colors are grey for unknown level of disruption, red for disruption without a solution, yellow for disrupted with a solution and progress and includes estimate time to stabilization, green for stable, and blue for administrative purposes. The toolkit provides planning factors and stabilization targets to evaluate the conditions in a quantitative manner, some key factors include safety and security, food, water, shelter, medical, energy, and hazardous material management.

To ensure adequate design and operation of a DER, local laws and regulations must be considered in conjunction with all applicable international standards. The Institute of Electrical and Electronics Engineers (IEEE) standard 1547-2018: Interconnection and Interoperability of Distributed Energy Resources with Associated Electric Power Systems Interfaces outlines several practices [63]. Special emphasis is placed on prioritization of DER Responses under Chapter 4.7 and Intentional Islanding under Chapter 8.2 from the standard. The former describes the frequency and reactive voltage responses that must be monitored when operating a DER, including deviations from the averages. The latter describes how scheduled and unscheduled islanding can occur; the latter is expected to occur following a natural disaster, whereas the former is expected to occur once the grid has returned to baseline conditions. Furthermore, categories for islanding are provided, including uncategoryed, intentional island-capable, black-start capable, and Isochronous-capable. This work aims to design a system that is intentional island-capable and black-start capable. Isochronous-capable (capable of independent voltage and frequency regulation) calculations are not within the scope of this project, but are referenced from previous work by Lozano Inca [43].

### 3 Scientific Approach

Literature review reveals there is neither an existing configuration for the UPRM nor a load-shedding scheme for the campus. The implementation of a campus-wide microgrid requires detailed analysis and consideration for the technical, economic, social, political, and environmental aspects. The methodology of this study can be separated into two major topics:

1. **Microgrid Design:** This focuses on the technical and economic aspects surrounding the design of the microgrid itself. The software Hybrid Optimization of Multiple Energy Resources (HOMER) Pro is used to perform the system optimization based on the component inputs and constraints defined due to the system configuration optimizer value it provides.
2. **Energy Oasis:** After a microgrid design is identified, it is used as the foundation for understanding the social impacts it has when applied to disaster relief efforts. This disaster relief operation, hereafter referred to as the Oasis, will be analyzed to determine the potential recovery services that the microgrid can support and understand the impact that their added electrical loads have on the normal operation of the grid.

The methods followed in this study are outlined below and shown via a flowchart in Figure 2:

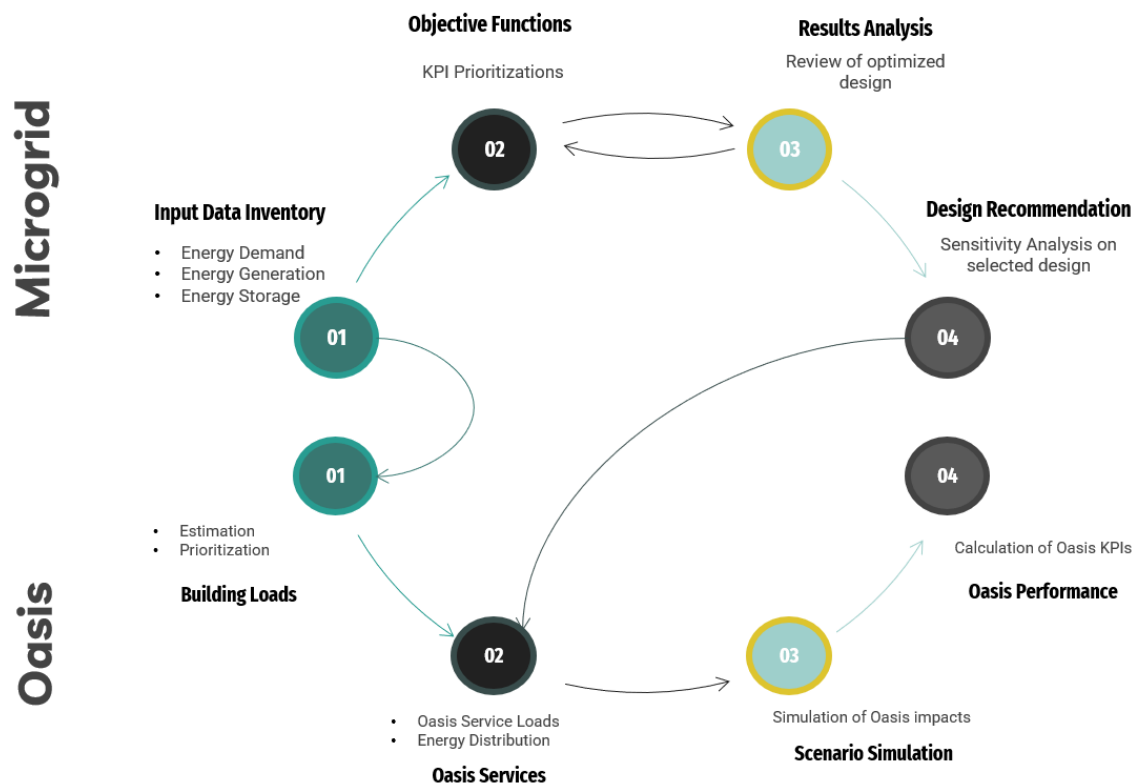


Figure 2: Flowchart outlining the methodological approach used in this study.

#### 1. Microgrid

- 1.1. **Input Data Inventory** – Defining all input values for the HOMER simulation (Energy demand values for campus used as input for 2.1 Building Loads)
- 1.2. **Objective Functions** – Outlining the key performance indicators (KPIs) and their prioritization for the design selection process
- 1.3. **Results Analysis** – Comparison of system designs as provided by HOMER, may require iteration to balance objective functions with non-quantitative needs of the Oasis
- 1.4. **Design Recommendation** – Final proposal of a system design (Capacity used as an input for 2.2 Oasis Services)

#### 2. Oasis

- 2.1. **Building Loads** – Estimation of individual building loads and their prioritization for load shedding
- 2.2. **Oasis Services** – Definition of Oasis services, their energy demands, and the distribution of energy within the Oasis
- 2.3. **Scenario Simulation** – Comparison of simulations for analysis of Oasis impact
- 2.4. **Oasis Performance** – Calculation of Oasis performance as defined by the chosen KPIs



## 3.1 Microgrid Design

This section covers key considerations for microgrid design based on existing standards, relevant research publications, and the local requirements of the project. The methodology is defined by three key steps:

- 1) Input data inventory
- 2) Microgrid KPIs
- 3) Results Analysis
- 4) Design Recommendation

The methodology follows the approach used by Maestre et al. to optimize renewable generation plants and hydrogen storage sites in Spain [64]. The methodology in this study has one key deviation, however, in Maestre et al., they optimized the sizing and location of the system in parallel to the system optimization itself, this is largely a result of having the entirety of the country of Spain at their disposal. In contrast, the space limitations of the UPRM campus are much more limiting, and as a result are used as boundary conditions for the system sizes in the proposed microgrid.

The system is expected to be within the size range spanned by the Adjuntas Pueblo Solar (220 kW solar PV, 1 MW second life Li-Ion batteries [20]) and the Babcock Ranch (74.5 MW solar PV [35]).

### 3.1.1 Input Data Inventory

The first step of the methodology involves a study of the total energy demand of the campus. This is followed by the defining of the power generation systems which begins with an analysis of the availability of renewable resources in the area. If the resource has a large enough pool of energy, then technological and economic parameters (such as conversion efficiency and capital expenditures, or CAPEX) are defined for component input in HOMER. The specifics of what parameters are needed depend on what is required in HOMER. Finally, different energy storage systems are considered and included to reduce dependence on the PR grid and improve performance during Oasis mode operation.

#### 3.1.1.1 Energy Demand

The University campus is divided into 63 buildings of varying sizes, construction dates, and functions. A preliminary literature review through Google Scholar, Science Direct, and direct contact with UPRM faculty revealed the energy consumption data is limited to monthly totals for the entire campus. There is currently minimal information regarding the energy consumption profiles of the buildings. A thesis conducted by Garcia et al provides consumption profiles for the Medical center, Biology laboratories, and an estimate of the Immigration and Accounting Office [41]. Contact was established with the Director of Mechanical Engineering, Ruben Diaz PhD, and the Dean of Administration, Omar Molina PhD. who were able to confirm there is no information on the subject as the buildings are not equipped with local electricity meters. Rather, the electricity is supplied to a central substation for distribution throughout the campus where the total consumption is totaled by the month. These monthly utility bills, provided for the purpose of this study by the campus administration, define the annual consumption profile that will be used in the HOMER simulation. Further resolution will be automatically calculated by HOMER according to a carefully selected profile that most closely matches the expected profile of the campus.

#### 3.1.1.2 Energy Generation System

Since this study is confined to the UPRM geographical boundary, a preliminary assessment of viable energy resources will be conducted by making use of the Solar Global Atlas, the Global Wind Atlas, an estimate of biomass availability based on agricultural and forestry/landscaping waste from the campus, estimates of local hydropower capabilities, and literature review for geothermal and tidal/wave energy potential.

These values will then provide the inputs necessary to simulate potential microgrid designs for the campus. An optimal component for each resource will be selected based on performance, economics, and durability. In this case, performance is defined as the ability for the potential design to meet the demand of the campus with minimal-to-no dependence on fossil fuel technology. The economic comparison will aim to minimize the costs of the selected component by comparing the costs of technologies available on the market. The resilience of the technologies will be considered as a prerequisite to performing any simulations: for example, a PV panel that is built with shatter resistant glass and mounted using ballasted mounts that have been proven to withstand Cat5 hurricane winds will be selected over a competitor with identical performance but weaker design characteristics, even if the cost of the former is slightly above the latter.

### 3.1.1.3 Energy Storage System

Most, if not all, commercial microgrids benefit substantially from having behind the meter (BTM) energy storage solutions in place [65]. This is especially true for the PRREO system, as the grid will likely be disconnected following disaster scenarios. An adequate storage design will be optimized via HOMER within predefined constraints. Ideally, the system will be capable of storing an energy equivalent to 1-5 days of the campus load. This is based on the average installation times for renewable energy systems [66] which are considered equal to the replacement time. Additionally, it would provide a significant buffer for Oasis operation after a SWE, if minor repairs or debris clearing are necessary before the microgrid can generate electricity again.

### 3.1.2 Microgrid KPIs

The selection of the optimal design is based on the results of the techno-economic assessment of the simulation results. This is accomplished by measuring and comparing the systems by three metrics: LCOE, renewable fraction (RF), and CAPEX. The primary focus being the minimization of the LCOE. It is calculated by Equation 1 in HOMER.

*Equation 1: LCOE*

$$LCOE = \frac{C_{ann,tot}}{E_{served}}$$

Here,  $C_{ann,tot}$  is the total annualized cost of the system (\$/yr) and  $E_{served}$  is the total electrical load served (kWh/yr). The LCOE of a system is the price at which electricity must be sold for revenue to equal project costs, including a return on investment (ROI) equal to the discount rate [67]. The lower a project's LCOE, the more likely the project will be profitable.

The RF measures the fraction of the energy delivered to the load from renewable power sources (Equation 2). Maximizing this value reduces the campus's dependence on the PR grid by reducing the amount of energy purchased from the grid. This is expected to have a two-fold benefit for UPRM. First, the reduction of purchased electricity improves the long-term savings of investing in the microgrid. This can be measured by a reduction in operating costs from grid purchases for the microgrid as RF increases. Secondly, it reduces the impact of PR grid outages from SWE on the campus operations and improves Oasis operations by increasing the fraction of the load served by reliable sources that can continue to generate after a SWE.

*Equation 2: Renewable fraction*

$$RF = 1 - \frac{E_{prod} - E_{ren}}{E_{served} - E_{grid,sales}}$$

Where,  $E_{prod}$  is the total electrical production from all generation sources including energy from a grid connection (kWh),  $E_{ren}$  is the energy produced by renewable sources (kWh), and  $E_{grid,sales}$  is the amount of energy sold back to the grid (kWh). RF is traditionally expressed as a percentage. Maximizing RF is done after minimizing LCOE to prevent situations where an RF of 100% is achieved at exorbitant system costs that make the design infeasible.

Lastly, CAPEX is utilized over the more traditional net present value (NPV)<sup>1</sup> metric as it provides a better understanding of the initial investment the project requires. In contrast, NPV provides knowledge of whether the project will be profitable in the long run. By minimizing CAPEX over maximizing NPV, the odds of approval for the selected design are improved as the short-term costs are lower than for competing designs. The total project CAPEX is the sum of the initial capital costs for each component in the system (Equation 3).

*Equation 3: CAPEX*

$$C_{CAPEX} = \sum_{j=component}^i C_{CAPEX,j}$$

---

<sup>1</sup> NPV is used interchangeably with net present cost (NPC) in this report

### 3.1.3 Results Analysis

As mentioned in the previous section, the optimal design is selected by first minimizing the LCOE to obtain a high ROI. Then, should more than one design have the same LCOE, the RF is maximized to select the design with the least dependence upon the PR grid. And lastly, if there is still more than one design at this point, the selection will be achieved based on the lowest CAPEX to minimize the initial investment of the project and increase the likelihood of project approval.

Once the optimal design is selected, an analysis of its resiliency will be discussed. This will focus on the diversity and size of the generation systems as well as whether it includes a storage system. Based on these points, a new selection may be added (e.g., two or more generation resources are required, or the design must include a storage system) and the above selection process repeated to find a new optimal system. The purpose of this analysis is to ensure that the recommended microgrid meets the unique requirements of the UPRM campus and needs of an energy oasis.

### 3.1.4 Design Recommendation

After the iteration of simulation and results analysis is completed, a final system design is selected. This microgrid will be optimized quantitatively as per the KPIs outlined above in Section 3.1.2 and qualitatively to meet the unique demands of the Oasis operation. Once this design is finalized, a sensitivity analysis is performed to understand how it responds to variations in inputs.

#### 3.1.4.1 Sensitivity Analysis

A sensitivity analysis based on component cost variations is then performed to understand how changes in market conditions impact the selected KPIs and whether they change the optimal configuration. The analysis will consist of costs for all components being adjusted together depending on three anticipated market scenarios, as defined by the Technology Innovation Scenarios for the NREL's Annual Technology Baseline (ATB) [68]:

- **Conservative:** No significant change in technology design, investments into R&D decreases. Has the highest prices of the three.
- **Moderate:** Technological innovations continue to spread at their current pace, current rates of R&D investment continue. This is the scenario used as a baseline for this study and the costs associated are used for the optimal design analysis.
- **Advanced:** Cutting-edge innovations become successful and proliferate throughout the market; investment into R&D increases. Has the lowest prices of the three scenarios.

In addition to this cost sensitivity analysis, a study of the performance of the recommended design at a range of demands is performed. In this, the annual average energy consumption of the campus is increased by 30% and decreased by 30% while the capacity of the microgrid is kept constant. The increased load simulates additional loads added to the campus. The reduction simulates the implementation of energy efficiency measures aligned with the PR100 goals. The impact these have on the RF, operational expenditures (OPEX), and the quantity of excess energy generated by the microgrid. The latter values are further used in the analysis of the microgrid during Oasis operation mode.

## 3.2 Energy Oasis

This section provides an overview of how the Oasis system is expected to be designed and how its performance will be measured. The overall approach can be separated into four distinct steps:

1. Definition of building loads
2. Outline of the services provided
3. Definition of scenarios
4. Oasis performance as defined by KPIs

The primary goal of an Energy Oasis is to provide the surrounding community with alternative access to reliable electricity in the event a natural disaster incapacitates the local grid. Furthermore, the Oasis will be designed to serve as a "Recovery Zone" where critical functions can be supplied with electricity including but not limited to medical services, telecommunications, water purification, food preparation and storage, and equipment recharging. These services are provided within the geographical boundary of the campus, but a flow of people from the surrounding community who are in need is expected to enter the geographical boundary.

To properly design and simulate the Oasis operation of the microgrid, a few improvements and considerations have been assumed. Firstly, the renewable energy system is designed in such a way as to prevent damage from hurricanes, natural disasters, and other events. In other words, it is resilient enough to be considered fully operational after an event that disrupts the national electric grid. The second assumption is that the electrical system of the university has been updated with the necessary number of independent electrical meters so as to assess the consumption of electricity at any point in time from each building. Thirdly, there is demand side management software with load shedding hardware installed for each building. The final assumption is that the estimates for consumption do not vary significantly throughout the projected 20-year lifetime of the system.

### **3.2.1 Building Loads**

To properly perform demand side management and optimize the Oasis performance, the campus demand profile must be broken down into individual building load profiles. This process is separated into two distinct steps to properly simulate the campus-wide demand side management. First, the load profiles for each of the 63 buildings on campus are estimated. After which each building is given a prioritization to rank how critical its electricity needs are compared to the rest of the campus.

#### **3.2.1.1 Estimation**

As mentioned previously, very limited data exists for the energy consumption of individual buildings around campus. Moreover, there is no available information regarding the cooling load and electrical load of the existing rooms.

To work around this limitation, each buildings consumption is estimated based on values obtained from a study by Garcia et al. [41]. This provides an estimate for the average consumption per area of seven buildings based on their primary functions, such as lecture halls or laboratories. Each building on campus is then categorized based on which of the seven buildings it most closely resembles. Thus, energy consumption is estimated based on this correlation and the total area of the buildings. This process is explained in further detail in Section 4.2.1.

#### **3.2.1.2 Prioritization**

Oasis mode serves to maintain continuity of operations within the UPRM and to preserve the progress of sensitive research being conducted. However, there is an opportunity for non-essential loads to be intentionally disconnected, thereby liberating the supply of electricity for use within the Oasis system. Suitable candidates for load shedding are found from interviews and assumed from expected importance based on priorities across the campus. The priorities include administratively critical functions, academic research, remote access capability (i.e. lectures), among others.

The highest priority loads serve the primary and critical roles for the entity being supplied. In this study, this highest priority is identified as “Priority 1”, as the criticality of a load decreases it is reflected by an increase in the priority number. In the UPRM case they have been requested by the Dean of Administration and are described in detail in Section 4.2.1. To better understand the consumption from these buildings, an inquiry of the building-responsible is necessary for acquiring the installed components requiring electricity. This is also detailed in Section 4.2.1, where the loads are divided by their function as per the method explained in Section 3.2.1.1.

Further levels of prioritization are assigned to every building across campus. This creates a tiered structure across the buildings that can be used to easily select which buildings will be shed from the load based on the existing severity. As the severity of the situation increases and more energy is required for the Oasis, subsequent levels of prioritization can be shed in groups to provide pre-calculated chunks of energy for the Oasis. Grouping the buildings together in such a way simplifies the load shedding mechanism and reduces the infrastructure required for demand side management. These prioritization levels are also explained in detail in 4.2.1.

### **3.2.2 Oasis Services**

To adequately describe the services being provided two different pieces of information are required:

1. The energy consumption per person served for each service.
2. The amount of energy in the Oasis that goes towards that service.

Six functions are enabled by the Oasis microgrid within this study, although variable amounts of services can be provided based on the recovery effort needs. In this study, these include Emergency medical aid (Medical), water filtration (Water), food preparation (Cafeteria), communications (Telecom), debris management (Debris), and personal usage (Personal).

The energy consumption per person is estimated for each of these functions. This is ideally accomplished through literature review as this provides the most accurate estimation available. Should there be insufficient information for a service, a bottom-up analysis of the service is used.

With these values, the calculation of the number of people or duration of access can be calculated given a set quantity of energy for the services. To begin, the proportion of the total energy in the Oasis simulation that goes to each service is determined by the criticality of that service compared to the others. The criticality order used in this study can be found in Table 2 below. The higher the criticality the larger the proportion of energy provided to that service. A more detailed explanation of the quantity of energy provided in each service can be found in Section 4.2.2.

*Table 2: Order of criticality of the Oasis services utilized in this study.*

Service	Criticality
Medical	5
Water	4
Cafeteria	4
Telecom	3
Debris	2
Personal	1

Because this order is self-defined for this analysis, and because there have been no similar studies analyzing the concept of an Energy Oasis, the results of this initial approach are expected to be suboptimal. As a result, this is used solely as a starting point for the distribution of energy within the Oasis. Further iterations are performed based on these initial results to optimize this distribution.

**3.2.3 Scenario Simulation**

To better understand both the performance of the prioritization structures and the scale of the impacts they can have, a series of different scenarios are simulated. These impacts are measured via select KPIs that are defined in Section 3.2.4. To provide a baseline for comparison, the impacts of the campus on disaster relief efforts are calculated in a business-as-usual (BAU) scenario. This is without any microgrid installation and therefore no Oasis capabilities.

With the baseline defined, the system impacts are recalculated for each prioritization level of load shedding (from lowest priority through to everything except the highest priority shed). This is performed first for the standard consumption profiles estimated for the buildings.

After which, the prioritizations are re-simulated with the assumption that the campus achieves the PR100 efficiency goals with the installation of the microgrid. In this scenario, the microgrid capacity is kept identical as the scenario before. The only change is an energy demand reduction of 30% per building, creating a large pool of energy available to the Oasis before load shedding occurs. A diagram of these scenarios can be found in Figure 3.

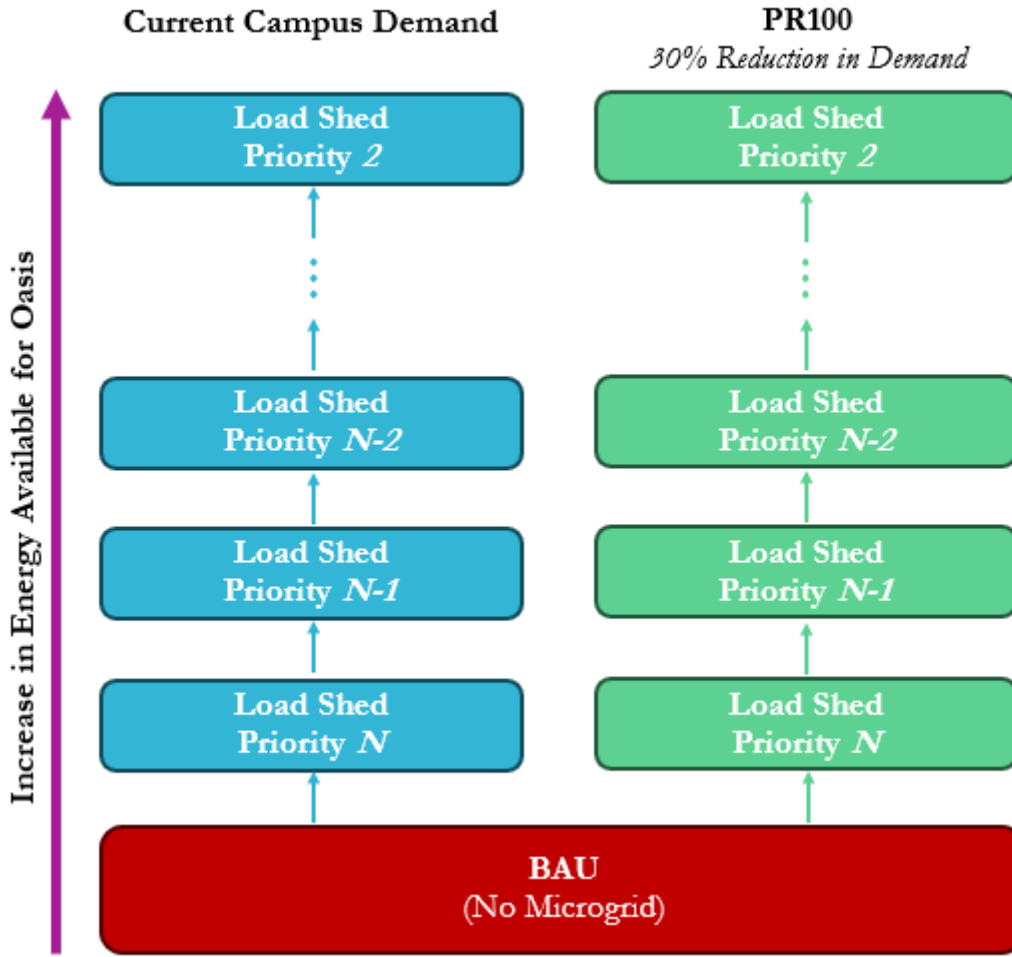


Figure 3: Diagram of the relationship between the different scenarios simulated for the Oasis performance.

### 3.2.4 Oasis KPIs

To assess the performance of an Oasis system, a set of metrics is proposed to improve understanding of the Oasis and allow direct comparison with a grid-only electricity supply. The KPIs considered are Oasis access time, number of people served, and disaster relief.

The overall objective of any Oasis system is minimization of recovery time ( $t_r$ ) for a community. This is defined in Equation 4 as the difference between the total blackout time ( $t_b$ ) a community experiences due to a disaster event minus the total access time ( $t_a$ ) they have to the Oasis grid.

Equation 4: Recovery time

$$\min(t_r) = \min(t_b - t_a) = t_b - \max(t_a)$$

Since total blackout time is entirely dependent upon the severity of the event, the current state of the existing grid, and the effectiveness of recovery efforts by governing bodies it is outside the control of the microgrid. As a result, the maximization of access time becomes the target variable that can be measured and controlled by the proposed system. The longer the period of access that the microgrid can provide is, the less time the community is without power for basic services during the grid blackout. Total access time is a sum of the access time provided by each service ( $t_{a,i}$ ) served in the microgrid. These are a function of the total energy ( $E_{O,i}$ ) provided to the service in kWh, divided by the product of the number of people served ( $n_i$ ) and the unit energy ratio for the service ( $\rho_i$ ), in kWh/person, which is a constant for the amount of daily energy consumed per person for the service (Equation 5).

Equation 5: Total access time

$$t_a = \sum_{i=service}^6 t_{a,i} = \sum_{i=service}^6 \frac{E_{O,i}}{n_i \cdot \rho_i}$$



For any renewable microgrid system, the quantity of energy supplied by the renewable microgrid has a daily maximum. Because of this, there is a limit to the number of people that can be served for each service in a day. Exceeding this value in the simulation is equivalent to overloading the generation capabilities of the microgrid. To calculate this limit, the annual energy provided to the Oasis for each load shedding scenario outlined in Section 4.2.3 is used to calculate the average daily generation capacity for the Oasis ( $E_{O,i}$ ). This quantity of energy is then partitioned into each service using a weighted average, based initially on the allocated disaster relief value given to each service in Section 3.3. Using the energy capacity for each service's access time, as defined in Equation 5, the maximum number of people that can be served is equal to the total energy capacity per day divided by the energy ratio for that specific service.

*Equation 6: Maximum number of people served per day for a service.*

$$\max(n_i) = \frac{E_{O,i}}{\rho_i}$$

The performance of an Oasis is characterized by the quantity of people served that are external to the generating entity. In this case, the metrics consider how many people of the surrounding Mayagüez community are provided access to electricity during a SWE. This concept considers all relief and recovery efforts to reduce the overall strain on the grid, as evidenced by the 2017 FEMA reports documenting efforts to re-establish the baseline grid conditions[3].

The disaster relief fraction is used to measure the overall performance of the Oasis ( $\epsilon_{OS}$ ), as shown in Equation 7. This dimensionless metric provides a ratio of how much energy is provided to the Oasis ( $E_O$ ) for a set access time compared to the energy produced by the microgrid in a year ( $E_M$ ).

*Equation 7: Disaster relief fraction*

$$\epsilon_{OS} = \frac{E_O}{E_M} = \frac{\sum_{i=service}^6 E_{O,i}}{E_M}$$

This, like the number of people served, will be calculated for a range of access times to provide more insight into how the duration of operation effects the impact of the Oasis system on the standard operations of the campus.

### 3.3 Sustainability Analysis

The recommended microgrid design and its use as an energy oasis is analyzed to understand the impacts on five sustainability categories: land use, energy consumption, food availability, water access, and social impact. This largely entails summarizing the anticipated impacts the microgrid and Energy Oasis have on each category, such as expected land transformation for any installed electricity generation systems.

Energy that is dedicated to relief efforts will have varying degrees of impact depending on their end usage. Charging personal phones is not on the same level of relief as providing electricity for medical equipment or water filtration purposes. However, significantly more people can be served if they are only seeking to charge their phones as opposed to receiving medical treatment. As a result, the proportionality of energy distribution to services within the Oasis is expected to have a high impact on the number of people that can be served.

Thus, the concept of an “Oasis Score” (OS) is proposed by this study to measure the social impact by an energy oasis, specifically during recovery efforts. To evaluate the effect of each end use on recovery, a point system is defined to scale their overall benefits to one another. This scale is based on the criticality of the services they provide (e.g., the ability to provide medical aid and save a human life is considered a higher priority than charging electronic devices for personal communication after a disaster). Table 3 below shows a proposed point system.

Table 3: Disaster relief multipliers for the different services included in the Oasis.

Service	Disaster Relief Multiplier
Medical	5
Water	4
Cafeteria	4
Telecom	3
Debris	2
Personal	1

To calculate the overall points of the Oasis, the disaster relief multiplier ( $DRM_i$ ) is multiplied by the energy supplied to that service by the Oasis ( $E_i$ ) and the actual number of people served ( $n_i$ ). This value is then divided by a constant for the microgrid: the product of the maximum number of people that can be served in a day for the service ( $n_{i,max}$ ) and the average total campus load served by the microgrid in a day ( $E_M$ ). The scores from each of the four core services (medical, water, cafeteria, and telecommunication) are summed together to provide the total Oasis Score (Equation 8).

Equation 8: Oasis score

$$Oasis\ Score = \sum_{i=service}^4 \frac{DRM_i \cdot E_i \cdot n_i}{n_{i,max} \cdot E_M}$$

It is important to note that this score, at its initial calculation, is an arbitrary metric. To understand how the OS can provide insight into the performance of an energy oasis, further data from alternative designs and real-life trials are required. As knowledge of the OS expands, a sense of scale can be developed to help provide initial target values for an Energy Oasis, or to improve allocation of resources.



## 4 Methods

This section outlines the inputs and constraints used in the study. All relevant research and assumptions are contained within.

### 4.1 Microgrid Design

Defining an Energy “Oasis” requires knowledge of the energy grid during “business-as-usual” (BAU) operation. Without a good model for the BAU microgrid, the full available capacity for Oasis operation cannot be analyzed. The development of the model required an iterative process to simulate multiple grid designs that meet the demand to optimize the most economical design within the system constraints. To accomplish this, HOMER Pro v3.14 software was utilized as its capacity to simultaneously simulate multiple component designs to find the economically optimum allowed for minimum post processing of results [69].

The energy generation system must be sufficiently sized so that any design will have the capacity to meet the BAU load without significantly relying upon the island’s existing grid. This is measured by the Renewable Fraction (RF) of the proposed designs, which is the amount of final energy generated (as a percentage of total energy produced) that comes from renewable sources. Ideally, the RF would be 100%, however, given space and technoeconomic limitations of UPRM a lower value with some grid reliance may be more reasonable.

The energy generating system components are scaled to meet the maximum daily energy demand as well as peak load of the campus. Since 97% of the island grid is currently powered by fossil fuels, transitioning the university from the island grid to renewables will have the added benefit of reducing the emissions associated with the University’s energy consumption [23], [34]. The energy generating system components are scaled to meet the maximum daily energy demand as well as peak load of the campus.

To improve the reliability of a renewable energy system, an energy storage system will be included in the design. By integrating storage systems, the intermittent nature of some renewable resources like solar and wind can be smoothed out to meet load demands during periods of low generation and to improve efficiency of the system by storage excess energy generated.

#### 4.1.1 System Demand

The electricity demand on the microgrid was modeled within HOMER Pro using pre-defined load profiles for hourly and monthly demand. The location was set to the city of Mayagüez, Puerto Rico. The university campus being studied is located approximately 0.5 km north of the center of town (Figure 4).

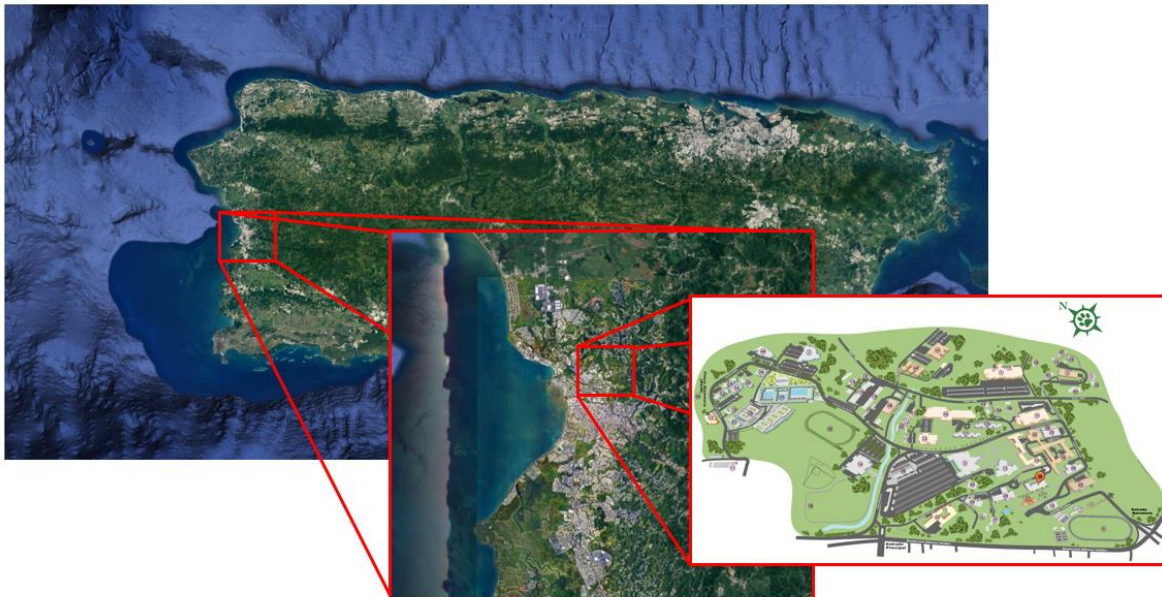


*Figure 4: Location of UPRM campus.*

The load profile for the university has been approximated using data provided by UPRM to define a scale that adjusts a preset HOMER load profile. The data gives the total monthly consumption of the campus between June 2020 and September 2022 as well as the total cost of the electricity for each month (Appendix

A), as shown in Figure 4. This data comes directly from the monthly electricity reports that accompanied the bills. They were provided for this study by the UPRM Mechanical and Electrical Engineering departments. Appendix A details the change of consumption and average cost of electricity (\$/kWh) for each month of data provided. No total cost value was provided for April 2022, as a result, an electricity rate could not be determined for this month. This value was excluded whenever electricity costs were analyzed in the simulation. These consumption values were averaged to obtain an estimate for the daily demand of the system.

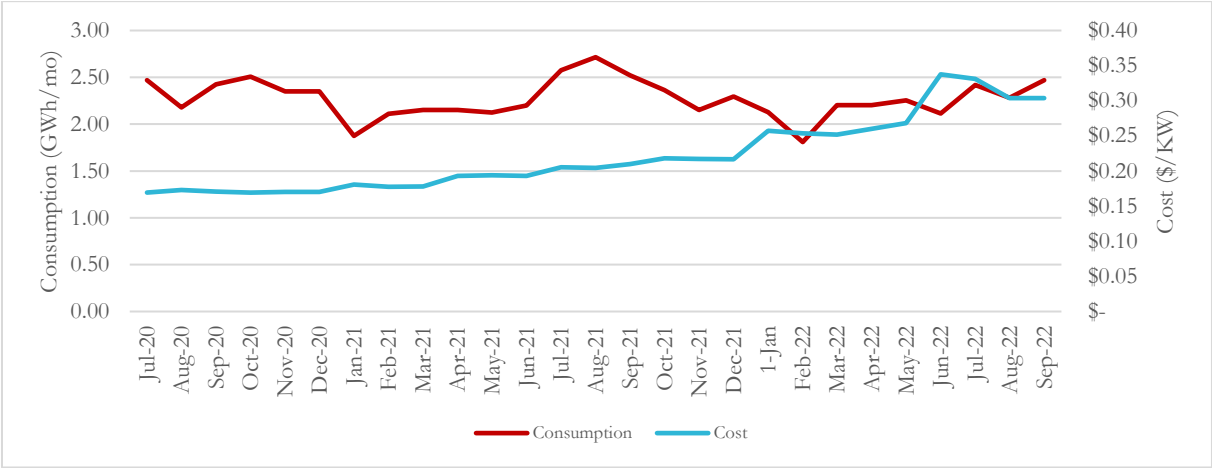


Figure 5: Monthly consumption (red line - left axis) and cost (blue line - right axis) for UPRM between July 2020 and September 2022.

A pre-defined profile found in the HOMER database was used to represent the hourly profile within each month. For this system, the location of the Mayagüez campus on the west coast of the island falls into the Köppen-Geiger climate classification system of “Am”, which is an equatorial climate with precipitation in the ‘monsoonal’ category [70].

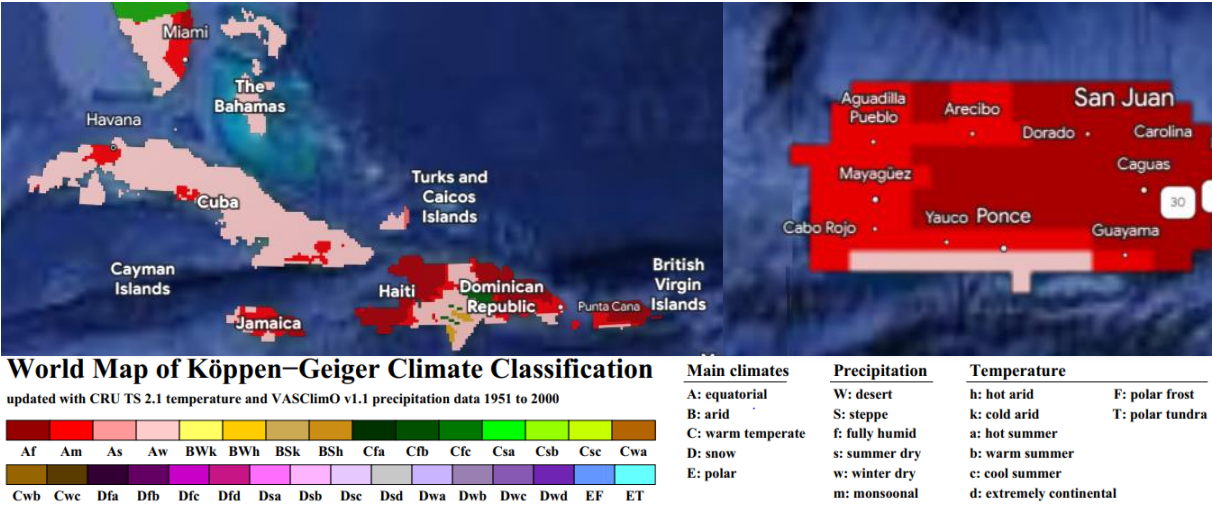


Figure 6: Climate Classification map of Puerto Rico and the northern part of the Caribbean showing that Miami and Mayagüez share the same classification. Images were captured from Google Earth with Climate Classifications overlaid using data provided by Vienna University. [70], [71].

Within this climate classification, a load profile representing a secondary school in the Homestead Air Force Base, Florida was selected as it is the closest match to the expected daily profile of the UPRM campus due to the share focus as educational institutes. However, it is important to emphasize that this is a limitation of the simulation as the secondary school does not also provide on campus housing and continuous research laboratories and therefore does not completely match the expected daily load of UPRM’s camps.

This profile was modified to better fit the known demand of the UPRM campus. This was done by scaling the daily demand from a default value of 15,055.21 kWh/day to the calculated average value of 74,962.36 kWh/day.

4.1.2 Input Data Inventory

The following subsections describe the parameters and components used in HOMER Pro to model the proposed microgrid. The microgrid consists of components that fall into three distinct categories:

- **Campus Load:** The simulated load profile for the campus as outlined in Section 3.1.1.1.
- **Energy Generation Systems:** Any system that is a source of energy (e.g., solar PV, wind turbines, etc.). It includes a component connecting to the existing electrical grid on the island. Any converters needed to transform DC current to AC current, and the reverse, are also included in this category.
- **Energy Storage Systems:** This category covers any simulated energy storage components, such as Li-ion batteries or electrolyzers, as well as any tanks or containers that are required to store the energy medium.

#### 4.1.2.1 Energy Generation

The selection of which of the available technologies for capturing renewable resources is one of the most important decisions in the designing of a microgrid. To narrow down the list and identify the optimal products on the market for the selected resources, the optimal technologies were chosen based on three primary characteristics:

1. **Resource availability:** the total potential of the renewable resource that is available at the chosen location of Mayagüez, Puerto Rico [kWh/year]
2. **Cost:** the total capital, operational/maintenance, and replacement costs of the product [\$USD]
3. **Durability:** the ability for the product to withstand the extreme conditions that are common to Puerto Rico and still function adequately

Durability does not have a simple quantifiable value or unit and must be analyzed subjectively on a case-by-case basis.

### Solar PV

With its location in the Caribbean between the equator and the Tropic of Cancer, the island of Puerto Rico has relatively consistent hours of daylight between winter and summer months [72]. This has the benefit of removing seasonal variations that traditionally create challenges for designing solar PV systems. Data provided by the National Solar Renewable Database (NSRDB), a database developed and maintained by the National Renewable Energy Laboratory (NREL), between 1999 and 2017, confirm this assumption, showing little difference between the global horizontal irradiance (GHI) for Mayagüez across the year. Figure 7 shows the variation in GHI per month throughout the year, Figure 8 shows the little variation between daylight hours throughout the year [73].

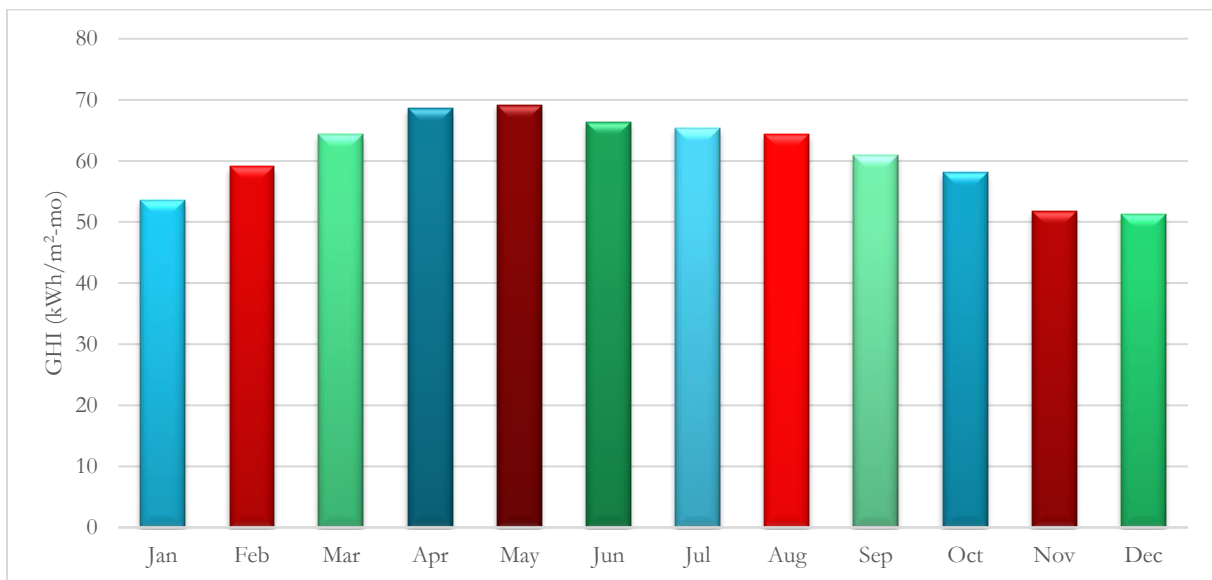


Figure 7: Average monthly GHI for Mayagüez, generated using data from the NSRDB [73].

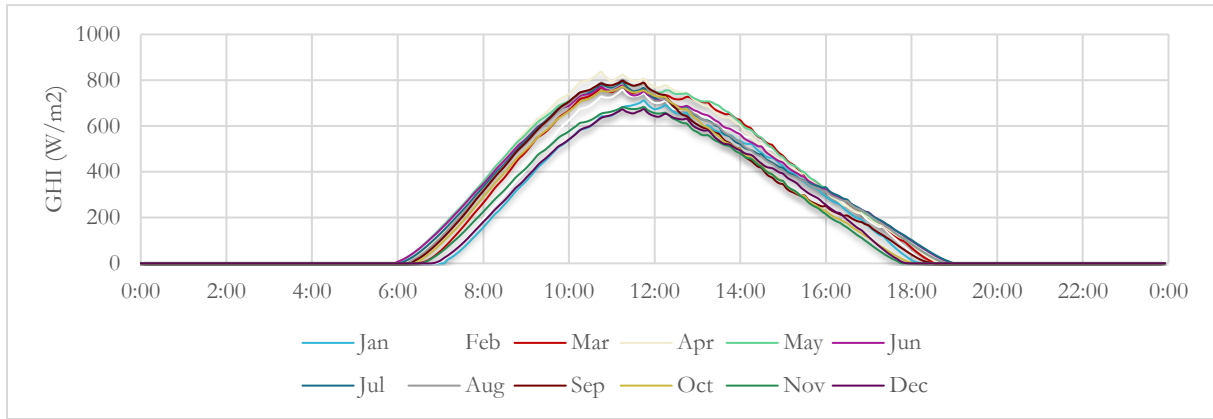


Figure 8: Average daily GHI for each month of the year in Mayagüez, generated using data from the NSRDB [73].

Simulation data for the GHI specific to the location of the university campus was downloaded from the National Aeronautics and Space Administration’s (NASA) Prediction of Worldwide Energy Resource (POWER). This database provides a statistical monthly average for the GHI based on measurements over a 22-year period between July 1983 and June 2005 [74].

Since 2000, global installed PV capacity has grown from virtually non-existent at the turn of the century to over 800 GW of power in 2021 [75]. Currently, newer PV models are able to achieve conversion efficiencies of above 20% with maximum power outputs of over 500 W at standard testing conditions (STC) [76]–[78]. To determine which model to use to define the technical specifications for the simulation, a decision matrix was created to compare them. The comparison categories characterize either the performance or durability of the cells in question and are listed along with the values in Table 4. The cost is not considered as it is estimated independently of the selected model for this study.

Table 4: Decision matrix table for the three PV modules.

Criteria	Jinko JKM550M-72HL4 [76]	LA Solar Group LS550 BL [77]	Phono Solar Tech 550 M6-24TH [78]
Rated Power	550	550	550
Efficiency	21.33	21.28	21.28
Material Warranty	12	25	12
Output Warranty	25	25	25
Output @ EOW	84.8	85	80.2
Snow	5400 Pa	5400 Pa	5400 Pa
Wind	2400 Pa	2400 Pa	2400 Pa
Hail	25mm @ 23m/s	25mm @ 23m/s	25mm @ 23m/s
Fire	IEC 61730	IEC 61730	IEC 61730

The performances of the three different models are almost identical across the board. The only differences being a slight increase in efficiency for the Jinko model, a longer warranty on the materials for the LA Solar Group model, and small differences between the output efficiencies at the end of the output warranty period. As a result, the system specs for the LA Solar Group LS550 BL model have been used for the simulation model despite the Jinko model having a better efficiency. This is due to the longer material warranty of the LA Solar Group LS550 BL, which will be beneficial in terms of durability and replacement costs, and its higher end of warranty output efficiency compared to the other two.

Based on this selection, the relevant input values used in the HOMER simulation were pulled from the model’s datasheet. These values can be found in Table 5, the full datasheet can be found in PV Model Datasheet.

Table 5: Relevant simulation input variables for the LA Solar Group LS55BL PV module [77].

Parameter		LA Solar Group LS550 BL
Maximum Power	W	550
Component Efficiency	%	21.28
NOCT	°C	45 ± 2
Module Size (LxWxH)	mm	2279x1134x35

The Nominal Operating Cell Temperature (NOCT) of a panel defines the temperature of the cell under normal operating conditions: an irradiance of 800 W/m<sup>2</sup> at 20°C with a wind speed of 1 m/s and an air mass (which defines the spectrum of the incoming light) of 1.5 [76], [78]. The actual operating temperature of the cell is an important design consideration as there is an associated drop in efficiency as temperatures deviate from NOCT. For the three models compared previously, the change in efficiency as a function of temperature is a drop of 0.35% for every °C away from NOCT [76]–[78]. Equation 9 gives the relationship between ambient air temperature, NOCT, solar irradiance, and the cell’s operating temperature:

Equation 9: PV cell temperature [79]

$$T_c = T_a + \frac{NOCT + 20}{80} \cdot S; [^{\circ}C]$$

Where,

$$T_c = \text{Cell temperature } [^{\circ}C]$$

$$T_a = \text{Air temperature } [^{\circ}C]$$

$$S = \text{Solar irradiance } \left[ \frac{mW}{cm^2} \right]$$

For UPRM, the solar irradiance has a maximum value of 10.022 W/m<sup>2</sup> and an average value (during daylight hours when irradiance >0 mW/cm<sup>2</sup>) of 4.274 W/m<sup>2</sup> throughout the year.

Due to temperatures in Mayagüez typically averaging between 26-29°C [72], the average (27.5°C and 4.274 W/m<sup>2</sup>) and maximum (29°C and 10.022 W/m<sup>2</sup>) cell temperatures for the selected PV model are 62.22°C and 110.43°C, respectively. In the worst-case scenario (the hottest day of the year with the maximum irradiance), the cell temperature is well above the recommended operating maximum (85°C) for the model. Even on the average day, cell temperatures can rise almost 20°C above NOCT. As a result, the temperature effects on PV efficiencies were included in all simulations using temperature data for the campus from NASA’s POWER database to improve accuracy and account for drops in performance.

Since most grids, and as an extension end-user systems, operate with an alternating current (AC), the direct current (DC) produced by a PV cell is not compatible with the grid and a DC-AC inverter is required to complete the coupling. The respective sizing of the PV system and an inverter is commonly described by a ratio, commonly called the ”DC/AC ratio” or ”inverter ratio”, between the maximum power produced by the PV system (in DC) and the maximum AC power that the inverter is capable of converting from DC (Equation 10).

Equation 10: Inverter ratio

$$r_{inv} = \frac{P_{PV}}{P_{inv}} = \frac{P_{DC}}{P_{AC}}$$

Throughout the year, the amount of solar irradiance fluctuates and rarely achieves the maximum. This variation results in a PV system only producing the maximum rated power a small percentage of the year. Figure 9 graphs the number of hours throughout a year that any PV system in Mayagüez produces a range of power, normalized to the maximum irradiance received in a year equaling 100% power output.



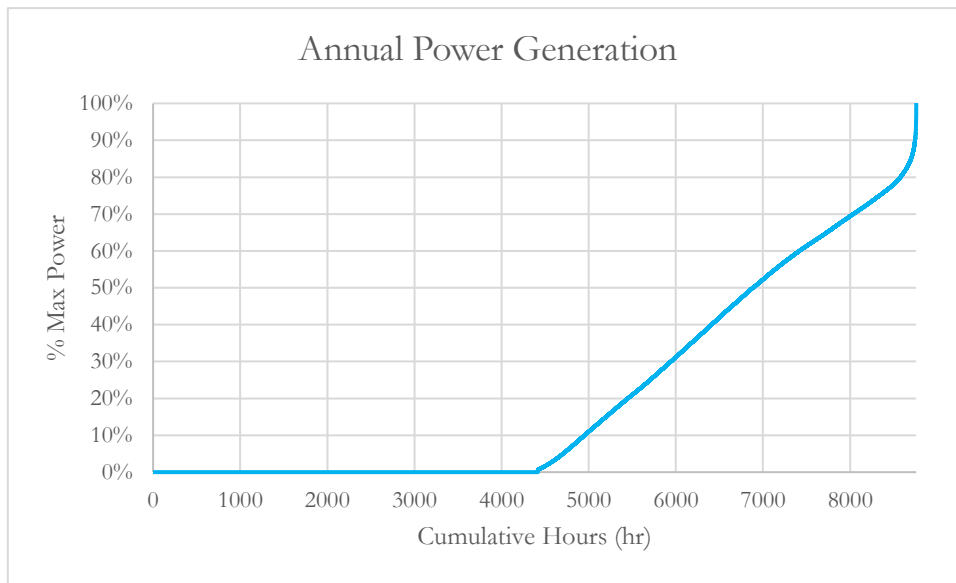


Figure 9: Cumulative annual time that the PV system produces at a power level, shown as a percentage of the maximum power produced for the system.

As a result, an inverter sized to the full capacity of the PV panel would only operate at this level for a small fraction of the year. In order to save on costs and improve the performance of the inverter, most systems are designed with an inverter ratio of 1.25 as this results in less than 1% of the total annual power produced to be unconverted, a procedure known as "clipping".

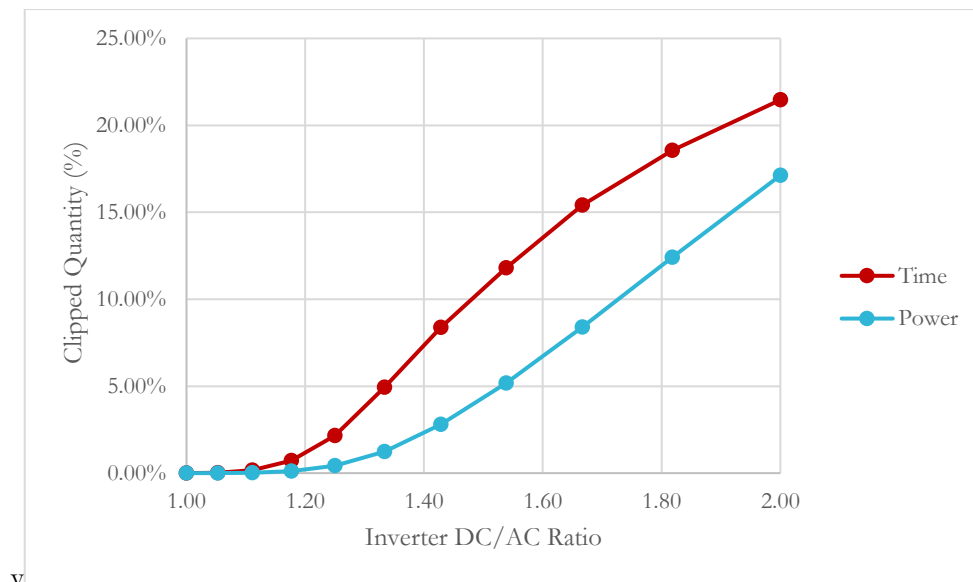


Figure 10: Amount of time throughout the year that clipping occurs (red) and the amount of power that is clipped (blue) for different inverter ratios at UPRM.

For the irradiance profile of UPRM, the inverter ratio has been set at 1.31 which results in 1% of the annual power clipped over 4.25% of the year (Figure 10).

For the purposes of simplification, a single inverter is modeled for the system as a whole. In reality, each rooftop or parking lot is recommended to have its own dedicated inverter. This will prevent any individual section of modules from reaching the maximum rated voltage or currents. Additionally, this configuration improves the resiliency of the microgrid, if one inverter were to fail then a smaller section of modules would be offline than if there were only one inverter for the entire system.

Mounting racks for PV systems are usually not independently defined when scoping systems as the industry standard of connected rows of PV panels along one single mounting rack. However, while this configuration is sufficient in many PV systems, the nature of the interconnected rows prevents the panels from flexing or bending when under extreme conditions such as high-speed winds. The alternative system selected for this project is the application of ballasted mounts (Figure 11) [80]. These anchors are not interconnected together or to the roof but rather ballasted with concrete blocks that allow the panels to behave like chain links by bending and flexing between panels in extreme winds. A PV system installed with this mounting system on

top of the Veteran’s Affairs hospital in San Juan has survived two back-to-back category 5 hurricanes in 2017 with no damage to the installed system, operating at 100% capacity after the storms had passed.



*Figure 11: Sollega Inc.'s ballasted roof mounts installed into a PV system [81].*

This type of mounting structure does have fixed angles for the panels (5°, 8°, and 10° for the Sollega FastRack models). As a result, the PV tilt angle was adjusted in the simulation from the optimal for the location (18°) to 10°.

A full economic assessment specific to the site and system designed is outside the scope of this study. As a result, ranges for the components have been acquired from estimates provided by the NREL. These include individual component costs (modules, inverters, mounts, etc.), installation costs (labor and installation equipment), and development overhead costs. The analysis, completed in 2022, used price points from 2021 to approximate cost per kW for the capital expenditure (CAPEX) of a PV system in a residential, commercial (ground and rooftop mount), and utility scales [82]. equipment), and development overhead costs.

For the purpose of the UPRM microgrid, ranges were obtained from the modeled market price (MMP), the current market price, and minimum sustainable price (MSP), the optimal price in a perfectly competitive market, benchmark values for a 200kW commercial rooftop system. These two values were used as the upper and lower bounds, respectively, to determine the cost sensitivity of the system. CAPEX values for the PV system were considered independent of the selected PV model, inverter, and mounting components. The breakdown of the cost components for both values along with a mean value between the two, given in USD \$ per watt of DC power of the PV system, are found in

Table 6.



Table 6: CAPEX breakdown for PV system [82].

	MSP (USD \$/W <sub>DC</sub> )	Mean (USD \$/W <sub>DC</sub> )	MMP (USD \$/W <sub>DC</sub> )
Developer Profit	0.11	0.115	0.12
Contingency (4%)	0.04	0.045	0.05
Developer Overhead	0.32	0.34	0.36
Sales Tax	0.04	0.045	0.05
Permits/Inspections/Interconnection	0.09	0.09	0.09
Engineering, Procurement, and Construction Overhead	0.17	0.175	0.18
Installation Labor/Equipment	0.15	0.15	0.15
Electrical Bill of Sale (BOS)	0.15	0.18	0.21
Structural BOS	0.12	0.125	0.13
Inverter	0.05	0.055	0.06
Module (w/ supply chain)	0.40	0.425	0.45
<b>Total CAPEX</b>	<b>1.63</b>	<b>1.74</b>	<b>1.84</b>

These provide an upper and lower bound for PV CAPEX which, along with the mean value of 1.74\$/W<sub>DC</sub>, creates an indication of system costs in three possible markets. This costing scheme is mirrored for all other system costs, both within solar PV (replacement and OPEX) as well as for other generation and storage components.

The selected model has material and output warranties that cover the full 25-year lifespan of the project, which would normally cover any replacement costs for the panels should they fail. However, due to the frequent potential for severe weather damage, which is not covered by the product’s warranty [83], a replacement cost and forecast was included in the design. Solar panels, especially those equipped with a ballasted racking system as is included in this design, have shown to be remarkably resilient even Cat5 hurricane conditions [51]. To consider a “worst-case-scenario”, it was assumed that 30% of the PV panels would be damaged and require replacement every 10 years. This was modeled in HOMER by setting the lifespan of the panels to 10 years and the replacement cost to 30% of the initial CAPEX. Only sales tax, installation labor/equipment, and module costs were included; all other CAPEX component costs were considered irrelevant and excluded from the replacement cost (Table 7).

Table 7: Replacement cost breakdown for PV system.

	MSP (USD \$/W <sub>DC</sub> )	Mean (USD \$/W <sub>DC</sub> )	MMP (USD \$/W <sub>DC</sub> )
Sales Tax	0.04	0.045	0.05
Installation Labor/Equipment	0.15	0.15	0.15
Module (w/ supply chain)	0.40	0.425	0.45
Total Replacement	0.59	0.62	0.65
<b>w/ 30% adjustment</b>	<b>0.177</b>	<b>0.186</b>	<b>0.195</b>

The annual operating and maintenance expenses (OPEX) are typically low for PV systems as they require little maintenance after installation aside from the occasional cleaning. As mentioned previously, the NREL

provides an Annual Technology Baseline (ATB) that projects, among other values, the OPEX for many renewable systems [84]. Costs were projected for the next 20 years from CAPEX values that are based on 2020 market data for each of three different scenarios:

- **Conservative:** assumes that levels of research and development (R&D) are lower and that technology advancement is minimal for the solar PV industry in the coming decades
- **Moderate:** assumes R&D and technology advancements are identical to current levels
- **Advanced:** assumes that there is an increase in R&D investments and technological advancements increase

Like the CAPEX cost used, the OPEX is also per  $W_{DC}$  produced by the PV system.

*Table 8: OPEX values (low, medium, and high) used for the solar PV design.*

	Conservative (% CAPEX)	Moderate (% CAPEX)	Advanced (% CAPEX)
% CAPEX	1.1412	1.2491	1.2618
¢/ $W_{DC}$ -yr	1.86	2.17	2.32

For the use in this study, the relationship between OPEX to CAPEX, represented as a percentage of total CAPEX for a system, was calculated for each of the 20 years. The values were then averaged together within each scenario to provide three multipliers that give a lower, median, and upper OPEX cost for the system (Table 8).

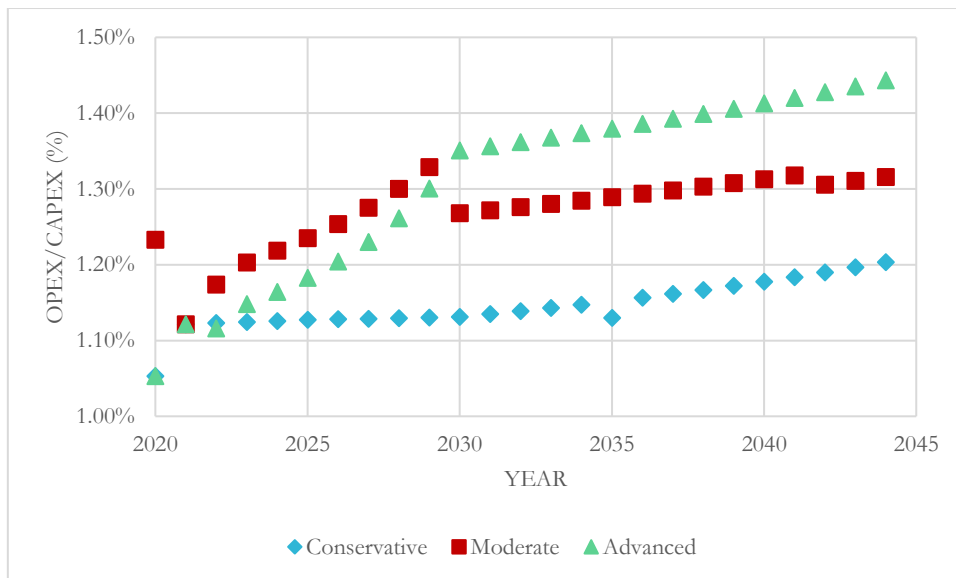


*Figure 12: Extrapolated values for expected OPEX costs expressed as percentages of the projected CAPEX for the same year [84].*

Figure 12 shows the small amount of deviation that occurs in the ratio of OPEX/CAPEX within each scenario. Standard deviations for each were relatively small: 0.03% for Conservative, 0.05% for Moderate, and 0.12% for Advanced, indicating that the ratios remain relatively constant as actual values shift over time.

The maximum system size for the PV panels was estimated from available space on the university campus. For this project, only a fraction of the total campus footprint was considered for the size of a PV system to prevent oversizing and requiring the entire area to be converted into a solar PV farm. The following areas were considered in the listed prioritization:

1. **Rooftops** – The primary space considered was the available rooftop areas of all campus buildings. This has the highest priority for first use due to not requiring further construction.
2. **Parking** – Should the system require further area for an appropriately sized PV network then the next space considered was large parking lots with the assumption that the PVs would provide a passive benefit of shaded parking spaces for employees, students, and visitors. This would require sufficiently stable support structures to raise the panels above regulation heights for covered parking areas.

The available rooftop area for each building was calculated using imagery from Google Earth in conjunction with Google’s Project Sunroof [71], [85]. Project Sunroof is a software developed by Google that provides users with insights into the available space for a PV system on a rooftop, the potential amount of energy

that can be produced by a PV system of the previously mentioned size at that location (taking into consideration shading and orientation), and an estimate of the economics of the proposed system. For the purposes of this study, only the information for the available space of a rooftop for a PV system was utilized from the software. The economic analysis is ignored. Google Earth’s functionality to measure areas has been used to estimate the available area of 10 large parking lots on campus. The total available rooftop space provides approximately 69,209 m<sup>2</sup> of area for a PV system. With the 10 parking lots, an estimated area of 74,274 m<sup>2</sup> is added to make a total of 143,483 m<sup>2</sup> of available space for the PV system.

The maximum capacity for PV modules in an area requires knowledge of the footprint of the selected model. The LA Solar Group LS550 BL has a footprint of 2.58 m<sup>2</sup> as seen from the dimensions in Table 5 [77]. On top of this panel area, the added space between adjacent panels and the space between rows of panels must be estimated as well. Using the Solega FastRack mounts, no space is added between adjacent panels, but 330 mm are added to accommodate spacing between rows and the space on the leading edge of the front row. This brings the new total area to 3.34 m<sup>2</sup> per panel, with a length and width of 2.279 m and 1.464 m, respectively.

The maximum solar capacity from rooftop space and parking lots on campus is calculated in this study by dividing the total areas from buildings and parking lots with the area of the panel, including the spacing. This calculation gives the maximum number of panels that can be installed. Multiplying this by the rated power of one panel provides the maximum rated solar capacity for the proposed area (Table 9). The total maximum rated capacity is the upper bound for the optimization of the solar system in HOMER.

*Table 9: The maximum capacity (kW) and the maximum number of panels that are estimated utilizing building rooftops and parking lots across the UPRM campus.*

	<b>Total Area (m<sup>2</sup>)</b>	<b># of Panels</b>	<b>Max Rated Capacity (kW)</b>
Buildings	69,209	20,743	11,409
Parking Lots	74,274	22,261	12,244
<b>Total</b>	<b>143,483</b>	<b>43,005</b>	<b>23,653</b>

This approximation is used to gain an estimate of the capacities available on campus without allocating new areas to a solar farm. A detailed study of each rooftop and the necessary infrastructure requirements for solar panels over the parking lots is needed for a fully accurate PV system for the entire campus.

### **Wind Turbines**

Simulation data for the wind profile specific to the location of the university campus was also downloaded from NASA’s Prediction of Worldwide Energy Resource (POWER). This database provides, in this case, a statistical monthly average for wind speeds at a height of 50 m above the ground based on measurements over a 30-year period between January 1984 and December 2013 [74]. Although frequently struck by tropical storms, the location of Mayagüez on the leeward side of the island opposite of the prevailing winds that bring the storms across the Atlantic shelters the city from strong winds most of the year. The average annual wind speed was only 3.59 m/s in 2017 and almost entirely from the northeast, with speeds between 3-5 m/s 54% of the year (Figure 13).

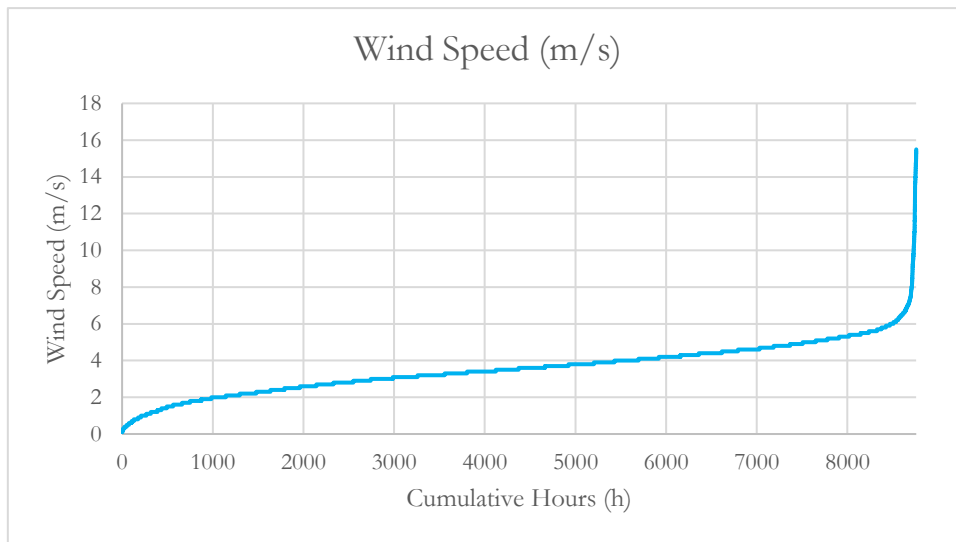


Figure 13: Cumulative wind speeds by hour for UPRM in 2017. Data provided by NASA's POWER database [74].

Most wind turbines have cut-in speeds of 3-5 m/s, indicating that the region will provide significant amounts of power from wind energy. However, in the effort to diversify the microgrid and add resilience to the overall design, the model included wind turbine models to determine their potential impact in the optimized design. Homer Pro allows for two separate model designs to be simulated simultaneously, for these purposes a generic wind turbine model and one designed specifically to survive the high wind speeds that are characteristic of tropical storms.

To start, the Generic 1.5 MW wind turbine component was selected from Homer Pro's built-in catalog. This design was chosen to include a standard onshore wind turbine model into the system. Many standard wind turbines do not fare well during extreme weather events: nacelles and blades can be damaged by high wind speeds, either from excessive torque or from debris. One study found that the probability of turbine damage rises from almost 0% certainty of damage to over 80% as wind speeds rise from 50 to 70 m/s (the difference between category 2 or 3 hurricanes and category 4 or 5) [52].

As a result, an additional turbine model has been considered to include a more durable turbine in the model. In this case, the RW600, an onshore turbine being designed by the Icelandic company IceWind, has been selected as it is rated to withstand speeds up to 75 m/s [86]. The RW500, which is the predecessor to the RW600 (Appendix D), has been proven to withstand category 4 wind speeds (60 m/s) [87].



Figure 14: The IceWind RW500 ground mounted (image courtesy of IceWind Inc.) [88]. The RW500 is the predecessor to the new RW600 that is used in this study.

The generic wind turbine, rated at 1.5 MW power output, is expected to have a very different performance than the much smaller RW600, rated at only 600 W. This assumption is largely due to the hub height of the generic turbine operating at 80 m above the ground, allowing it to capture much of the little wind that is available in the area. In contrast, the RW600 operates at only 2 m above the ground. Even when mounted

to the exterior of buildings on the campus, the amount of energy loss from the terrain and infrastructure will significantly reduce the amount of wind that the RW600 can harness.

The power curves for the two models can be found in Figure 15 and emphasizes a few major distinctions between the two turbines. The IceWind RW600 has a cut-in speed of 3 m/s, lower than the 4 m/s of the generic 1.5 MW turbine. Due to the relatively low average wind speed in the region, this allows the RW600 to capture 65.91% of the annual wind resource compared to the 34.97% of the generic model. In contrast, the generic turbine reaches max power production at 14 m/s, compared to the RW600 which does not achieve max power until 18 m/s. Both turbines have cutout speeds of 25 m/s and are assumed to have a lifespan of 25 years.

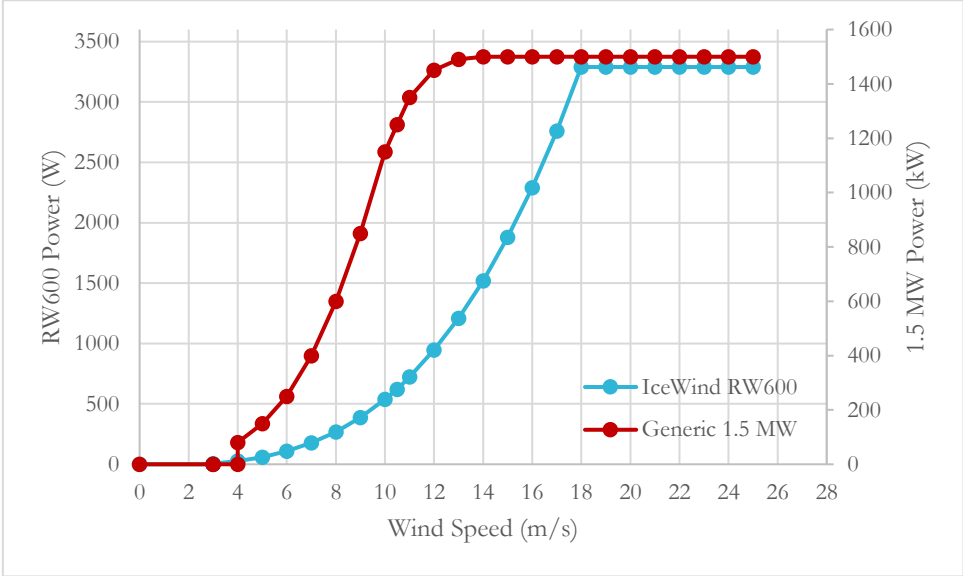


Figure 15: Power curves for the IceWind RW600 and the Homer Pro Generic 1.5 MW wind turbines.

Additional parameters for the generic wind turbine were pulled from the NREL’s 2021 Cost of Wind Energy Review, in which they analyze the costs of land-based, offshore, and distributed turbines of various sizes [89]. One of the distributed turbines studied was sized at 1.5 MW and, as such, many of the performance parameters were used to improve the accuracy of the model. Specifically, the losses associated to the turbine were included in the simulation: an availability loss of 5% and a generic loss of 6.9% were included to provide an overall loss of 11.550% for the generic turbine model. The RW600 does not currently have performance losses available. As such, it was assumed that the losses were identical to the generic 1.5 MW turbine model.

As mentioned previously, the cost of the generic wind turbine was estimated based on values provided in the NREL’s 2021 review. The results showed that the total CAPEX of the turbine consisted of the turbine components and the bill of sale (BOS) component costs. For 2021, these were found to be \$2,589 USD/kW and \$951 USD/kW, respectively, for a total CAPEX of \$3,540USD/kW or \$5,310,000 USD for a 1.5 MW turbine [89]. Cost data for the RW600 was provided directly by IceWind. The CAPEX of the RW600 is estimated to be \$10,500 USD for one unit: \$8,000 USD for the unit itself and an additional \$2,500 USD for electronics.

When considering replacing a damaged or malfunctioning turbine, only the cost of the turbine components was included, not the BOS component costs. Making the replacement cost \$2,589USD/kW or \$3,883,500 USD. The RW600 was analyzed in an identical manner, with only the cost of the unit itself being considered. Thus, the replacement cost is \$8,000 USD for one unit.

The OPEX of the generic turbine was set as \$35 USD/kW/yr, or \$52,500 USD/yr for the 1.5 MW unit. Table 10 below summarizes the costs of each model used in the simulation. No OPEX value was currently available for the RW600. As a result, the same ratio of OPEX/CAPEX found from the NREL report for

the generic turbine (approximately 1%) was used to determine an appropriate OPEX value for the IceWind model.

*Table 10: Standard pricing values used to simulate the generic 1.5 MW and the IceWind RW600 turbines.*

	Generic 1.5 MW	IceWind RW600
CAPEX (\$ USD/unit)	5,310,000	10,500
Replacement (\$ USD/unit)	3,883,500	8,000
OPEX (\$ USD/yr/unit)	52,500	104

Using the same Annual Technology Baseline from the NREL as was used for the cost structure of the PV system, forecasted values for CAPEX costs of a large-scale (>1 MW) distributed wind turbine were used to provide upper and lower bounds for the sensitivity analysis [90]. These projected values follow the same three scenarios outlined in Solar PV above: Conservative, Moderate, and Advanced (Figure 16).

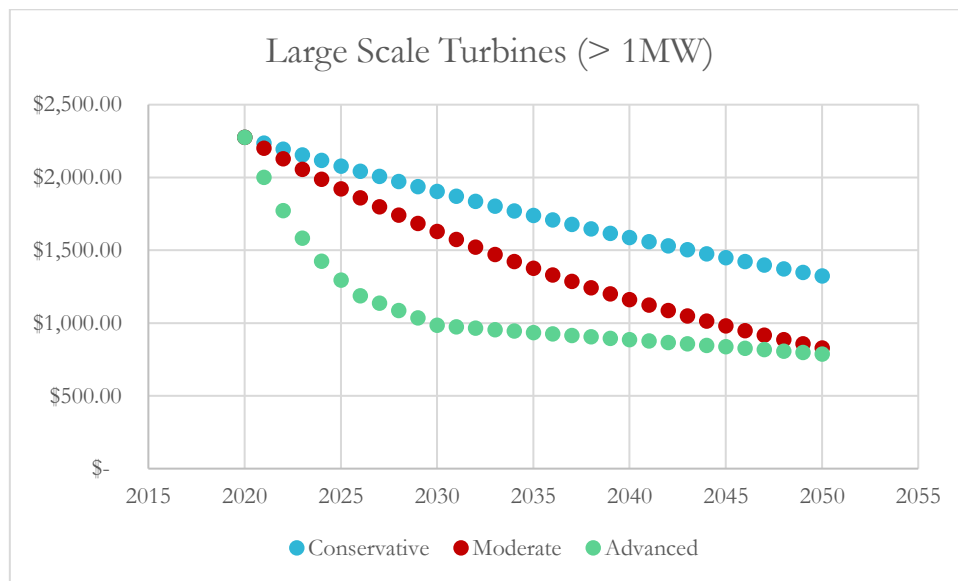


*Figure 16: Comparison for projected CAPEX costs of a large scale wind turbine for three different levels of market growth between 2020 and 2050 [90].*

For the purpose of acquiring upper and lower bounds for the cost sensitivity, a multiplier has been derived from these projections. For the upper bound that is used in the conservative scenario, the maximum ratio between the conservative and moderate projections provides the multiplier for the conservative scenario. Similarly, the minimum ratio between the advanced and moderate scenarios provides the multiplier for the advanced scenario. The standard pricing values in

Table 10 are used for the moderate scenario. All sensitivity prices are defined in Table 11.

*Table 11: Component costs for the two wind turbine models in each of the three market scenarios.*

	Generic 1.5 MW			IceWind RW600		
	Conservative	Moderate	Advanced	Conservative	Moderate	Advanced
<b>CAPEX</b> (\$ USD/unit)	8,496,000	5,310,000	3,186,000	16,800	10,500	16,800
<b>Replacement</b> (\$ USD/unit)	6,213,600	3,883,500	2,330,100	10,080	8,000	3,780
<b>OPEX</b> (\$ USD/yr/unit)	52,500	49,875	47,250	21.00	19.95	18.90



The addition of wind turbines creates a similar problem to the inclusion of solar PV panels when designing the system. In order to avoid oversizing the number of turbines, and therefore require more than can be feasibly installed onto the campus, upper bounds must be included. For the RW600, it is assumed that due to the small height of the turbines, the slightly smaller RW500 is only 2.2 m in height, 1.3 m in diameter, and 85 kg, placing them along the ground would not provide a significant amount of energy due to the high surface roughness of the urban area because of the surrounding buildings and dense vegetation. However, they can be easily installed to the roof edges of sides of the buildings. Here it was assumed that at most each building could support two individual RW600 units without significantly impacting the PV production (if they are placed on the roofs along with the PV panels) or structural integrity of the buildings (should they be installed on the sides of the building that are not wind- nor -leeward). At 63 individual buildings, this comes to a maximum of 126 RW600 units for the system.

With a height of 80 m and a rotor diameter of 77 m, a 1.5 MW turbine requires significantly more space than the 2.2 m tall RW600. Although most estimates for land requirements by wind turbines are based on studies of large scale wind farms (>20 MW installed capacity), some estimates for the land use and spacing were extrapolated from them [91]–[93]. The NREL performed an analysis in 2009 on 172 existing or proposed wind farms in the United States to understand the land-use requirements of such farms [91]. As part of the study, they defined both temporary (land utilized during construction and installation) and permanent (land permanently occupied by the turbines and utility structures) land use (Figure 17). For the purposes of this study, both the temporary land use (both roads and installation areas) and the permanent service road were excluded from the estimates for the turbine placement. The former due to it not being a permanent requirement and the latter based on the assumption that the roads already exist in some capacity throughout the campus. The resulting area requirement for a wind turbine includes the land used for the turbine pads and the clearings and was found to be  $3000 \pm 3000 \text{ m}^2/\text{MW}$  for the wind farms studied. An average value of  $3000 \text{ m}^2/\text{MW}$ , in the shape of a circle centered on the turbine tower, was used to estimate the land requirements from each turbine installed on the campus. For the 1.5 MW turbines, this requires a radius of 37.85 m around the tower to be cleared.

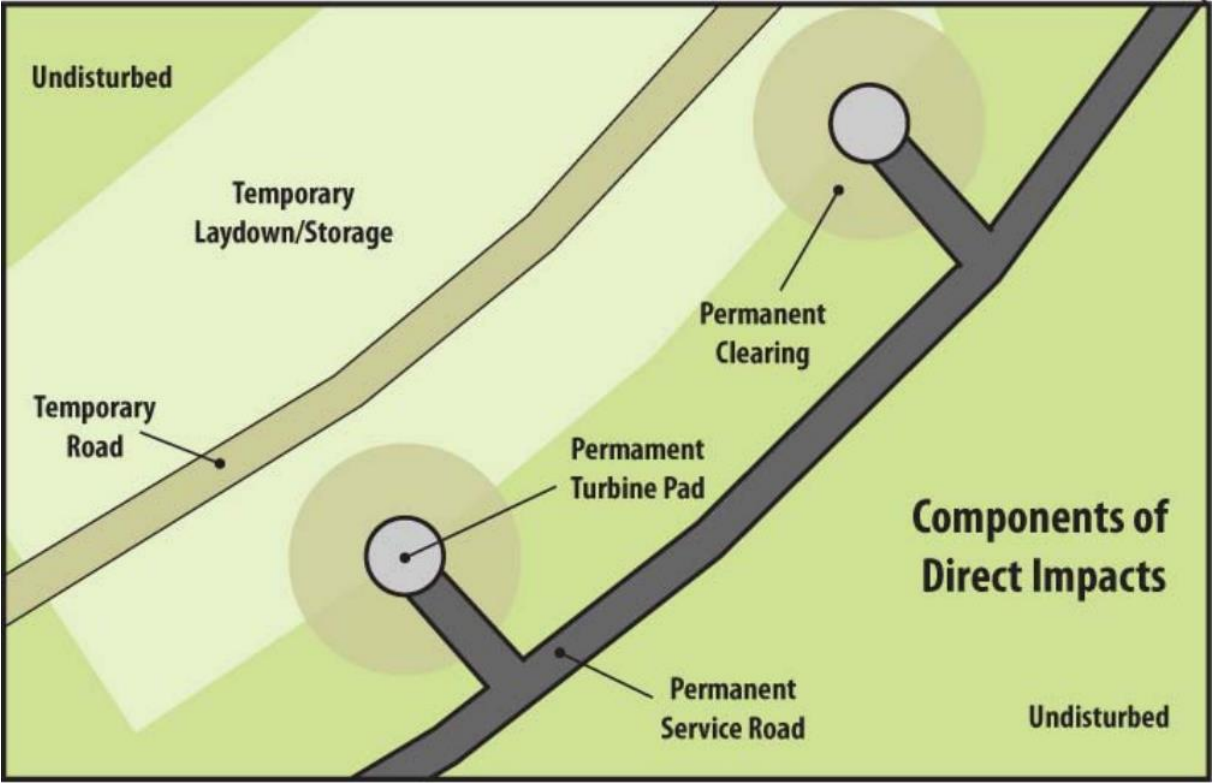


Figure 17: Labeled diagram of temporary and permanent land use requirements for a wind farm. Image courtesy of the NREL. [91].

Based on industry standards from the Danish Wind Industry Association, it was assumed that turbines should be no less than 4 times the rotor diameter apart in the direction perpendicular to the prevailing winds (coming from the northeast) and 7 times the rotor diameter apart in the direction of the prevailing winds [93].

Another consideration that limits the location and number of turbines is their noise emissions. Noise ordinance in the Commonwealth of Puerto Rico limit the permissible level of noise based on the



classification of the location in question [94]. The campus grounds themselves are classified as Zone I (Residential) along with the residential areas bordering the campus, while other areas bordering the campus are commercial centers which are considered Zone II (Commercial). Based on these classifications, the lowest threshold for noise levels is 50 dB for these zones. Considering most wind turbines produce up to 110 dB at the rotor, the closest building would need to be over 150 m from the center of the rotor [95]. For a turbine with a tower height of 80 m, this is equal to about 130 m from the base of the tower.

With this limitation in mind, only 2 suitable locations have been identified within the campus grounds (Figure 18). The first site is east of the CID of Puerto Rico at Mayagüez, where the solar boat shop and the Casa EcoSolar buildings are located. The second is located over 1 km away on the northern end of the campus between the offices on the edge of campus and the La Finca Alzamora agricultural grounds. Both would require landscaping and the removal of trees and other vegetation in a radius of 38 m around the base of the towers. Optimization of the system in Homer will determine if both sites, one, or none are needed. Should only one be needed, the second site near La Finca Alzamora is the preferred location as it is farthest from any zoned areas.



*Figure 18: Map of the UPRM campus. The two selected sites for the 1.5 MW turbines are labeled as red dots.*

## Biomass

Although the availability of biomass throughout the campus is limited, it was included in the study as it is a viable source of energy for the microgrid and could provide valuable diversification to the system design. Specifically, three sources of biomass were investigated to determine the production rates they could provide:

- **Yard Waste (YW):** from the maintenance of the green spaces and vegetation across campus
- **Food Waste (FW):** from the cafeterias
- **Municipal Solid Waste (MSW):** from waste disposal and collection

Data on the quantity and composition of the YW collected was provided by the UPRM Department of Buildings and Grounds (DBG). The DBG uses Ford F-450 trucks for their YW removal, filling up 3-4 truckloads of YW each day from lawn clippings, vegetation trimming, and fruit disposal from the numerous fruiting trees across campus (mainly mango trees). There are over 100 fully mature mango trees (>20 years old) across the campus which are capable of producing up to 600 kg of fruit in a year each [96]. Therefore, for the purposes of this study, it is assumed that 20% of the YW is mangoes. With a cargo volume of 2.192 m<sup>3</sup> [97] and an average density of 148 kg/m<sup>3</sup> for YW, provided by the U.S. EPA Volume-to-Weight Conversion Factors [98], this equates to an average of 908 kg/day of YW, excluding the mangoes and other fruits which are included in the FW.

Interviews with the cafeteria manager revealed that approximately 1000 meals are served each day on campus. An estimated 10% of each meal was assumed to be disposed of each day. An average weight of 1

lb per meal (0.454 kg/meal) was assumed to provide an estimate of 45.4 kg/day of FW from the cafeteria. Combined with the mangoes and other fruits from the YW, a total of 272 kg of FW is generated each day.

The DBG is also responsible for municipal solid waste collection and disposal on the campus. They collect and dispose of 15.29 m<sup>3</sup>/week of MSW, which is equal to 2.18 m<sup>3</sup>/day. According to the same Volume-to-Weight Conversion Factors, MSW has a density of 81.87 kg/m<sup>3</sup> [98]. With an assumed value of 34% organic fraction (OF) [99], this provides 61 kg of organic matter in the MSW generated each day.

In total, the biomass availability on campus from all three sources was estimated at 1,242 kg/day. This was used as the Scaled Annual average value for the biomass resource in HOMER. The gasification ratio and lower heating value (LHV) of biogas were kept at their preset values: 0.7 kg biogas/kg biomass and 5.5 MJ/kg biogas, respectively. The carbon content of the biomass was adjusted to match the weighted average (on a mass basis) of the carbon content of each source of biomass. Table 12 below provides the breakdown of the values.

*Table 12: Carbon contents and mass flow rates for each source of biomass studied on the UPRM campus.*

Source	Mass (kg/day)	Mass Fraction (wt %)	Carbon Content (wt %)	Source
YW	908	76.93 %	45.2 %	[100]
FW	272	23.07 %	45.7 %	[100]
MSW	61	5.17 %	70.4 %	[101]
<b>Total</b>	<b>1,242</b>	<b>100 %</b>	<b>48.6 %</b>	

The component used to simulate the biogas generator was the Generic 500 kW Biogas Genset model. The performance metrics for the component (Minimum Load Ratio, Fuel Curve Intercept, and Fuel Curve Slope) were not adjusted from their preset values.

Values for the costs of a biogas generator system were based on the 2021 report on Renewable Power Generation costs from the International Renewable Energy Agency (IRENA) [102]. All values were specific to the North American market and for a system size between 0-5 MW. CAPEX and replacement costs were assumed to be equal for the biogas generator at 3,331\$ USD/kW on average. For the sensitivity analysis, the upper and lower costs come from the 95<sup>th</sup> and 5<sup>th</sup> percentiles, \$5,997 USD/kW and \$592 USD/kW respectively, for the category selected (Table 13). The OPEX consists of two components: the fixed OPEX, which is assumed to be 6% of the CAPEX, and the variable OPEX, which has a cost of \$0.005 USD/kWh. Because HOMER requires the OPEX to be a function of the operating hours of the generator, the final OPEX requires iteration within the simulation. As a result, the initial OPEX will be set to the fixed OPEX cost of 6% of the CAPEX.

*Table 13: Cost values for the biogas generation system [103]. The OPEX value will be adjusted to an accurate value for the size of the system through iteration.*

		Conservative (95 <sup>th</sup> Percentile)	Moderate (50 <sup>th</sup> Percentile)	Advanced (5 <sup>th</sup> Percentile)
<b>CAPEX</b>	\$ USD/kW	5,997	3,331	592
	\$ USD/unit	2,998,500	1,665,500	296,000
<b>Replacement</b>	\$ USD/kW	5,997	3,331	592
	\$ USD/unit	2,998,500	1,665,500	296,000
<b>OPEX</b>	\$ USD/kW	6% CAPEX + 0.005 \$/kWh * (Energy Generated/yr)		

## Ocean Tidal & Wave

A resilient microgrid design ideally has a diverse portfolio of generation technology. The city of Mayagüez is located on the west coast of Puerto Rico in the Bay of Mayagüez. With the UPRM campus being situated one kilometer from the coastline, the potential application for tidal or wave energy generation is also investigated for the design.

The preliminary 2008 investigation surrounding renewable energy potential in Puerto Rico performed one of the first studies looking into tidal energy potential around the island. The results indicated that the topology of the ocean floor surrounding the island does not allow for the minimal tidal range (height

difference between high and low tides) required for a system to produce hydrostatically generated electricity [104].

The same 2008 study found that the island had a potential of over 17 TWh of wave energy [8]. In 2019, a study from the UPRM Center for Applied Ocean Science and Engineering (CAOSE) was published that further investigated wave energy potential around Puerto Rico. They analyzed the wave energy using high resolution data from 2013-2015 and concluded that the island has good potential, especially between November and March, for wave energy along the northern coast [105]. Unfortunately, as seen in Figure 19, the wave energy potential in the Bay of Mayagüez (marked by the red point on the map) is close to 0 kW/m due to the shielding effects of the surrounding coastline. A 2021 study performed by the NREL confirmed these values [106]. This eliminates wave energy as a possible resource for the UPRM microgrid design.

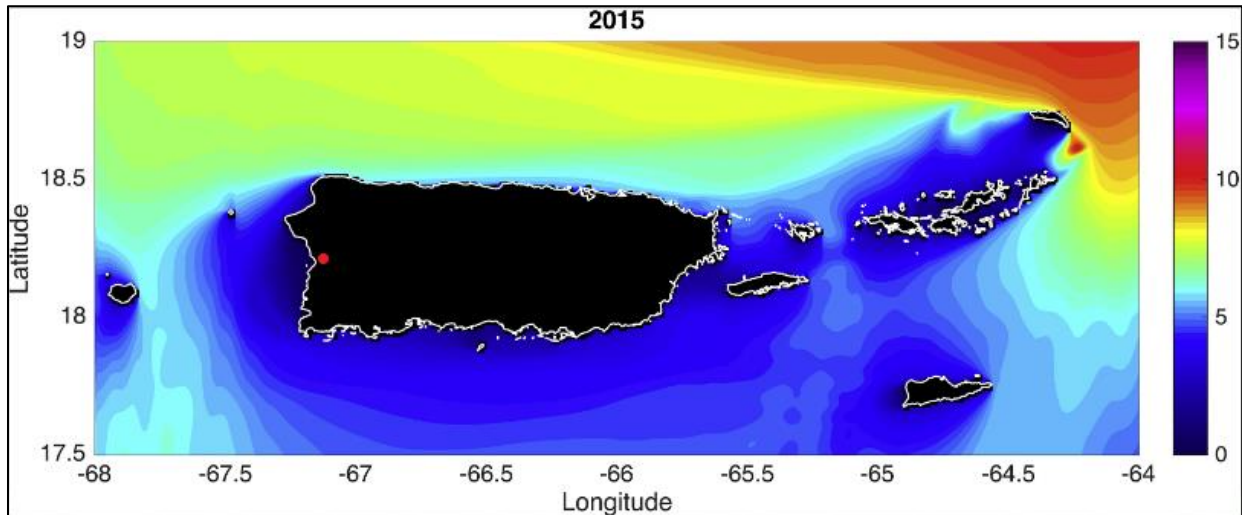


*Figure 19: Heat map of wave energy potential around Puerto Rico and the US Virgin Islands in 2015 [105], the color gradient is measured in kW/m. The approximate location of UPRM is given by a red dot.*

The 2008 report further investigated ocean energy for Puerto Rico, looking into both current energy and ocean thermal energy [104]. The available currents surrounding the coastline of the island are not fast enough (they average only 0.5 m/s) to produce sufficient energy to warrant installation of a generation system. Regarding ocean thermal, the southeast coast near Punta Tuna has one of the best conditions in the world for ocean thermal energy conversion, with a temperature gradient of over 22 between the ocean surface and 1 km of depth located only one mile off the shore. Unfortunately, the location of this site is too far from the UPRM campus to be of use for the microgrid preventing the inclusion of any source of ocean energy into the system design.

## Geothermal

Like nuclear energy, geothermal resources can provide a constant output of energy for a grid, providing a baseload, renewable substitute for carbon-intensive energy generation. Within the Caribbean, the islands of Dominica, St. Lucia, and Guadeloupe all exploit geothermal gradients along their coastlines to offset some of their fossil fuel demand [107].

Around Puerto Rico, a 1991 study investigated the heat flow from an unsuccessful hydrocarbon wellbore located west of San Juan in the region of Toa Baja. In this study, it was found that a heat gradient existed approximately 2 km beneath the surface, indicating geothermal energy potential [108]. The geothermal potential was further studied at the Organization of American States (OAS) for a master's thesis from Utrecht University. As part of the thesis, an analysis of the geological profile of Puerto Rico and the surrounding seabed was performed to provide insight into locations with high geothermal potential. The results indicate that more wells are required to fully understand the geothermal profile of the island [109].

As a result of this lack of reliable data, the inclusion of a geothermal electricity generation system was excluded from the UPRM microgrid design.

## Hydro

Puerto Rico has a broad range of annual rainfall across the island with averages ranging from over 430 cm in the tropical rainforest of El Yunque on the eastern side of the island to below 75 cm parts of the dry southern coast [110]. Around Mayagüez, the annual rainfall is typically between 125-200 cm (Figure 20).



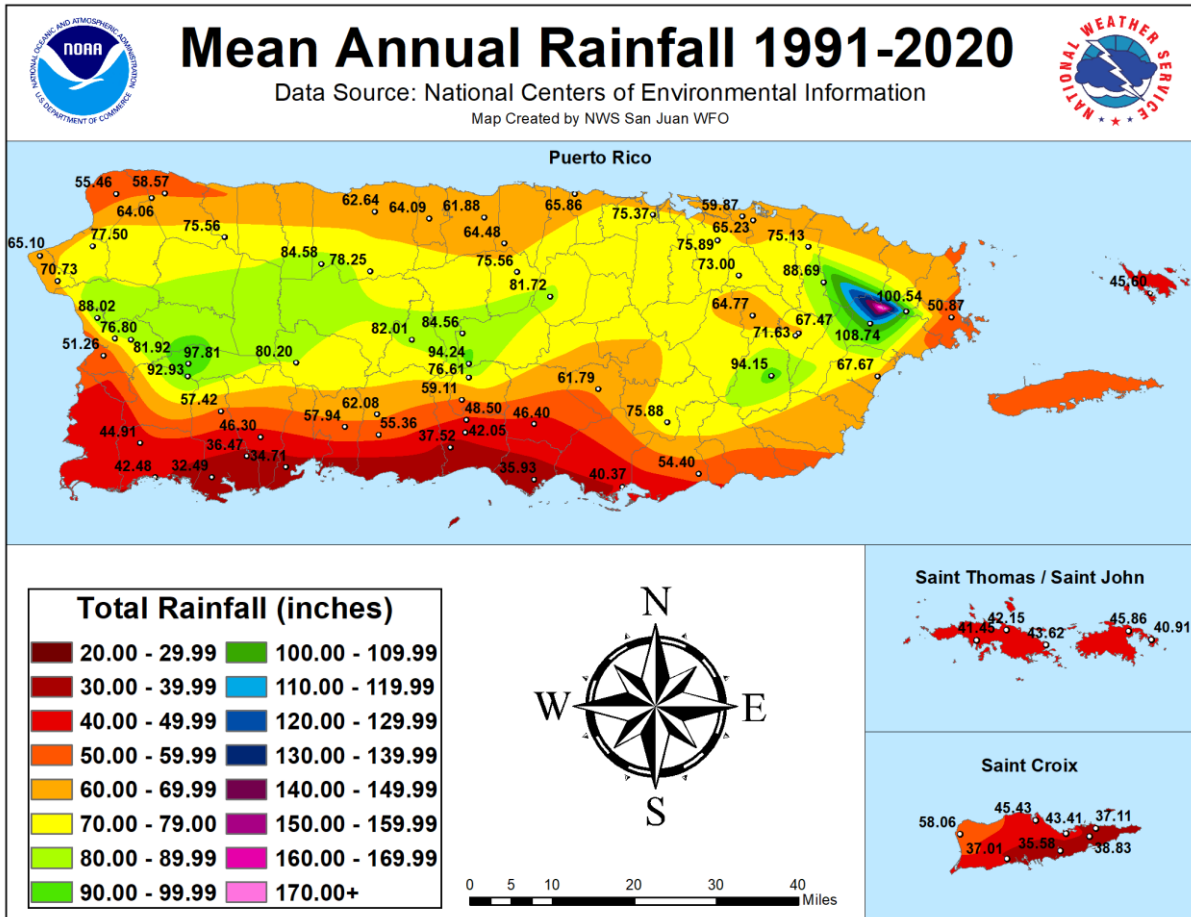


Figure 20: Heat map of the mean annual rainfall for Puerto Rico and the U.S. Virgin Islands. Image courtesy of the U.S. National Oceanic and Atmospheric Administration [110].

This rainfall leads to a significant amount of watershed across the island that brings with it the potential for hydro electrical generators. Estimates from the 2008 study of renewable resources in Puerto Rico indicate that the total watershed of the island could produce 3.08 MW of hydro-powered electricity. This is due to most of this watershed, approximately 67%, being directed to the coasts along the northern and southern watersheds of the island. However, only 0.1 MW is from the watershed region around Mayagüez [111]. All this energy is produced along the Rio Loco, Rio Rosario, and Rio Guanajibo rivers (Figure 21).

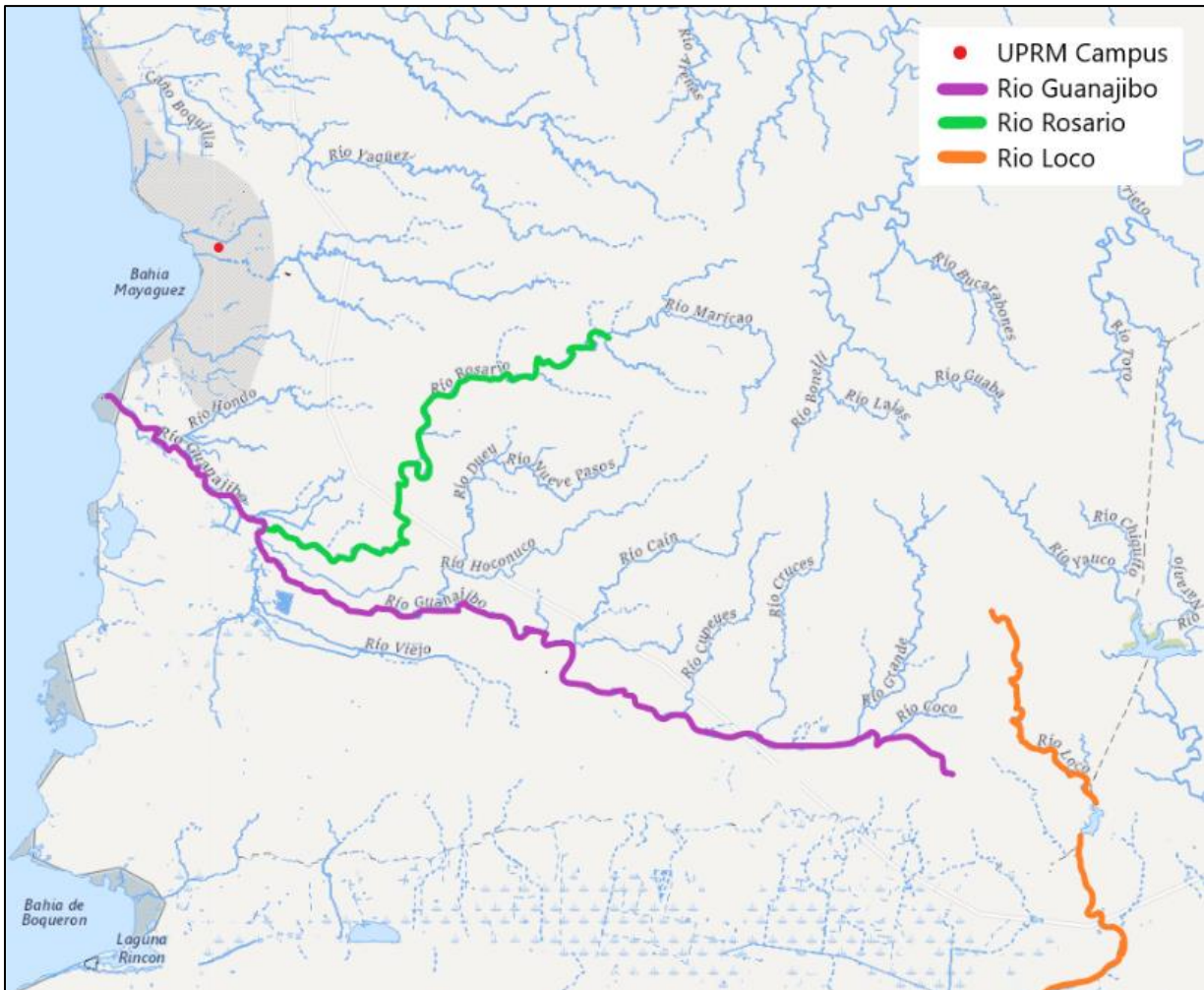


Figure 21: Watershed map of western Puerto Rico surrounding Mayagüez [112].

Based on the low estimated energy output and the large distances between the viable rivers and the campus, hydroelectric generation was ruled out for the system.

## Grid Connection

One of the largest financial benefits of a microgrid system is the reduction, or complete elimination, of expenses on energy consumption. Since the purpose of the model is to propose a renewable microgrid capable of completely meeting the campus demand, the savings for these 100% renewable systems was calculated post hoc to provide accurate economic valuation over the project's lifetime.

A grid connection was included to provide insight into how the microgrid could interact with the main grid during standard and Oasis operation. In these systems, electricity prices were set current rates of around \$0.30/kWh, based on the data provided by the university. Buy-back rates for excess energy provided to the grid set to the current rate on the island of \$0.10/kWh [113].

By setting the minimum renewable fraction to 100% in the simulation, the optimization algorithm was prevented from using the grid as a source of energy. This was a useful method of measuring the excess load available during operation. In BAU mode, this was expected to be near zero as the system was designed to store all energy exceeding the load. However, this became an important metric when simulating the system during Oasis operation. By maintaining the system size and decreasing the load to match the proposed amount of Load shedding (intentional blackouts of loads during Oasis mode, explained in more detail later in the report), the amount of energy sold to the grid was a direct indication of how much excess energy was available for crisis response efforts.

### 4.1.2.2 Energy Storage

Many of the renewable energy sources applied to the microgrid have high intermittency: solar irradiation is subject to daytime hours and dependent upon weather conditions, and wind can occur at any hour of the day but is highly inconsistent in most regions. As a result, the energy produced from these sources can be

higher or lower than the average measured value. To accommodate this limitation, an energy storage system is included to capture excess energy for use when conditions are not favorable enough to produce adequate amounts of energy or sufficient amounts of power to meet demand.

### Chemical Batteries

Currently, there are numerous different battery chemistries on the market, each with their own benefits and limitations. For instance, lead acid batteries are the oldest chemistries and, as a result, have the most mature market presence and, therefore, are one of the cheaper options available. However, they lack sufficient power and energy density (Figure 22) for large scale implementation and have traditionally been used in automobiles, even though they are almost 3 times heavier than a Li-ion of the same energy capacity. Within the purposes of this study, two chemistries were pinpointed for the battery energy storage system (BESS): Li-ion and redox flow batteries (RFB). The ideal chemistry was selected based on energy/power density, discharge time and power rating, cyclability, and scalability.

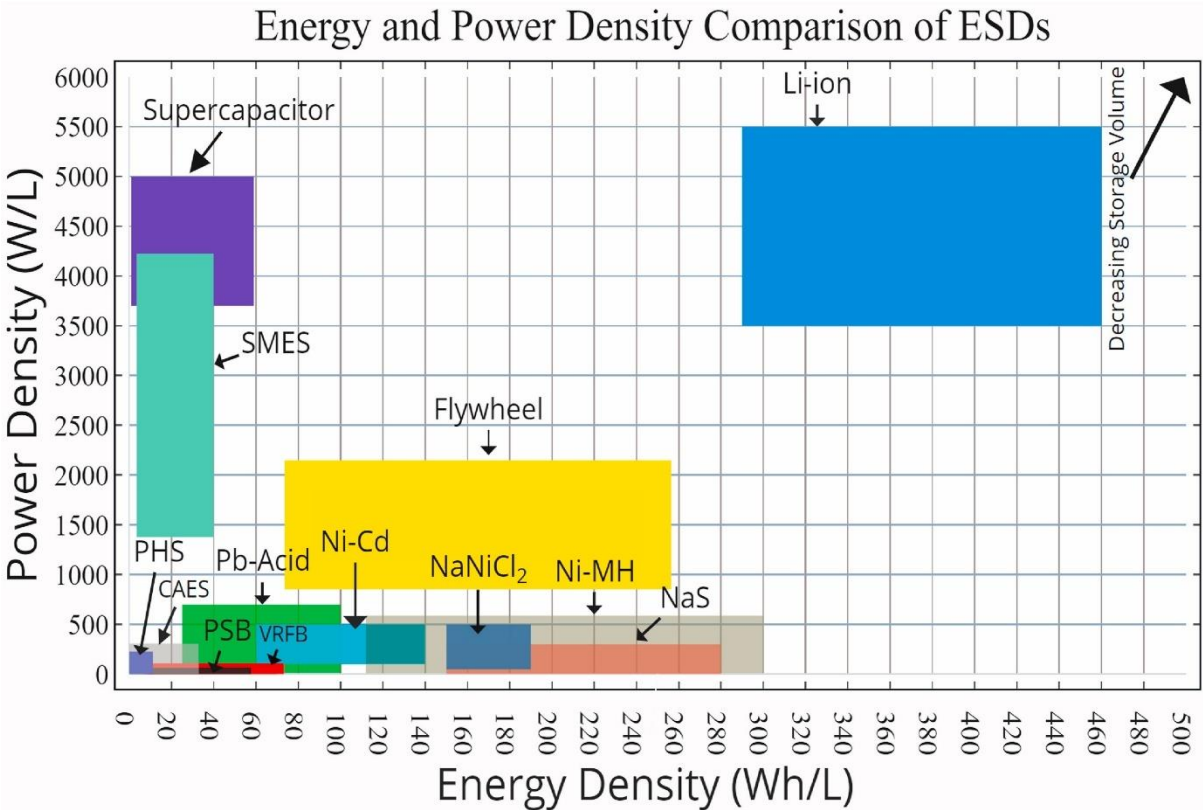


Figure 22: Ragone chart of difference energy storage devices [114].

Energy and power density of a chemistry directly corresponds to the required size of the system. The higher the densities the smaller the BESS for a given load. This has a double benefit of requiring less land use while also reducing costs by requiring less battery. As seen in the Ragone plot in Figure 22, the energy density and power density of Li-ion energy storage devices vastly outperforms all other storage systems and chemistries. In comparison, vanadium redox flow batteries (VRFB), which is the most common chemistry for RFB, have a very low energy and power density in general.

The discharge time at the power rating of a BESS impacts how it can be utilized within the energy system. BESS with faster discharge times (on the scale of seconds), the storage device can be used to improve power quality and voltage control within the system. For BESS with slower discharge times (hours or longer), they could provide energy management to the system. Due to the intermittency of solar and wind energy, which are expected to be the primary energy generators for the microgrid, and the anticipated reliance upon the island grid during the night, as solar PV systems will not be producing energy, a BESS with a high-power rating and long discharge time is preferable for this system. As shown in Figure 23, both Li-ion and VRFB have long discharge times at their rated powers, with VRFB being longer at higher power levels than Li-ions.



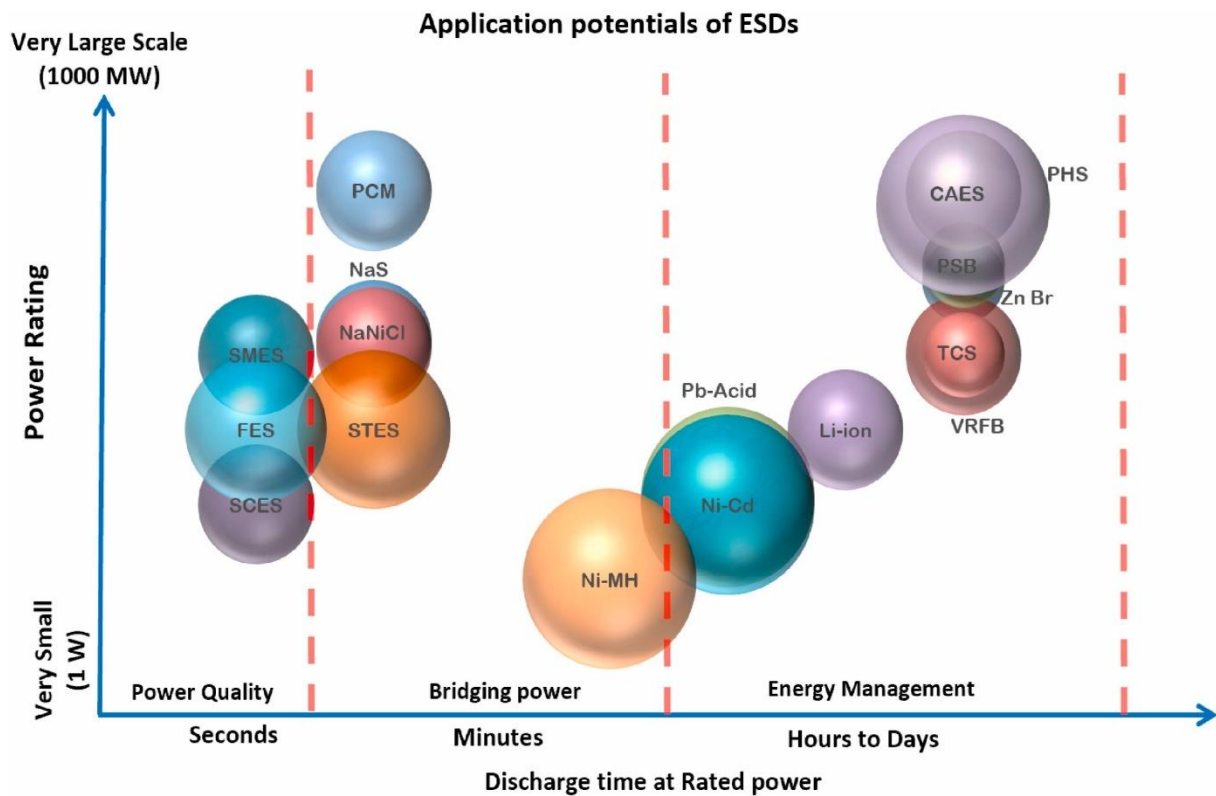


Figure 23: Comparison graph of discharge times and power rating for energy storage devices [114].

The cyclability of a BESS defines its ability to charge and discharge energy. It describes both the number of full cycles that the BESS can undergo without loss of performance (regarding energy stored and power provided), as well as the maximum depth of discharge (DoD) during each cycle. A higher maximum DoD means that more of the total available energy can be discharged during a cycle without effecting the cycle life [115]. Li-ion batteries typically have a maximum DoD of around 80-90% to avoid lithium dendrite formation that could short circuit the cell. With this maximum DoD, many Li-ion batteries have a lifespan of 3,000-6,000 cycles (assuming discharge at the rated current) [116]–[119]. In comparison, RFBs typically have maximum DoD of 100% and cyclabilities over 10,000 cycles [119], [120].

As mentioned before when discussing the energy and power density, Li-ion batteries have a high density making them smaller than redox flow batteries of the same capacity. However, a key advantage of redox flow batteries is the separation of power and energy within the system allowing each to be scaled independent of the other. This is due to the design of the system separating the cation/anion solutions (the volume of these tanks defines the energy capacity) from the stacks (the size of which defines the power capacity). In other battery chemistries, the relation of power and energy capacity is intrinsically linked because of the battery design.

A few additional comparatives exist between the two chemistry that were outside the primary criteria considered but still had an impact on the selection process. As a result of the system design of a RFB, they have almost no self-discharging over long periods of idle storage, require no thermal management (a good feature in terms of resilience and durability of the system should it be damaged), and have a good tolerance for overcharging and over-discharging. In contrast, Li-ion batteries have an estimated self-discharge of up to 5% total charge per month, require thermal management (lest thermal runaway occur and the battery be irreparably damaged in sometimes violent circumstances), and is sensitive over-charging/discharging as it negatively impacts the lifespan of the battery [120]. However, due to the maturity of the two technologies, the costs of Li-ion batteries are lower than RFBs per installed kWh and kW. Additionally, RFBs have a lower roundtrip efficiency (~70% vs. 90% for Li-ion) [121]. Although, the ability to independently scale the energy capacity of the RFB can mitigate both of these disadvantages. By reducing the LCOE (\$/kWh) and by increasing capacity to compensate for efficiency losses at a lower additional cost (since only tank size would need to increase, not the entire system).

Due to these criteria, the RFB chemistry has been selected for the microgrid system. The specific model was chosen from the available components within HOMER. In this case, the Gildemeister 250kW-8hr Cellcube FB250-2000, a VRFB with a rated capacity of 2,480 kWh, has the highest capacity of the RFBs modeled within the HOMER catalog. The full datasheet can be found in Appendix E. An added benefit of

the selected component is its high structural durability. The Cellcube FB 250-2000 is comprised of 4 shipping containers stacked as in Figure 24, the bottom 3 units used for energy demand and the top unit for power demand response [122]. The containers are rated to the ingress protection standards of IP54 and have a total weight of 245 tonnes. These make them reasonably secure against all but the largest debris during SWEs while also being too heavy to become debris themselves. These enclosures do not require a large footprint in comparison to the entire campus (12.2 m x 7.4 m) and therefore can be placed at a numerous points across campus without large scale planning to accommodate them [123].

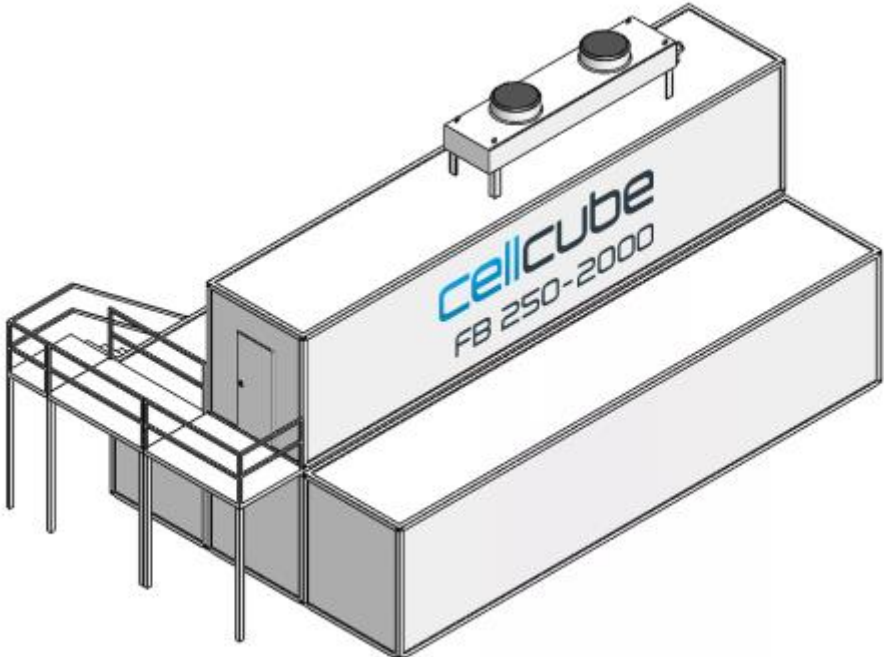


*Figure 24: Rendering showing the setup of the CellCube FB 250-2000 system [122].*

The design variables for the component were kept at the preset values: a 25-year lifespan, a string size of 1 cell with a voltage of 700 V, an initial state of charge of 100%, and a minimum state of charge of 0% due to the maximum DoD being 100% for this chemistry. The sizing of the battery was defined in increments of 3 (e.g. 0 strings of cells, 3 strings, 6 strings, etc.) for HOMER to optimize from. This is due to the assumed structure of the microgrid as it is modeled for the Oasis. The explanation of the design can be found in Section 4.2.1.

The costs of the system were pulled from the 2019 characterization report by HydroWires, a joint initiative focused on renewable energy technology that works closely with U.S. DOE national laboratories . The report provides project costs for BESS of different chemistries in 2018 as well as projected costs for 2025. An average of the two values for the total project costs (in \$ USD/kW) were used as the CAPEX and replacement costs of the BESS for the microgrid in the moderate scenario. The higher value, from 2018, provides the upper cost for the conservative scenario, and the lower value from 2025 for the advanced scenario during the sensitivity analysis. The OPEX costs were defined in the same way [119]. All values within the sensitivity cases are defined in

Table 14 below.

Table 14: Costs, both per kW and per unit, for the BESS in all three sensitivity scenarios used in the model [119].

		Conservative (2018)	Moderate (Average)	Advanced (2025)
CAPEX	\$ USD/kW	3,430	3,014	2,598
	\$ USD/unit	857,500	753,500	649,500
Replacement	\$ USD/kW	3,430	3,014	2,598
	\$ USD/unit	857,500	753,500	649,500
OPEX	\$ USD/kW/yr	10	9	8
	\$ USD/unit/yr	2,500	2,250	2,000

## Hydrogen Storage System

Even with the inclusion of a BESS, it is expected that the microgrid will have periods of excess generation that is either curtailed or sold back to the grid. Figure 25 shows the amount of excess generation by a simple microgrid in UPRM for a random 10-day period. The microgrid was simulated with a 1 MW solar PV system, one 1.5 MW wind turbine, and one 250 kW VRFB as outlined above. In this period of time alone, 77.6 MWh of excess energy is generated.

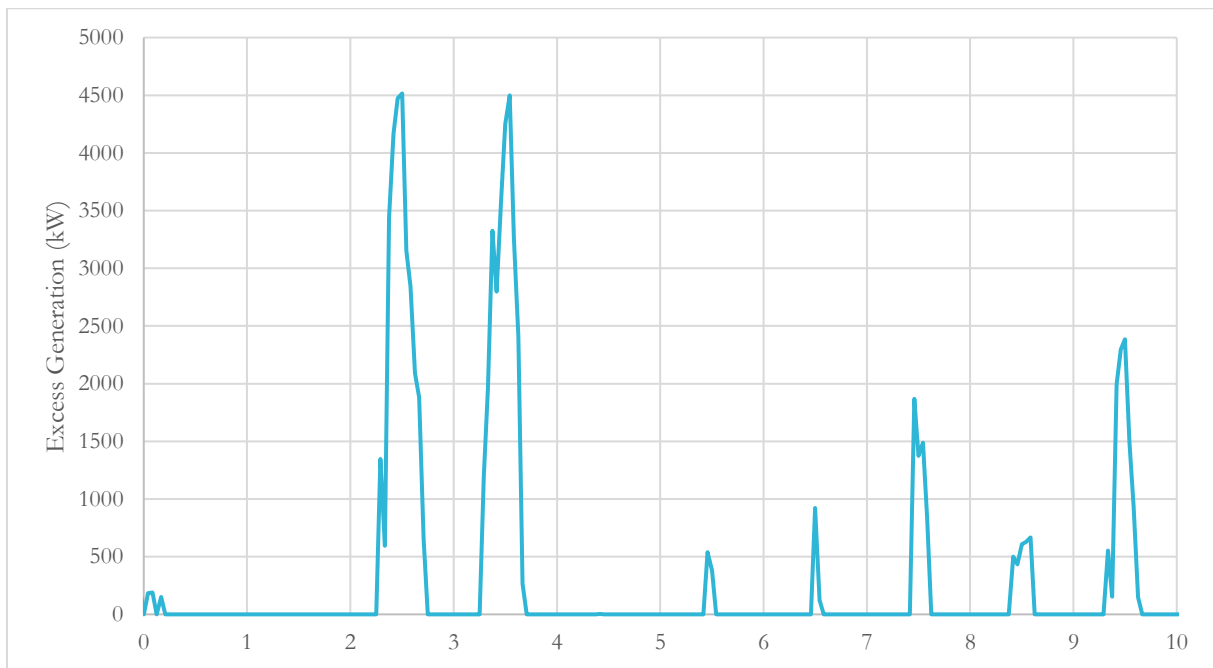


Figure 25: Excess electrical generation by a 1 MW solar PV system, 1.5 MW turbine, and one 250 kW VRFB on the campus for a random 10-day period throughout the year, as simulated by HOMER Pro.

With the inclusion of a sufficiently sized H<sub>2</sub> generation system, all of this excess could be converted into H<sub>2</sub> for long term storage. This much energy could produce 1,629 kg of H<sub>2</sub> from the electrolysis of water, given that H<sub>2</sub> has an energy density of 33.33 kWh/kg and assuming a 70% conversion efficiency.

Three main technologies currently exist for hydrogen generation via electrolysis: alkaline electrolysis (AE), proton exchange membranes (PEM), and solid oxide electrolytic cells (SOEC). Standard operating conditions for each of the three types of electrolyzers are shown in Table 15. Of the three, SOECs operate at the highest temperatures, over 700°C, and typically operates in tandem with a system that has high heat generation as a byproduct to reduce the energy consumption of operation (such as gas turbines). Although SOECs have the highest efficiency of the three types, due to the UPRM campus not having any existing infrastructure that produces excessive amounts of heat above these high temperatures, this technology is not considered for the UPRM microgrid system.

Table 15: Typical operating conditions of AE, PEM, and SOEC [124].

		AE	PEM	SOEC
<b>Operating Pressure</b>	bar	10-30	20-50	1-15
<b>Lower Partial Load Range</b>	%	20-40	0-10	-
<b>Power-to-Hydrogen Efficiency</b>	%	50-60	65-70	90-95
<b>Operating Temperature</b>	°C	60-90	50-80	700-1000

Between the remaining two technologies, AE and PEM, the PEM technology was chosen for the system design. This selection was based primarily on the higher efficiency and a lower partial load range (which allows it to continue producing hydrogen at lower energy consumptions) [124]. Although, it could just as easily be designed with an AE, as the differences are not significant.

For the system setup in HOMER, the electrolyzer component uses a Generic Electrolyzer model to control the performance and costs of the component. The selection of electrolysis chemistry as PEM impacts the performance inputs for the component. Specifically, the efficiency was set to 70% and the minimum load ratio was kept at 0% to provide the optimal performance.

A benefit of electrolysis technology is its reversibility. Typically, an electrolysis cell can operate in reverse as a fuel cell (FC) to consume the generated hydrogen and produce electricity and water. HOMER requires separate components for the electrolysis and fuel cells; therefore, the fuel cell was modeled with the Generic 250kW Fuel Cell component. The fuel curve for the FC was set to match the H<sub>2</sub> consumption of a PEMFC. The intercept coefficient, which describes the fuel consumption rate when the FC is idling, is set to 0 kg H<sub>2</sub>/hr/kW<sub>rated</sub>. The referenced PEMFC consumed 0.03 kg H<sub>2</sub>/hr for the 0.6 kW system; this provides a fuel curve slope, describing the consumption rate of fuel as a function of power output, of 0.5 kg H<sub>2</sub>/hr/kW<sub>output</sub> for the component [125]. All other performance values were kept at the preset values.

With the size of the generic FC fixed to 250 kW, the range of sizes for the electrolyzer was kept in a similar range to avoid oversizing or under sizing either side of the system. As such, the initial range of values was set to 5 even values between 0 and 1 MW: 0 kW, 250 kW, 500 kW, 750 kW, and 1,000 kW.

The costs for both the electrolyzer and the FC were considered the same, due to their reversibility, for the CAPEX of the systems. The replacement costs and OPEX are assumed to be unique to each component due to different operating requirements. The CAPEX was set to the average value of existing electrolyzer projects as defined by the IEA's 2022 Global Hydrogen Review. Conservative and advanced scenario costs were set to the upper and lower values, respectively of this range [126]. Replacement costs were set at 30% and 40% of the total CAPEX for the electrolyzer and FC, respectively. An electrolyzer OPEX of 2% CAPEX each year was used [64]. The FC OPEX was set to a flat rate of 0.01 \$ USD per operating hour, as opposed to a percentage of the CAPEX like the other values, due to HOMER's requirement of a generator OPEX being in terms of operating hours instead of per kW [127]. Table 16 provides the costs for the electrolyzer, Table 17 provides the costs for the fuel cell.

Table 16: Costs for the electrolyzer [64].

Electrolyzer		Conservative	Moderate	Advanced
<b>CAPEX</b>	\$ USD/kW	1,770	1,585	1,400
<b>Replacement</b>	\$ USD/kW	531	475.5	420
<b>OPEX</b>	\$ USD/kW/yr	35.4	31.7	28

Table 17: Costs ranges for the fuel cell [64], [127].

Fuel Cell		Conservative	Moderate	Advanced
<b>CAPEX</b>	\$ USD/kW	1,770	1,585	1,400
	\$ USD/unit	442,500	396,250	350,000
<b>Replacement</b>	\$ USD/kW	708	634	708
	\$ USD/unit	177,000	158,500	140,000
<b>OPEX</b>	\$ USD/op. hr.	0.01		

The inclusion of a H<sub>2</sub> tank is necessary to complete the loop of the hydrogen storage system. The tank itself must be sufficiently sized to store enough capacity for sustained use. For reference, the average daily demand by the campus of 74,962.36 kWh is equivalent to 2,250 kg of H<sub>2</sub>, assuming no losses in the conversion from and back to electricity. With this in mind, the optimal size of the tank was left to HOMER’s optimization abilities by defining the size to 100 kg increments between 0 and 1,000 kg to start. Further iteration was anticipated to narrow the optimum size of the system based on costs.

The tank CAPEX was a combination of the cost of the tank itself and the compressors needed to compress the gas to a sufficiently dense pressure (Figure 26). The cost of the tank is a function of the tank size, 100-130\$ USD/kg, while the compressor is a fixed cost for the system, 600-900\$ USD total. A pressure of 300 bar was targeted as it increases the density of H<sub>2</sub> to 24.6 kg/m<sup>3</sup> [64]. Replacement and OPEX were set to 85% and 1% of the total CAPEX, respectively. Sensitivity values for the conservative and advanced scenario costs were set to the upper and lower bounds of the 300-bar steel vessel system. The full table of costs for the hydrogen tank can be found in Appendix F.

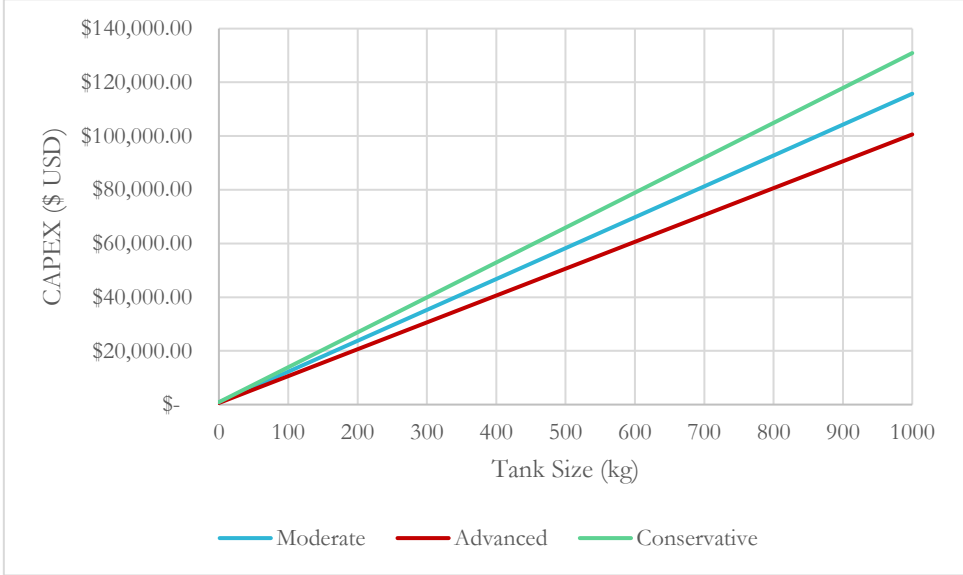


Figure 26: H<sub>2</sub> tank CAPEX as a function of tank size for three market scenarios [64].

## 4.2 Energy Oasis

This section provides methods for estimating the building loads based on priority level, the Oasis service energy intensities, and the scenario setups. The priority levels are also discussed in more detail, along with procedures to determine priority levels for other academic institutions. A majority of the calculations are based on HOMER Pro output files, which are renamed within the equations that use them.

### 4.2.1 Building Loads

Load shedding schemes require a significant degree of detail from the loads and the energy supply to achieve intended results. There are many methods to undertake these operations that provide building managers with various degrees of flexibility in operation [128]. Much like with the microgrid design, the first step is to get a detailed understanding of the energy loads connected to the energy source [129].

The average campus energy consumption of 27,361.26 MWh per year sets the baseline for the building demand calculations as it ties in directly to the designed capacity of the microgrid. The lack of energy metering on the UPRM campus necessitates the use of estimates taken from Garcia et al [41]. The study provides monthly loads for seven buildings across the campus. These loads are used to determine the annual energy consumption and specific consumption per unit area for each building. The buildings reviewed in Garcia et al. Are then assigned to a usage class based on their general function and installed equipment as this allows the remainder of the campus to be classified on a similar basis. Table 18 depicts the classified buildings and estimated loads. The complete dataset is available in Appendix H.

Table 18: Sample building loads and classifications. Courtesy of Dr. Yuly Garcia [41].

Building Name	Class #	Total [kWh/year]	Specific Consumption [kWh/m <sup>2</sup> ]	Class Description
MuSA	1	28,099.0	10.6	Storage
Coliseum	2	470,635.9	42.5	AC and Lighting
Business Admin.	3	1,145,048.2	57.9	Lectures
Civil Engineering	4	470,635.9	62.1	Engineering Lectures and Labs
Medical Services	5	204,949.0	117.9	Medical Services
Biology	6	4,349,512.7	133.4	Labs & Classes
Natatorium	7	923,510.9	141.3	Water Pumping, AC, and lighting

The specific consumption serves to calculate the energy consumption for each building based on its total area. Each building's area is determined by measuring individual rooftops in Google Earth and multiplying by the number of floors within the building. At this point, each building in the campus is assigned a usage class from Table 18. The estimated energy consumption is then given by using Equation 12 below. A complete table with all building load estimates can be found in Appendix I.

Equation 11: Total building area

$$A_{Building} = A_{Roof\ top} * n_{floors}$$

Equation 12: Total energy consumption per building

$$E_B \left[ \frac{kWh}{year} \right] = A_{Building} [m^2] * c_c \left[ \frac{kWh}{m^2} \right]$$

Where  $c_c$  is the specific consumption of that building type.

Using this method results in an overestimate of the total annual energy consumption ( $E_{Tot}$ ) of 34,364,256 kWh/year, representing a 25.59% error when compared to the average annual consumption of 27,361,260 kWh/year. This necessitates a correction factor ( $k_{f,i}$ ) to be applied in each building demand estimate ( $E_{B,i}$ ) to obtain the corrected building demand estimate ( $E_{B,i}^{cor}$ ). These adjustments are performed in Equation 13 through Equation 15 below.

Equation 13: Total campus energy demand estimate

$$E_{Tot} = \sum_{i=0}^{63} E_{B,i}$$

Equation 14: Building consumption correction factor

$$k_{f,i} = \frac{E_{B,i}}{E_{Tot}}$$

Equation 15: Corrected building loads

$$E_{B,i}^{cor} = k_i * E_{B,i}$$

The resulting loads are then organized into their respective "electrical cabinets", which function similarly to busbars. It is assumed for the purpose of this study that the campus installs three (3) Microgrid interconnection devices (MIDs) in each electrical cabinet to manage the loads [130]. These will handle the connections between the three zones on campus (West, North and Center, East) and from them to the Mayagüez electrical grid. The maximum load of each MID is given by Table 19.



Table 19: MID Energy Consumption and Building Count.

MID#	Building Count	Annual Average Energy [MWh/year]	Comment
1	15	9244.3	West Area
2	22	9223.7	North/Central Area
3	26	8893.2	East Area

A prioritization scheme is proposed for each building. This allows microgrid demand-side management to systematically remove building loads based on their relative importance. The most important buildings have operation-critical functions and are of particular concern to the stakeholder. These stakeholder-request loads are designated Priority 1 as they must be maintained at all costs via the microgrid. An interview with Dr Omar Molina Bas, the stakeholder representative for the UPRM, revealed which buildings are categorically Priority 1: Chemistry, Biology, Chemical Engineering, Building and Grounds Division, University Police Dept. Telecommunications Center, IT Department, and Main Library.

The remaining priority levels are defined at the discretion of the parties involved in the system’s design; within this study the allocations are as follows:

- **Priority 2:** these loads provide high value functions but are not requested directly by the stakeholder, therefore it is at the discretion of the investigator to assign their qualities.
- **Priority 3:** the loads that provide basic functioning capabilities for the stakeholder but can otherwise be performed without having access to the physical site.
- **Priority 4:** these loads have marginal benefits to the overall campus functions.

Table 20 lists the specific priority characteristics for the UPRM load functions and is used to assign each building with a priority level based on its function. A graphical representation of the breakdown of the quantity of energy in each priority level within each MID is shown in Figure 27.

Table 20 Academic Institution Prioritization Scheme.

Priority 1	Priority 2	Priority 3	Priority 4
Stakeholder request	Essential Functions	Lecture Halls with technology	Lecture Halls without technology
Critical Research	Housing	Research Admin Offices	Workshops
Communications	Non-Critical Research	Function Enhancing Services	Storage Warehouses
Security Services	Lighting	Living Assistance	Athletic Areas
Medical Services		Funding	Event Spaces
		Administrative	Auxiliary Services
		Psychological Services	
		Laboratories with equipment	
		Computer Labs	
		Ancillary Services	

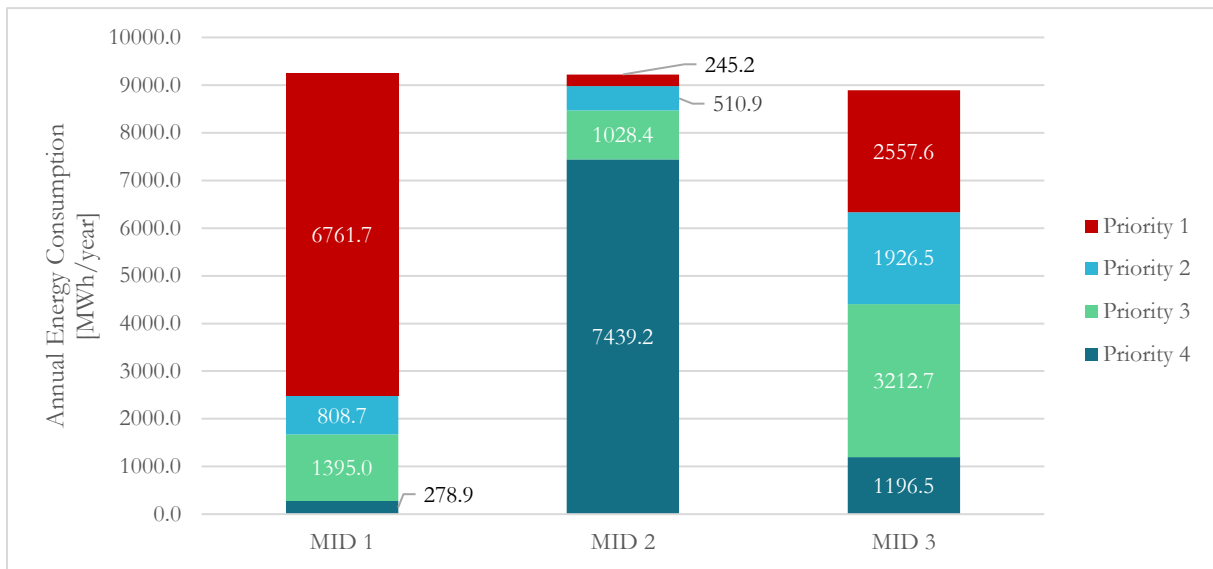


Figure 27: Electrical Energy Breakdown for Campus Buildings for each MID and Priority.

Using the estimated annual energy demand based on priority level as described above would yield an overestimate for the Oasis supply since the outage would be considered for 365 days. Therefore, it is necessary to calculate the energy demand for the duration of the hurricane season spanning from June to November. This can be done by manipulating the hourly primary AC load from the HOMER Pro simulation as a starting point to replicate the energy demand curves for each building. The adjustment of each building load from the previous assumption to the newly adjusted value is accomplished via a correlation factor, here called the energy consumption fraction. This fraction is the percentage of the total campus demand ( $E_{Tot}$ ) that is consumed for each hour of the year ( $E_t$ ). Equation 16 provides this relationship mathematically.

Equation 16: Fraction of energy consumption per hour per building

$$f_{AC,t} = \frac{E_t}{E_{Tot}}$$

Where,  $E_t$  is the building energy consumption in hour  $t$  (kWh),  $E_{Tot}$  is the total campus AC load in a year (kWh), and  $f_{AC,t}$  is the ratio of these two values (kWh). The  $f_{AC,t}$  is unique for each building and each hour of the year.

Once this matrix of fractions is calculated, the hourly energy consumption of each building ( $E_{B,t}$ ) can be found by multiplying the hourly fraction ( $f_{AC,t}$ ) with the total annual energy consumption of the building ( $E_{B,T}$ ) (Equation 17). The energy consumption fraction is then multiplied by the annual energy demand for each building as depicted in Appendix J. These generate the normal campus demand curves and require further manipulation to estimate the load-shedding scenarios, as discussed in 4.2.3.

Equation 17: Hourly energy consumption per building.

$$E_{B,t} = f_{AC,t} * E_{B,T}$$

#### 4.2.2 Oasis Services

The Oasis service loads are defined as the amount of energy required, on average, to meet the needs of one person for one day for the service in question. For example, the Oasis service load for water purification is the amount of energy required to filter and purify enough water to meet the daily needs of one person. These values are estimated primarily using assumptions from available literature and interviews and are summarized in

Table 21.

*Table 21: Estimated Oasis services and their corresponding daily energy consumption per capita.*

Recovery Activity	Specific Consumption per capita	Units
Medical	21.61649187	kWh/person day
Water	0.01	kWh/person day
Cafeteria	6.80	kWh/person day
Telecom	1.00E-05	kWh/person day
Debris	ND	kWh/person day
Personal	ND	kWh/person day

It is important to note that these exclude the service loads for debris management and personal usage, which are instead provided as total electricity for each when applicable. These categories capture a broader spectrum of tasks and devices than the other four and are assumed to be not as critical. Therefore, the analysis of their specific service loads is considered beyond the scope of this study.

### *Medical*

Bawaneh et al. describe the consumption for medical centers based on total area [131] with an average value of 738.5 kWh/m<sup>2</sup> per year. Whereas the average spacing requirements for hospitals in the USA range between 7.5m<sup>2</sup> and 13.9m<sup>2</sup> per person [132]. These values yield an estimated 21.616 kWh/person day as seen in Table 22.

*Table 22: Medical service load in the energy Oasis.*

Variable	Value	Units	Source
Energy Consumption per Area	738.5	kWh/m <sup>2</sup> year	[131]
Average Area per Patient	10.683845	m <sup>2</sup> /person	[132]
Average wait time	14.5	hrs/day	
Medical Consumption	21.61649187	kWh/person day	

### *Water*

Water filtration is calculated with a bottom-up approach using values for reverse osmosis seawater purification, which is 2.7 kWh/m<sup>3</sup>. The particular reverse osmosis system analyzed here, by Elemental Water Makers [133], is installed in a portable desalination unit that runs on solar panels. The activity level for water consumption per person is assumed to be active due to the recovery efforts and elevated stress levels of each individual person [134]. A step-by-step calculation of the specific service load for water purification is detailed in Table 23. The estimated energy value of interest is 0.01 kWh/day person as per Table 23.

*Table 23: Water service energy load and water demand per person.*

Variable	Value	Units	Source
Ambient Temperature	90	°F	Assumed
Activity Level	Active		Assumed
Daily Water Requirement @ 90 F	5	L/(day*person)	[134]
Recommended Intake	3.7	L/(day*person)	[135]
	0.0037	m <sup>3</sup> <sub>H2O</sub> /(day*person)	
Water Filtration Specific Consumption	2.7	kWh/m <sup>3</sup> <sub>H2O</sub>	[133]
Daily Energy Consumption per Capita	0.00999	kWh/(day*person)	
Max Water Production	1000	L/day	[133]

### Cafeteria

An interview with the UPRM cafeteria manager provides the average weekly propane consumption, estimated electrical appliance share, and approximate meals served per day. These values are used to estimate the energy consumption for an external cafeteria and daily energy consumption per capita. The estimated energy value of interest is 2.26 kWh/meal day from Table 24 which is multiplied by 3 to account for 3 meals each person eats in a day.

*Table 24: Cafeteria service load variables as provided by the UPRM cafeteria manager.*

Variable	Value	Units	Source
Meals Served	1000	per person per day	Interview
Electrical appliances	90%		Interview
Propane appliances	10%		Interview
Propane Weekly Use	360	Gal/week	Interview
Propane HHV	13.99	kWh/gal	[136]
Propane Density	1.885	kg/gal	[136]
Propane Energy Consumption	5036.4	kWh/week	
Total Energy Consumption	50364	kWh/week	
Electrical Energy Consumption	45327.6	kWh/week	
	6475.4	kWh/day	
Food Prep Share	35%		[137], [138]
Food Prep Electrical Consumption	2.3	kWh/meal day	
Average Electrical Consumption for Restaurant or Cafeteria	43.5	kWh/ft <sup>2</sup>	[139]
	468.22965	kWh/m <sup>2</sup>	

### Telecom

The telecommunications service makes use of a 5G network Cell-on-Wheels. The energy consumption for 5G vs 4G is slightly higher, however the newer network service has demand-side control strategies that can improve energy efficiency significantly. Moreover, the number of devices that are connected can be limited to those who have been allowed access to the Oasis network. The active runtime for the network is limited to 16 hours, starting one hour before the earliest class lecture time, and ending by the latest reasonable bedtime to conserve energy for other purposes. The variable of interest is 0.00001 kWh/device day per Table 25.

Table 25: Telecommunications service load and cell tower on wheels.

Variable	Value	Units	Source
Coverage Range	0.1	km <sup>2</sup>	[140]
Specific Consumption	1.4	kW/km <sup>2</sup>	[141]–[143]
Number of Cells on Wheels	1		[144]–[146]
5G device Density	1000000	devices/km <sup>2</sup>	
Connection Start time	6:00		Assumed
Connection End Time	22:00		Assumed
Total Hours Per Day	16		
Total Connection Hours per Oasis Period	2912		
Oasis Period	182		
Max # of Devices Served	2,240,000.00	devices/day	
Energy Consumption	22.4	kWh/day tower	
Max Devices Served per day		devices/day	
Specific Energy Consumption	0.000010	kWh/device day	

### 4.2.3 Scenario Simulation

Different scenarios are modeled in Excel that represent how certain changes affect the demand-supply relationships of the campus during a SWE. In this study the goal is to visualize the effects of the Oasis and load shedding functions on the energy demand for both campus and Disaster Relief services. A scenario representing Business-as-Usual (BAU) and the PR100 Study (PR100) are also included to represent scenarios where the UPRM microgrid is nonexistent. Table 26 provides an overview of the technical considerations for every scenario.

Table 26: Input considerations for each scenario; Y includes the variable whereas N excludes the variable.

Variable	Scenarios							
	BAU	PR100	P4	PR100 P4	P3	PR100 P3	P2	PR100 P2
30% Energy Efficiency Improvement	N	Y	N	Y	N	Y	N	Y
100% RE from Grid	N	Y	N	Y	N	Y	N	Y
Demand Side Management	N	N	Y	Y	Y	Y	Y	Y
Energy Storage	N	N	Y	Y	Y	Y	Y	Y
Solar	N	N	Y	Y	Y	Y	Y	Y
Wind	N	N	Y	Y	Y	Y	Y	Y
Biogas	N	N	Y	Y	Y	Y	Y	Y
Load-Shedding P4	N	N	Y	Y	Y	Y	Y	Y
Load-Shedding P3	N	N	N	N	Y	Y	Y	Y
Load-Shedding P2	N	N	N	N	N	N	Y	Y
Oasis Services	N	N	Y	Y	Y	Y	Y	Y

The Business-As-Usual total energy supply is reduced due to the seasonal disruption from Hurricane-related damage to the grid. For this study, it is assumed that disruptions last from the first hour of June to the final hour of November, represented by hours 3624 and 8015 respectively across the year. The same applies to the PR100 scenario with a key difference being the total campus demand decreases by 30% for the entire year.

The P4 Oasis supply during the hurricane season corresponds to energy demand of the P4 level buildings. Therefore, the energy supply to the Oasis is equal to the quantity of the hourly load shed by the campus buildings in the P4 scenario summed over entire the hurricane season. This is the same for the P3 Oasis

supply, to which the load shed demand from P4 and P3 buildings are summed. And congruently, the same applies to the P2 Oasis supply, in which the P4, P3, and P2 load shed demands are summed.

When accounting for the energy efficiency measures in the PR100 derivative scenarios, the overall consumption for each building is reduced by 30%. Therefore, it is necessary to include these energy savings in the Oasis energy supply calculation ( $E_{Campus,PR100}$ ). This is done by subtracting the seasonal load shedding for the desired priority level ( $E_{Campus,PR100}$ ) from the seasonal campus load before energy efficiency measures ( $E_{Campus}$ ), as shown in Equation 18. The  $E_{Oasis,PR100}$  value can then be added to any Oasis scenario as a standard increase to the Oasis energy volume.

*Equation 18: Oasis energy provided by PR100 energy efficiency measures.*

$$E_{Oasis,PR100} = E_{Campus} - E_{Campus,PR100}$$

The disruptions from the grid necessitate a re-estimation of the available energy going into the campus. This is due to the optimization method used by HOMER to improve the ROI, which curtails excess production from the microgrid through sales to the AEE grid. Therefore, the grid sales ( $E_{GS,t}$ ) and grid purchases ( $E_{GP,t}$ ) must be re-integrated into the microgrid generation mix. To do this in each hour within the blackout, as seen in Equation 19, the grid sales for the hurricane season ( $E_{GS,t}$ ) are added to the campus load served by the microgrid ( $E_{MG\ CL,t}$ ), which gives the total generation from the microgrid for the hurricane season ( $E_{MG}$ ). It is worth noting that these variables have been adapted from their HOMER nomenclature for convenience.

*Equation 19: Total Oasis energy for a defined period*

$$E_{MG} = \sum_{t=3624}^{8015} E_{MG\ CL,t} + E_{GS,t}$$

The total quantity of curtailed energy ( $E_{GP}$ ) in the outage period is the sum of the grid sales in that period of time ( $E_{GP,t}$ ), as seen in Equation 20.

*Equation 20: Total curtailed energy (or grid sales, if allowed)*

$$E_{GP} = \sum_{t=3624}^{8015} E_{GP,t}$$

At this point, it is possible to determine the campus differential demand ( $E_C^{Diff}$ ) by adding the seasonal campus load ( $E_C$ ) to the seasonal grid purchases ( $E_{GP}$ ) and then subtracting the seasonal microgrid generation ( $E_{MG}$ ), as seen in Equation 21. If  $E_C^{Diff} > 0$  then there is an unmet campus demand, and when  $E_C^{Diff} < 0$  then there is a surplus provided by the microgrid.

*Equation 21: Unmet or surplus energy of the campus during Oasis operation*

$$E_C^{Diff} = E_C + E_{GP} - E_{MG}$$

This value is then divided by the total seasonal duration ( $t_H$ ) to determine the daily average ( $\bar{E}_C^{Diff}$ ). The assumed duration of the season runs from the first hour of June 1st to the last hour of November 30th, corresponding to hours 3624 and 8015, respectively. Where  $E_C$  is in kWh, and  $t_H$  is in days (Equation 22).

*Equation 22: Daily average surplus or unmet demand for the campus.*

$$\bar{E}_C^{Diff} = \frac{E_C^{Diff}}{t_H}$$



## 5 Results & Discussion

In this section, the results of the models and simulations described above are discussed in more detail. A final recommendation for a microgrid design is provided and justified based on the criteria outlined in Section 3.1.3: Results Analysis. The impacts of the sensitivity variables are discussed, and the limitations of the study are reiterated and clarified. Within the Oasis analysis, the energy flow into the Oasis using the microgrid proposed in Section 5.1 are presented and discussed for all scenarios. The resulting KPIs are calculated and recommendations to further refine the proposed KPI equations are given. The same process is repeated for the overall Oasis Score for the system.

### 5.1 Microgrid Results Analysis

As outlined in Section 3.1.2, the optimal design was selected based on the three KPIs: LCOE, RF, and CAPEX. The highest priority KPI is the system LCOE. If there is more than one design with the same minimal LCOE, then they are further sorted to identify the highest RF. Should there still be more than one design after this point, then the system with the lowest NPC is the optimal design for the campus microgrid.

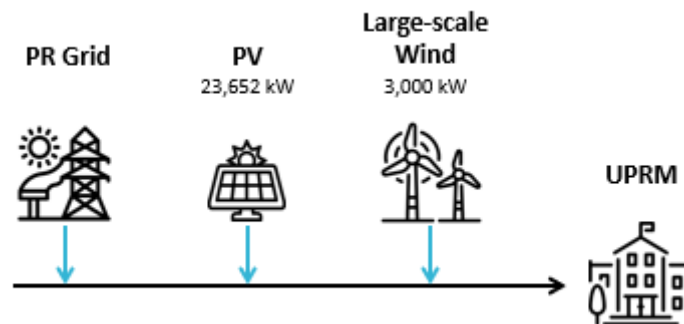


Figure 28: Microgrid design with minimized LCOE.

A full display of all input values can be found in Appendix G. From these results, the optimal microgrid design includes a 23,652-kW PV system and two 1.5-MW wind turbines as the electricity generators (Figure 28). There is no storage system included in the design, instead all periods with insufficient renewable generation are covered by the island grid. The generation capacity is able to achieve a RF of 88.3% even without a storage system. Figure 29 details the annual energy generation from each source, in kWh, over the course of the year.

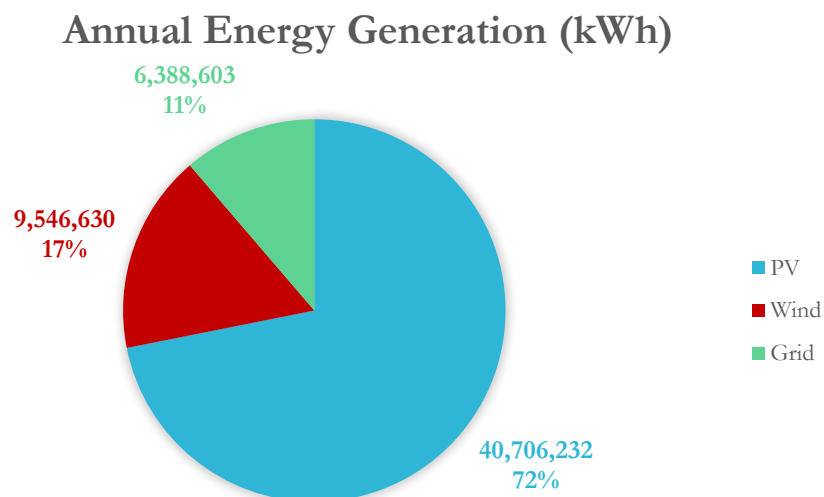


Figure 29: Total annual energy generation by source for the optimized microgrid design.

As mentioned before, the optimal design uses component costs from the mid-range moderate scenario. The economic assessment of the design results in an LCOE of 0.04637 \$/kWh and a NPV of \$32,737,030 over the 20-year project life. Table 27 below gives the breakdown of component costs for the CAPEX, replacement, and OPEX. As it is displayed here, values in parentheses are negative cash flows which is a

savings, not an expense. In this scenario, the grid OPEX is a savings due to the cost of the energy sold back to the grid exceeding the cost of the energy purchased from the grid.

Table 27: Economic assessment results of the optimal system design by component.

	CAPEX	Replacement	OPEX	Total
Wind	\$10,620,000.00	\$0.00	\$1,289,519.78	\$11,909,519.78
Grid	\$0.00	\$0.00	(\$26,962,001.79)	(\$26,962,001.79)
Solar PV	\$41,154,480.00	\$0.00	\$6,635,027.18	\$47,789,507.18
<b>System</b>	<b>\$51,774,480.00</b>	<b>\$0.00</b>	<b>(\$19,037,454.83)</b>	<b>\$32,737,025.17</b>

A base case (Figure 30) where no microgrid is installed and the campus load continues to be served by the PR grid for the same period of time is used for comparison. This baseline has an LCOE of 0.3000 \$/kWh and an NPV of \$106,113,948 for the 20-year lifetime.

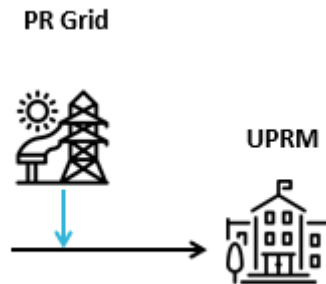


Figure 30: Baseline system for techno-economic comparison of microgrid designs.

Thus, the microgrid has a discounted payback period of 6.62 yr, a return on investment (ROI) of 14.7%, and an internal rate of return (IRR) of 18.4% compared to the base case.

The proposed design achieves the goal of minimizing the LCOE of the microgrid to 0.0464 \$/kWh, a reduction of over 83% from the current baseline LCOE of 0.30 \$/kWh. However, it lacks a storage system, which is a critical component for the effective utilization of the microgrid in the event of a total grid blackout. Therefore, the microgrid is re-simulated with either a hydrogen or VRFB storage system included, to determine the optimal storage system. The two new optimal systems are selected using the same criteria as before and compared to one another. In both simulations, the generation components are kept constant at the previously optimized capacities: 23,652-kW PV and 3-MW of large-scale wind. Additionally, the storage systems are designed to not be charged from the grid nor can their stored energy be sold back to the grid.

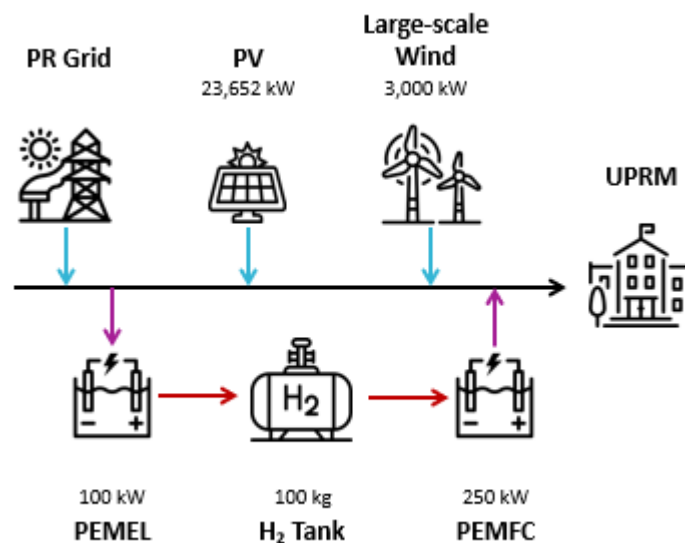


Figure 31: System design optimized for the Forced Hydrogen microgrid.

The new optimal design with a hydrogen storage (Forced Hydrogen) system consists of a 250-kW FC, a 100-kW EC, and a 100 kg H<sub>2</sub> tank at 300 bar (Figure 31). Interestingly, this microgrid has the same RF (88.3%) as the previous system (hereafter referred to as the Optimal LCOE). This is largely due to the small amount of energy that is stored in the system: under 0.5 MWh for a microgrid that generates over 50 MWh/yr of electricity. The EC produces 8,428 kg H<sub>2</sub>/yr and the FC generates 168,521 kWh/yr from this stored hydrogen.

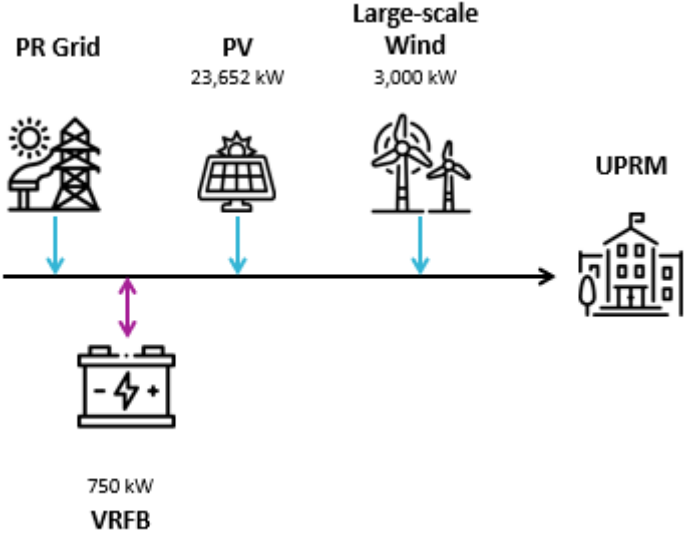


Figure 32: System design for the Forced VRFB microgrid.

The Forced VRFB microgrid is detailed in the line diagram above (Figure 32). The storage system contains three separate 250kW-8hr VRFBs and achieves an annual throughput of 1,993,363 kWh. The microgrid has the highest LCOE, (0.05326 \$/kWh) of the three designs, but also reaches the highest RF, at 90.8%, of the three. The VRFB storage system outperforms the hydrogen not only in annual throughput, but also in roundtrip efficiency with a value almost twice as high.

Table 28 below further compares the three systems. The results strongly suggest that the benefits of the VRFB outweigh the additional costs. While the LCOE increases by 15% from the optimal LCOE scenario, it is still an 82% reduction from the baseline system. Additionally, the CAPEX increases by only 4.4% compared to the 10% increase in NPV over the 25-yr project lifespan. All this while grid purchases are reduced by 25%, compared to a reduction of 0.7% with the Forced Hydrogen storage system. Having this large of a reduction on the PR grid dependence greatly improves the microgrids ability to meet the campus load during PR grid outages and to provide a larger energy reserve during Oasis operation. With these benefits and drawbacks in mind, the recommended microgrid system includes a VRFB storage system.

Table 28: KPI comparison between microgrid designs with the optimal LCOE, forced hydrogen, and forced VRFB.

		Optimal LCOE	Forced Hydrogen	Forced VRFB
<b>LCOE</b>	\$/kWh	0.04637	0.04801	0.05326
<b>RF</b>	%	88.3	88.3	90.8
<b>CAPEX</b>	\$	51,774,480	52,341,480	54,034,980
<b>NPV</b>	\$	32,737,030	33,861,630	36,011,150
<b>Grid Purchases</b>	kWh/yr	6,388,603	6,343,887	4,804,224
<b>Energy In</b>	kWh/yr	-	474,900	2,382,525
<b>Energy Out</b>	kWh/yr	-	168,521	1,667,767
<b>Roundtrip Efficiency</b>	%	-	35.5%	70.0%

To better understand the relationship that RF has on the economic KPIs, LCOE and CAPEX, the capacity of the microgrid is adjusted. In this analysis, three system designs are considered:

- **PV:** only contains PV generation in addition to a grid connection

- **PV+W:** Contains PV and two 1.5-MW wind turbines in addition to the grid connection
- **PV+W+Batt:** Contains PV and two 1.5-MW turbines plus three 250kW-8hr VRFB batteries for energy storage

The only capacity that is adjusted is that of the PV system, the quantity of the turbines and VRFBs are kept constant to simplify the study. Figure 33 clearly shows that while LCOE is linearly correlated to RF, the CAPEX of the system has exponential growth as the RF approaches 100%. This is an anticipated result due to the limitation of only adjusting the PV capacity and not also increasing battery capacity as well. A complete understanding of the most affordable design to achieve 100% RF for the UPRM campus requires an indepth study focusing specifically on that goal.

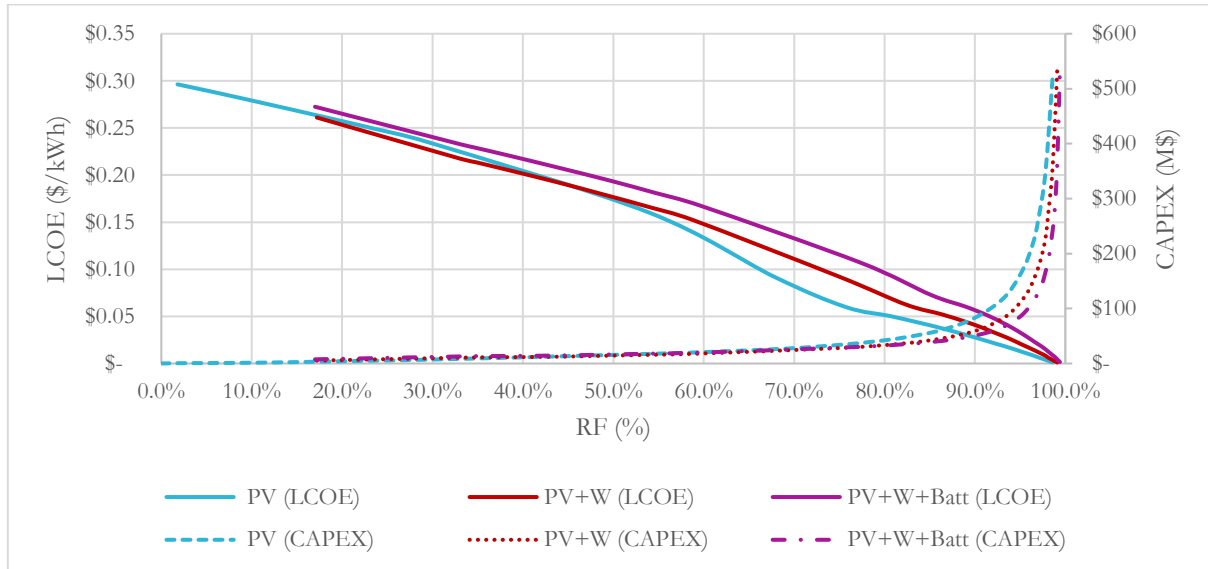


Figure 33: LCOE and CAPEX of the microgrid as a function of the renewable fraction for three different configurations

### 5.1.1 Sensitivity Analysis

#### Component Costs

The sensitivity of the optimal system to component cost variations is studied to understand how the costs impact a microgrid with the selected capacities (from the Forced Battery battery). In addition, a new optimal system design is identified based on the KPIs for the advanced and conservative scenarios. This is done to understand if changes to the market impact what the optimal microgrid design looks like. The component costs for each market scenario are outlined in Table 29.

Table 29: Values for sensitivity analysis on component costs within the system.

		Conservative	Moderate	Advanced
<b>Solar PV</b>				
<b>CAPEX</b>	\$ USD/kW	1,840	1,740	1,630
<b>Replacement</b>	\$ USD/kW	195	186	177
<b>OPEX</b>	\$ USD/kW/yr	23.20	21.70	18.60
<b>Generic 1.5-MW Wind Turbine</b>				
<b>CAPEX</b>	\$ USD/unit	8,496,000	5,310,000	3,186,000
<b>Replacement</b>	\$ USD/unit	6,213,600	3,883,500	2,330,100
<b>OPEX</b>	\$ USD/yr	52,500	49,875	47,250
<b>IceWind RW600</b>				
<b>CAPEX</b>	\$ USD/unit	16,800	10,500	6,300
<b>Replacement</b>	\$ USD/unit	10,080	8,000	3,780
<b>OPEX</b>	\$ USD/yr	21.00	19.95	18.90
<b>Generic 500-kW Biogas Genset</b>				
<b>CAPEX</b>	\$ USD/unit	2,998,500	1,665,500	296,000
<b>Replacement</b>	\$ USD/unit	2,998,500	1,665,500	296,000
<b>OPEX</b>	\$ USD/op. hr	0.85	0.48	0.09
<b>Gildemeister 250kW-8hr Cellcube FB 250-2000</b>				
<b>CAPEX</b>	\$ USD/unit	857,500	753,500	649,500
<b>Replacement</b>	\$ USD/unit	857,500	753,500	649,500
<b>OPEX</b>	\$ USD/yr	2,500	2,250	2,000
<b>Generic Electrolyzer</b>				
<b>CAPEX</b>	\$ USD/kW	1,770	1,585	1,400
<b>Replacement</b>	\$ USD/kW	531.00	475.50	420.00
<b>OPEX</b>	\$ USD/kW/yr	35.40	31.70	28.00
<b>Generic 250-kW Fuel Cell</b>				
<b>CAPEX</b>	\$ USD/kW	442,500	396,250	350,000
<b>Replacement</b>	\$ USD/kW	177,000	158,500	140,000
<b>OPEX</b>	\$ USD/op. hr	0.01		
<b>H<sub>2</sub> Tank</b>				
<b>CAPEX</b>	\$ USD/kg	<i>See Appendix F</i>		
<b>Replacement</b>	\$ USD/kg			
<b>OPEX</b>	\$ USD/kg/yr			

As was expected, adjusting the costs for each component in the same direction at once had a proportional impact on the final economics of the systems. In the advanced case, the optimal system designs in each case (lowest LCOE, forced hydrogen storage, and forced battery storage) are identical in configuration to those from the moderate case (Figure 28, Figure 31, and Figure 32), which is used as the baseline for the results.

In contrast, the conservative case results in a different generation system configuration compared to the others. With the increased costs, the optimal generation is made up of the same sized PV system (23,652-

kW) but instead of two 1.5-MW turbines, no wind generation system is included (Figure 34). This emphasizes the small impact that a wind-based generation system has on the entire system. When affordable, the large-scale turbines can provide 19% of the total renewable generation (17% of total generation when the energy from the AEE grid is included). Between the moderate and conservative costs, a tipping point occurs where the costs of the large-scale turbines outweigh the benefits gained by the energy generation.

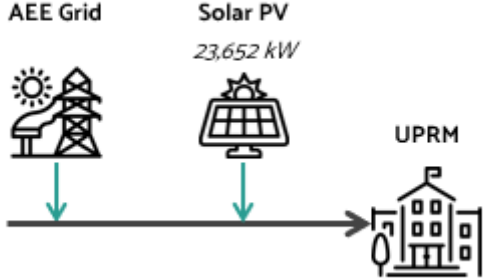


Figure 34: Energy generation system for the microgrid in a conservative market.

The forced storage systems utilized this same generation system for the conservative market with the same sized storage systems as in the advanced and moderate markets.

To provide a comparison between all three market cases, a conservative market with the same system configuration as the advanced and moderate markets is used. Figure 35 compares the discounted payback period for all system designs in each market (with both conservative systems). In addition, two extra systems are included: the optimized system that provides the highest RF and the optimized system that includes all component types (solar, wind, biomass, H<sub>2</sub> storage, VRFB, and AEE grid). Using the same system configurations, the increase in payback time has the expected increase from advanced to conservative markets. In the unrestrained conservative system, the system designs for the highest RF and full diversification include one 0.6-kW RW600 turbine instead of two 1.5-MW turbines. The significant difference in costs between these two components explains the large drop in discounted payback compared to the conservative market with the forced designs of the cheaper markets.

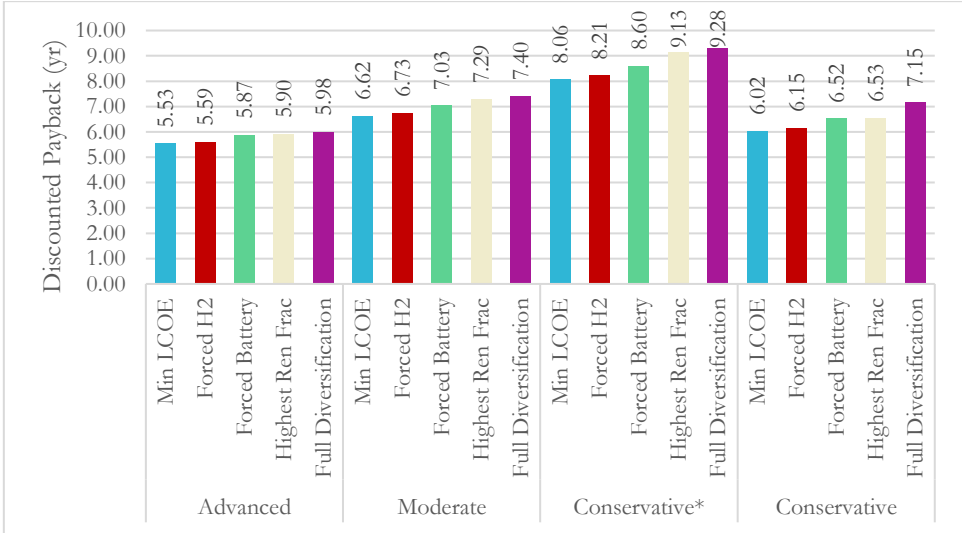


Figure 35: Discounted payback time for different design configurations from the three cost scenarios: advanced, moderate, conservative. The conservative systems marked by \* indicate the system design is forced to match the design for the advanced and moderate markets.

A full table of the system configurations and economic results for the scenarios is provided in Appendix L.

*Grid Price*

Returning to the chosen system design, the Forced Battery scenario, within the moderate market, a sensitivity analysis is performed to understand the impact of grid price on the system. As mentioned previously, grid prices have nearly doubled from 0.17 \$/kWh in July 2020 to 0.30 \$/kWh in September 2022. Based on this historical growth, and Puerto Rico’s dependence on imported oil for most of their energy generation, grid prices are expected to rise almost 0.07 \$/kWh each year (Figure 36). Therefore, the



Forced Battery system for a moderate market is re-simulated using grid prices ranging from 0.15 to 1.80 \$/kWh.

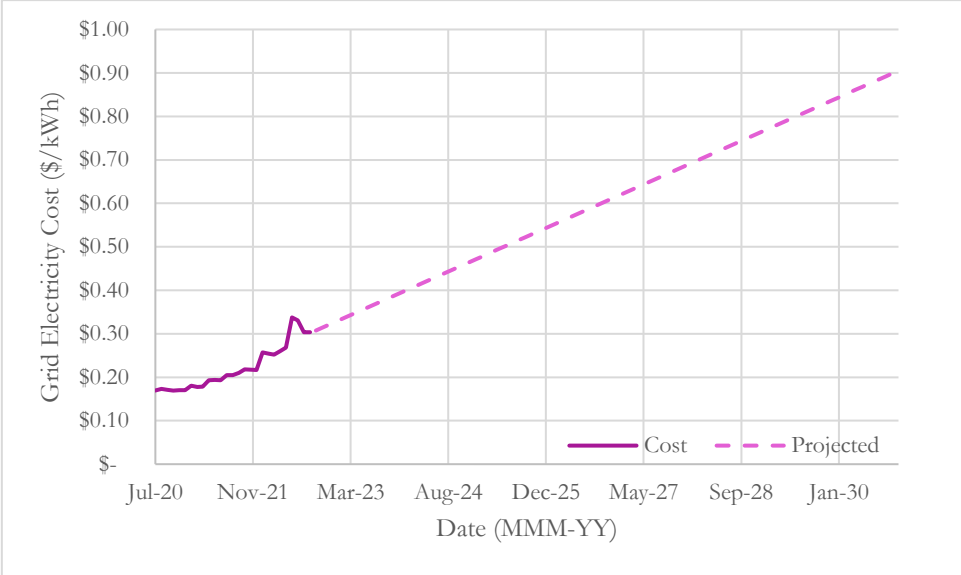


Figure 36: Projected growth in the cost of electricity (per kWh) from the PR grid based on current data trends.

Because no changes to the components are made for this sensitivity analysis, there is no change in RF, CAPEX, or OPEX. Only small changes in NPV and LCOE occur in a linear relationship to the grid price because of the price change for the constant quantity of energy purchased from the grid. Similarly, when compared to the existing baseline system of no microgrid with an AEE grid connection, the ROI and IRR increase linearly with grid price (Figure 37).

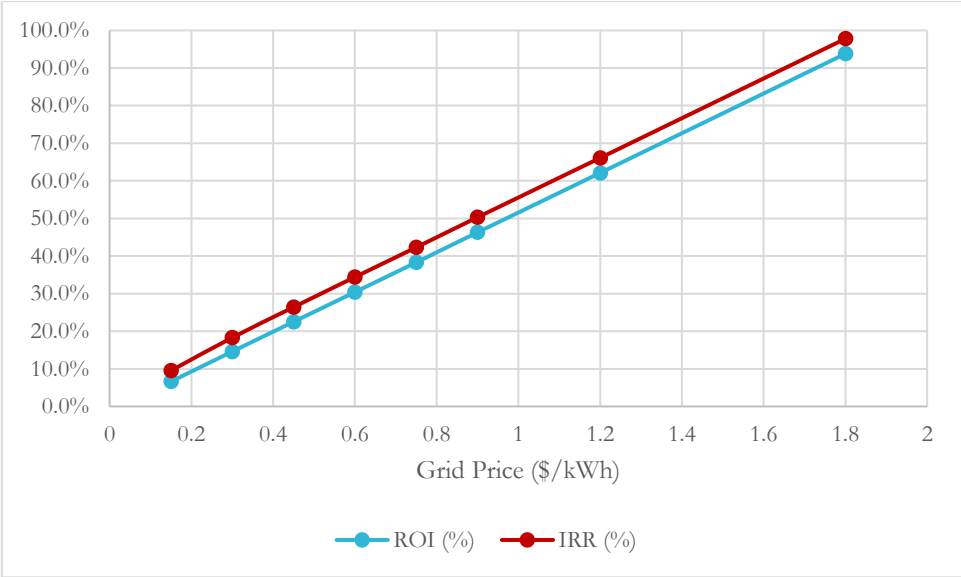


Figure 37: ROI and IRR for different costs of electricity from the grid.

Due to the asymptotic nature of discounted payback in general, the relationship with grid price indicates an exponential decay towards immediate payback. The largest reduction in discounted payback occurs at the lower ranges of grid prices. Given that prices are dynamic and not static, as is assumed for the running of these simulations, the financial benefit of investing in a microgrid for the campus is only expected to grow.

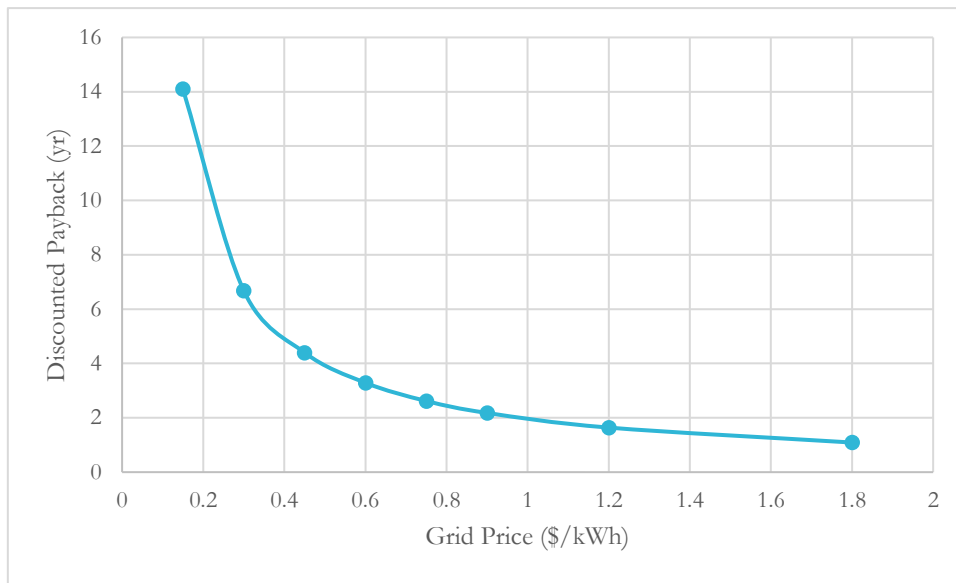


Figure 38: Discounted payback period for the optimal microgrid with an energy storage system: 23,652-kW PV, two 1.5-MW wind turbine, and three 250-kW/8-hr VRFB.

### Buyback Rate

Up to this point, all systems proposed have had a negative NPC for the project lifespan. The benefits of the microgrid come from the savings it provides compared to the current electricity costs that are incurred by relying entirely on the AEE grid. At best, the closest design to being profitable is, as expected, the advanced market system that minimizes LCOE (configuration as seen in Figure 28) with a total NPC of -24.8M\$.

To understand what it would take for these systems to be profitable, the Forced Battery systems are re-simulated with variations in the buyback rates. As this value is the only source of potential income, aside from any component salvage potential at the end of the project life, it is the only variable adjusted for this analysis. The current rate for the AEE grid is 0.10 \$/kWh, therefore, rates have been increased all the way up to 0.30 \$/kWh. This is equivalent to the purchase price of energy from the grid and, as such, is the upper limit to what is probable.

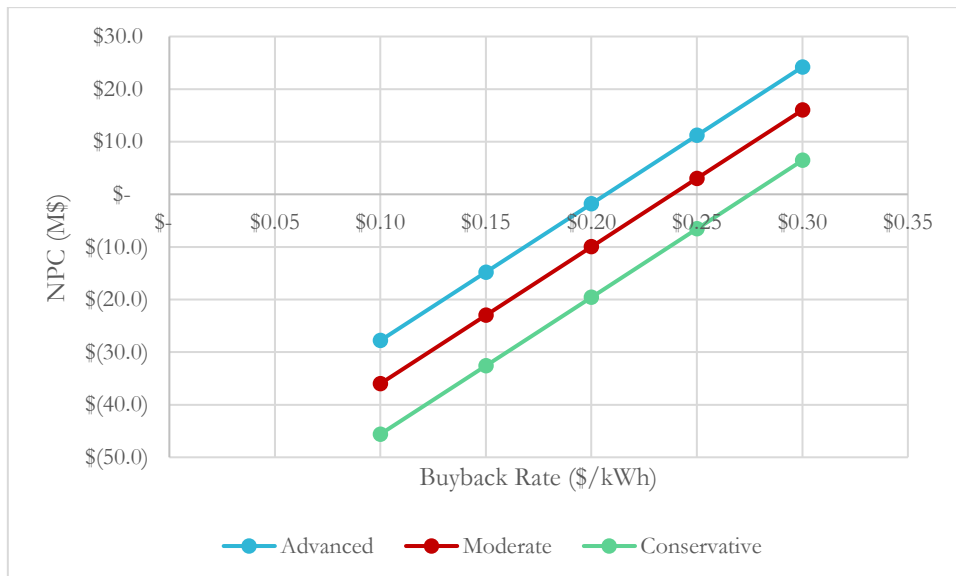


Figure 39: Variations in NPC for the selected design in a moderate scenario as buyback rate for energy sold to the grid increases.

Figure 39 shows the increase in NPC as a function of buyback rate for the Forced Battery system in each market scenario. All scenarios reach profitability above 0.20 \$/kWh but below the upper limit for the buyback rate. Table 30 shows the breakeven values for the buyback rate, above which the Forced Battery systems can achieve profitability.

Table 30: Minimum buyback rates that allow the Forced Battery system to be profitable in all three market scenarios.

	Advanced	Moderate	Conservative
Break Even Value	\$ 0.2069	\$ 0.2384	\$ 0.2752

## 5.2 Oasis Results

This section provides the final estimates for all Oasis related calculations. It includes the estimated annual energy consumption of each scenario for both the campus and Oasis, along with the seasonal energy supply for each Oasis service per scenario. The Oasis KPI are then calculated and analyzed leading into the discussion around system performance.

The Business-as-Usual scenario maintains the existing energy supply coming from the AEE grid and introduces an assumed disruption to the electrical supply lasting the entirety of the hurricane season. The simulated outage runs from June to November, spanning a total maximum of 183 days. During a disaster year the supplied electrical load to the campus from the grid reduces from a total annual of 27,361 MWh to 12,232 MWh, representing a 55.3% drop in supply.

In a similar fashion, the PR100 scenario assumes there to be a 30% energy efficiency improvement on all loads, while the grid is supplied by 100% renewable energy resources. It does not, however, implement any changes to the distribution system in the model. Therefore, the total nominal load for the campus decreases from 27,361 MWh to 19,152 MWh by 2030. Likewise, the disruption in the electrical grid causes the annual supply to dwindle from 19,152 MWh to 8,562 MWh, representing a 55.3% drop in supply. This scenario assumes that an energy metering system is in place to monitor the consumption per diem.

When the microgrid is introduced in the Oasis P4 scenario, there is still a reduction in the annual supply to the campus from 27,361 MWh to 24,415 MWh as there are no longer purchases from the grid. This 10.8% reduction represents a deficiency in supply that necessitates the "reclamation" of grid sales and curtailment to serve the total load if no load shedding is implemented. However, when looking at the Oasis P4 scenario, it becomes clear that there is enough supply from the microgrid to meet the campus demand. This is due to the reduced demand from 27,361 MWh to 22,432 MWh, or an 18% reduction, in this scenario. The Oasis scenarios P3 and P2 further reduce the annual campus demand to 19,315 MWh and 17,520 MWh, which represent a 29.4% and 36% reduction from the baseline, respectively. The reclaimed curtailment will be discussed in Section 5.2.1.

As mentioned previously with the PR100 scenario, introducing the energy efficiency measures reduces the campus load from 27,361 MWh to 19,152 MWh per year. This then translates to 15,702 MWh of annual demand after strategic load shedding for the Oasis PR100 P4 scenario, which is the same 18% reduction in demand as compared to the Oasis P4 scenario without energy efficiency measures. Furthermore, the demands for the Oasis PR100 P3 and P2 scenarios are reduced to 13,521 MWh and 12,264 MWh, which correspond to a 29.4% and a 36% reduction. The scenarios and their total campus energy demands are found in Figure 40.

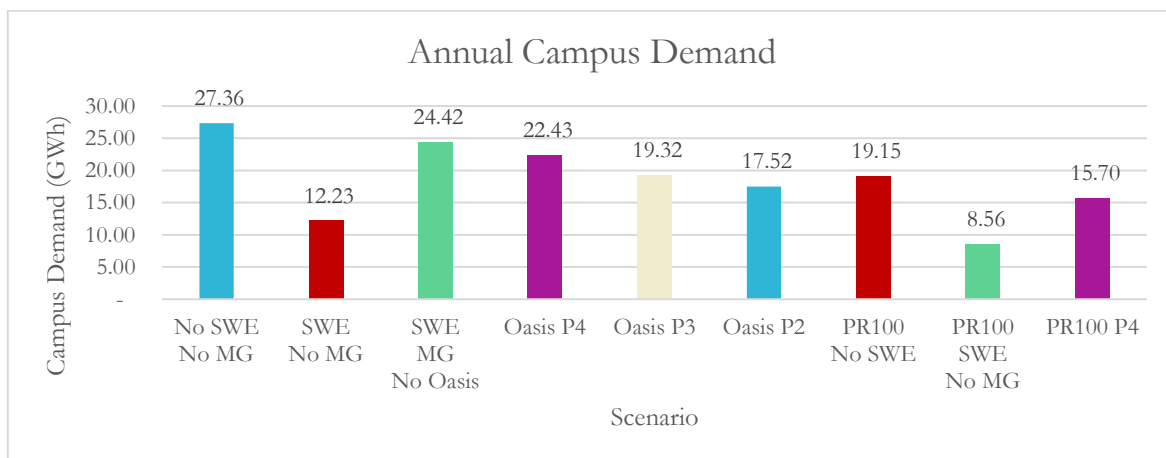


Figure 40: Annual campus demand across the different scenarios

## 5.2.1 Scenario Simulation Results

Having the capability to maintain Oasis services for a duration of 183 days provides the community with 2.18 times longer than the average disruption time of 84 days without electricity reported by Kishore et al. [147]. As expected, a larger amount of load shedding results in a greater quantity of energy provided to the different services, with the amounts varying as shown in Figure 41.

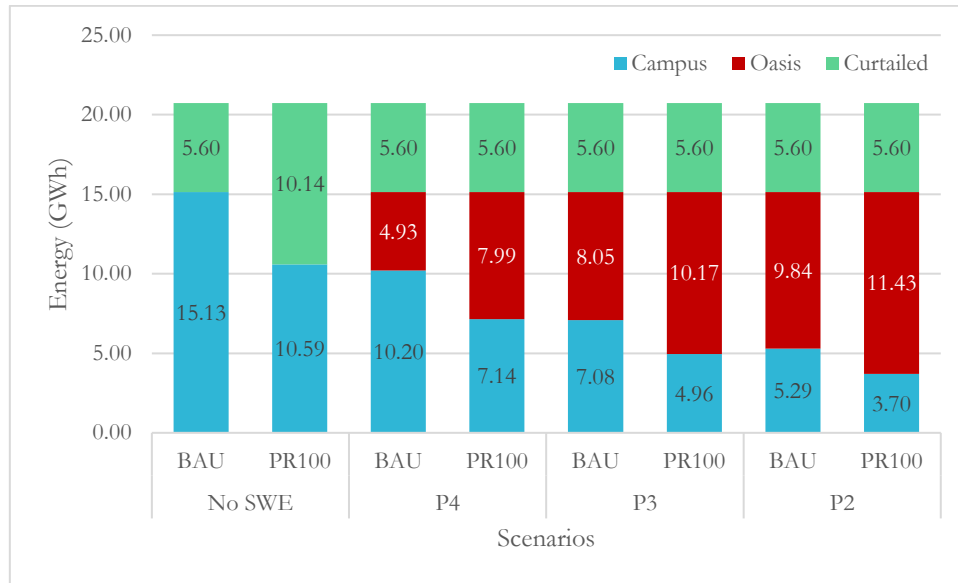


Figure 41: Breakdown of the flow of energy into the campus, the Oasis, or curtailed during hurricane season in the different scenarios.

When no SWEs are observed, there is an average campus demand of 82,671 kWh/day during the entire hurricane season (183 days). Similarly, when energy efficiency measures are accounted for the PR100 scenario yields a seasonal daily average of 57,870 kWh/day, or a 30% decrease as expected. Table 31 provides the complete set of scenarios and their seasonal daily energy supply averages.

Table 31: Energy supplies for campus and Oasis including seasonal daily average.

Load Shedding Level	Scenario	Campus		Oasis	
		Seasonal Supply [kWh/Season]	Seasonal Daily Average [kWh/day]	Seasonal Supply [kWh/season]	Seasonal Daily Average [kWh/day]
No SWE	BAU	15,128,973.34	82,671.99	-	-
	PR100	10,590,281.34	57,870.39	-	-
P4	Oasis	10,199,776.32	55,736.48	4,929,197.02	26,935.50
	PR100 Oasis	7,139,843.42	39,015.54	7,989,129.91	43,656.45
P3	Oasis	7,083,437.06	38,707.31	8,045,536.28	43,964.68
	PR100 Oasis	4,958,380.58	27,094.98	10,170,592.76	55,577.01
P2	Oasis	5,288,555.53	28,899.21	9,840,417.81	53,772.77
	PR100 Oasis	3,702,074.47	20,229.92	11,426,898.86	62,442.07

The HOMER Pro simulation data allows for the estimation of the energy curtailed from both the wind and solar generation. This is due to the simulation assuming that "curtailed" energy is sold to the grid and so by totaling the energy sold to the grid in this time period it is possible to calculate the total curtailed energy during hurricane season. It is important to reiterate at this time that the HOMER simulations are prevented from charging the storage systems with energy from the grid, from selling energy from the storage systems to the grid and prioritize charging the storage system over selling to the grid. This results in a surplus of 3,652 MWh per hurricane season and a seasonal average of 19,958 kWh/day. These later values are included in the Oasis KPI estimates in the following section.

### 5.2.2 Oasis KPI's

The KPIs outlined in Section 3.2.4 provide context to the Oasis performance for each scenario in the study. Since there is no Microgrid or Oasis implemented within the BAU or PR100 scenarios, their KPI values are excluded from these results. Because there is no starting point for the distribution of energy for each service, the Oasis scores are used as scalar multipliers for each service supply. This is done by dividing the score for the service by the total sum of scores from every service (ie. Medical = 5/16). The first iteration using Equation 6 provides the maximum number of people that can be served in a day by each for every Oasis scenario (Table 32).

Table 32: Maximum number of people served based on the available energy for each service in each load shedding scenario.

	Maximum People Served Per Day					
	P4	P3	P2	PR100 P4	PR100 P3	PR100 P2
<b>Medical</b>	389	636	777	631	803	903
<b>Water</b>	674,062	1,100,217	1,345,665	1,092,504	1,390,816	1,562,614
<b>Cafeteria</b>	990	1,617	1,977	1,605	2,044	2,296
<b>Telecom</b>	505,040,678	824,337,734	1,008,239,530	818,558,393	1,042,068,930	1,170,788,818

Using Equation 5, along with the scalar multipliers mentioned before, facilitates visualizing the total Oasis access time as a function of people that can receive access to services. A larger quantity of people results in a decreased amount of service access time as evidenced by Figure 42. It is important to point out that the lower limit of access time is 1 day, thus crossing the time axis (Y) at 1 would imply the maximum possible people have received access to services for the maximum time period. Any additional people receiving access would technically be consuming energy that will not be available until the next day, which is impossible.

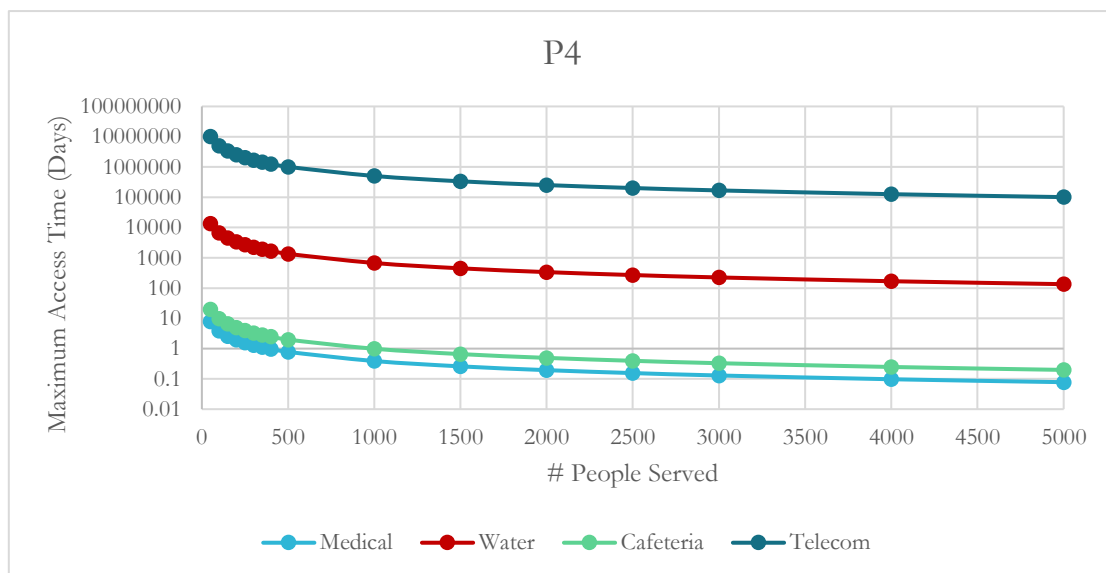


Figure 42: Maximum access time as a function of the population served for each service within the P4 Scenario.

From these values only a small number of people are served by medical and cafeteria services. In contrast, the telecom service is massively oversized, as it serves people in the scale of hundreds of millions, as well as water, which can service millions of people. This discrepancy is due to a combination of the significant difference in energy intensity for each service and the fact that the energy is distributed near-equitably amongst services, which is observed in Figure 43 below.

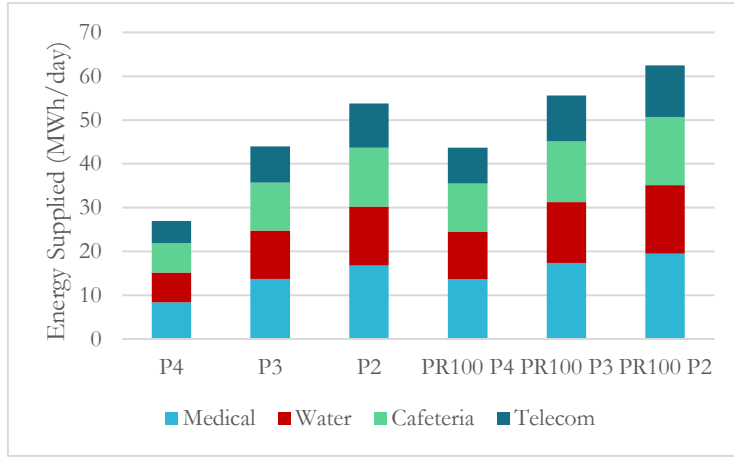


Figure 43: Energy supply to each Oasis service for every scenario.

This initial solution can be improved by modifying the relationship between the Oasis energy distribution, the Oasis score, and the number of people served via Equation. The constants  $n_M$ ,  $n_W$ ,  $n_C$ , and  $n_T$  relate the score for the medical, water, cafeteria, and telecommunications services respectively.

Equation 23: Sum of the energy service distribution

$$E_O = \sum n_i \cdot \rho_i = n_M \cdot \rho_M + n_W \cdot \rho_W + n_C \cdot \rho_C + n_T \cdot \rho_T$$

They are found by dividing the service score value for the service in question by the following service score value. These ratios serve similar functions to the scalar multipliers.

Table 33: Relationship between constants for redistribution of energy within the Oasis.

Constant	Relation to $n_M$
$n_M$	$n_M$
$n_W$	$\frac{5}{4} \cdot n_M$
$n_C$	$\frac{5}{4} \cdot n_M$
$n_T$	$\frac{4}{3} \cdot n_C = \frac{5}{3} \cdot n_M$

The equation is simplified to Equation 24 by substituting the constants with their relational values as per Table 33, remembering that  $\rho_i$  is the specific daily consumption per person for each service.

Equation 24: Simplified version of Equation 23.

$$E_O = n_M \cdot \left( \rho_M + \frac{5}{4} \cdot \rho_W + \frac{5}{4} \cdot \rho_C + \frac{5}{3} \cdot \rho_T \right)$$

Re-estimating the energy distribution using this version of the equation requires the number of people served be found first. This is accomplished by iterating the value of  $n_M$  until the differential between the calculated  $E_O$  (The equation is simplified to Equation 24 by substituting the constants with their relational values as per Table 33, remembering that  $\rho_i$  is the specific daily consumption per person for each service.

Equation 24) and the available  $E_O$  (as estimated from the load shedding) is zero. The energy for the service can then be calculated by multiplying the specific daily consumption by the number of people served. This approach is also done to estimate the KPIs using the curtailed surplus from the microgrid. The resulting values using the curtailed energy are added to the final values using the load-shed supply and are provided in Table 34 and Table 35.



Table 34: The maximum number of people served in a single day with adjusted energy distribution to Oasis services and the addition of curtailed energy.

	Maximum People Served Per Day					
	P4	P3	P2	P4 PR100	P3 PR100	P2 PR100
Medical	1,556	2,122	2,447	2,111	2,507	2,735
Water	1,946	2,652	3,059	2,639	3,134	3,419
Cafeteria	1,946	2,652	3,059	2,639	3,134	3,419
Telecom	2,594	3,536	4,079	3,519	4,178	4,558

Table 35: Adjusted energy values per service for each scenario including the addition of curtailed energy.

	Energy Per Scenario (kWh/day)					
	P4	P3	P2	PR100 P4	PR100 P3	PR100 P2
Medical	33,644.72	45,862.55	52,899.51	45,641.40	54,193.98	59,119.42
Water	19.46	26.52	30.59	26.39	31.34	34.19
Cafeteria	13,229.72	18,033.99	20,801.05	17,947.03	21,310.07	23,246.84
Telecom	0.03	0.04	0.04	0.04	0.04	0.05
<b>Total</b>	<b>46,893.92</b>	<b>63,923.10</b>	<b>73,731.19</b>	<b>63,614.87</b>	<b>75,535.43</b>	<b>82,400.49</b>

The data shows that the amount of people receiving access increases drastically when energy efficiency measures are in place for the campus. Specifically, there is nearly the same amount of people in the Oasis PR100 P4 scenario as there are in the Oasis P3 scenario. Whereas the Oasis PR100 P3 scenario surpasses the Oasis P2 scenario, this inflection point is due to the larger amount of energy being consumed by the P3 category buildings than the P2 category buildings. Figure 44 depicts the re-visited Oasis access times as a function of the population served for P4; note that water and cafeteria share the same values, thus they are superimposed on the same curve.

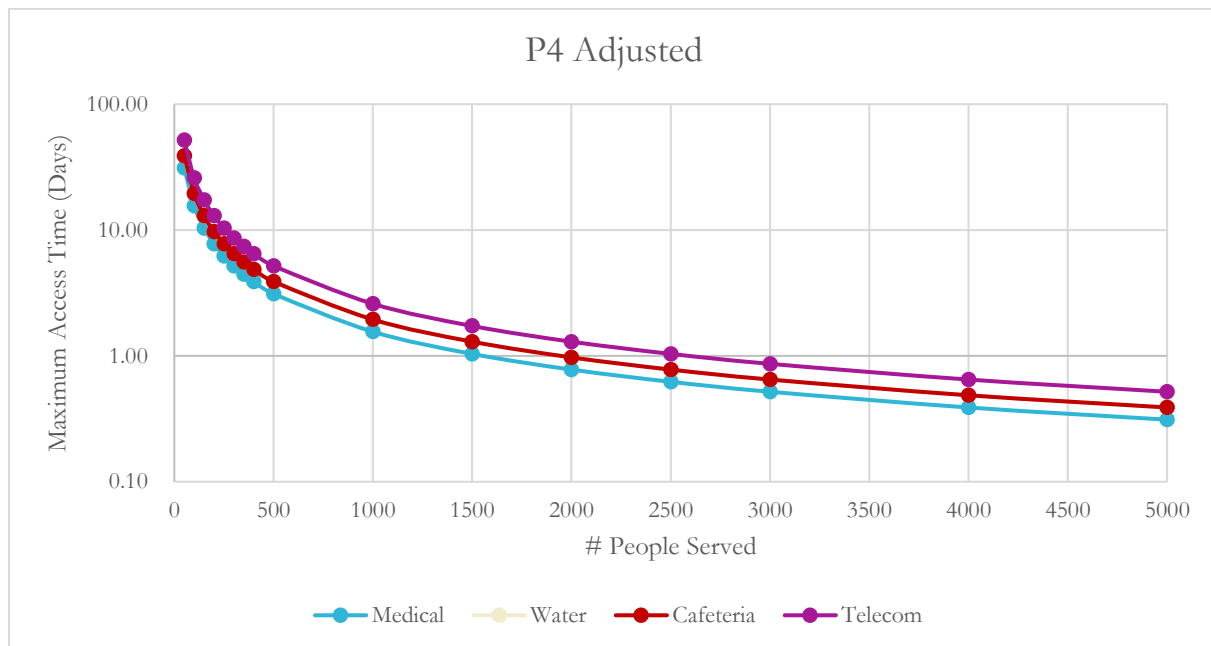


Figure 44: Correlation between number of people served and the access time for each service in the Oasis with the new energy service distribution for P4.

In terms of energy distribution, the medical service requires a much greater energy consumption in comparison to all other services for each scenario as evidenced by Figure 45 below. This is largely due to the amount of space that is required by law for patients to receive medical care within an emergency room. In the same vein, this quantity of people is expected to remain fixed for a period of time due to the physical recovery time associated with medical treatment received. In other words, a person receiving surgery or dialysis is expected to remain in the medical center for a longer period than a person waiting in line for food or water, as the latter services essentially function like assembly lines. This is further accentuated by the

telecommunications service. Since the service can be provided in smaller periods of time per person based on the intended use of the service.

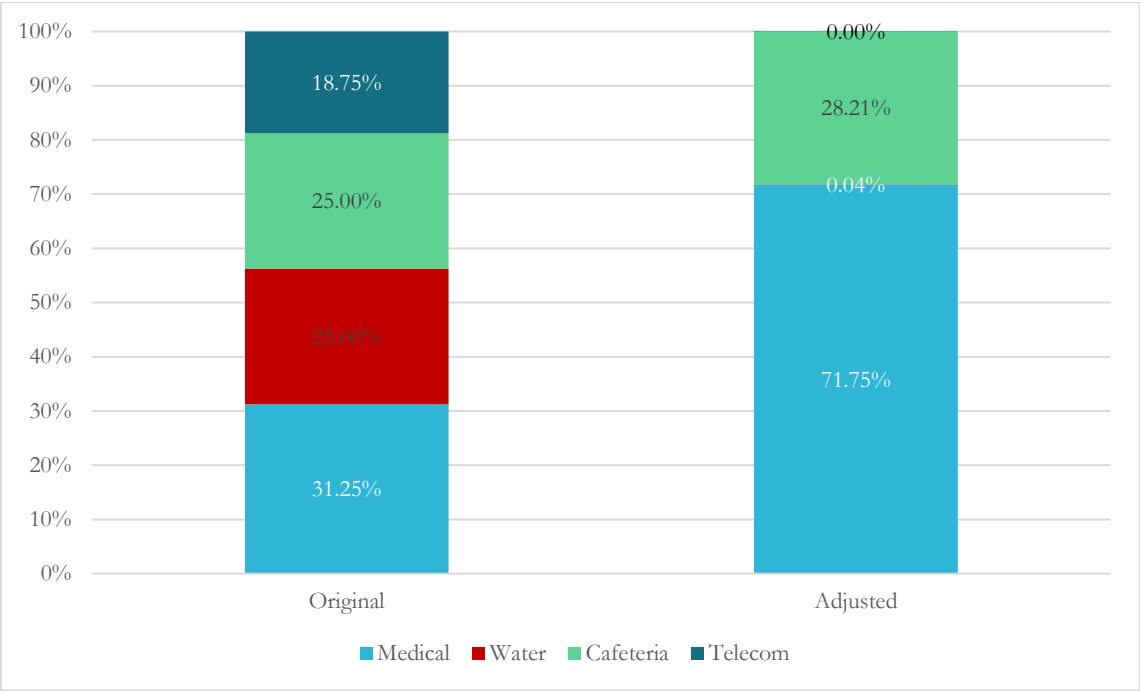


Figure 45: Comparison of energy distribution into the Oasis services between the original and the adjusted systems.

It is critical to point out that each service requires a different energy minimum value to function at the lowest possible value of people served. For example, the energy supply for the telecommunications service is well below the estimated energy consumption of the tower (22.40 kWh/day), resulting in a percentage difference between 199.12% and 199.46%. Since this value is estimated from the energy consumption per km<sup>2</sup>, it does not provide a minimum required energy demand for low-power operation. The same is true for the other services as there will likely be idle loads in the absence of people receiving the service. Therefore, a deeper understanding of energy consumption for each service is necessary to further optimize the energy distribution per service within this study.

Lastly, the disaster relief fractions for the different scenarios provide a glimpse into the potential aid that can be provided to the community as a function of the maximum generation from the microgrid. As hypothesized, a larger amount of load shedding results in a greater percentage of the disaster relief fraction, as seen in Table 36: Disaster Relief Fraction for each scenario as a function of Oasis duration. This effect is further compounded by the energy efficiency gains that can be achieved by the campus buildings.

The prioritization scheme for the UPRM campus prevents the disaster relief fraction from exceeding 47.65% for any given year as the equation uses annual energy. Similarly, the minimum Oasis duration of 1 day yields a relief fraction of 0.06%. A greater resolution for events lasting less than a day would require recalculating the distributed energy on an hourly basis. While this may be possible to achieve, there is a likelihood that the service deployment times may be longer than the duration of the service demand. To better understand the minimum number of days that the Oasis can provide access would require empirical results for the operation of such a system. Similarly, disaster recovery efforts exceeding 365 days are expected to re-calculate the relief fraction as this provides more readily interpretable performance across various years and Oasis systems.

Table 36: Disaster Relief Fraction for each scenario as a function of Oasis duration.

Oasis Duration (Days)	Disaster Relief Fractions ( $\epsilon_{OS}$ )					
	P4	P3	P2	PR100 P4	PR100 P3	PR100 P2
365	19.56%	31.93%	39.06%	31.71%	40.37%	45.35%
183	9.81%	16.01%	19.58%	15.90%	20.24%	22.74%
100	5.36%	8.75%	10.70%	8.69%	11.06%	12.43%
50	2.68%	4.37%	5.35%	4.34%	5.53%	6.21%
1	0.05%	0.09%	0.11%	0.09%	0.11%	0.12%

### 5.3 Sustainability Impacts

As is mentioned in Section 3.3, with the completion of the microgrid design and acquisition of the Oasis system performance in several scenarios, the Oasis Score (OS) is calculated. Initial values are found using Equation 8 and the original energy distribution to services in the Oasis, as defined in Section 4.2.2. The results are defined in Table 37 below.

Table 37: Oasis Score calculated for each of the load shedding scenarios with the current campus load as well as for the P4 load shedding with PR100 efficiency improvements.

Service	P4	P3	P2	P4 PR100	P3 PR100	P3 PR100
<i>Medical Services</i>	0.63	1.03	1.26	1.02	1.30	1.47
<i>Water Purification</i>	0.40	0.66	0.81	0.66	0.83	0.94
<i>Cooking</i>	0.40	0.66	0.81	0.66	0.83	0.94
<i>Communications</i>	0.23	0.37	0.45	0.37	0.47	0.53
<b>Total</b>	<b>1.67</b>	<b>2.72</b>	<b>3.33</b>	<b>2.71</b>	<b>3.44</b>	<b>3.87</b>

These results have the expected correlation based on the formula: scores increase as the quantity of energy in the Oasis increases (P4 vs. P2) and higher DRMs result in larger amounts of energy going to the service, both of which increase the score for the service. In these calculations, the number of people served is assumed to be the maximum that can be served. This is to show what the highest score capable is for the current Oasis system.

When the energy distribution within the Oasis is adjusted, as outlined in Section 5.2.2, the OS increases compared to the original distribution. This indicates a people-normalized energy distribution, as opposed to an equal distribution of energy per service, improving the operation of the Oasis. Further adjustments to the ratios defining the distribution of energy in the Oasis could yield even higher scores and provide a more optimal system performance.

Table 38: The Oasis Score using the recalculated distribution of energy to the services.

Service	P4	P3	P2	P4 PR100	P3 PR100	P2 PR100
Medical Services	1.45	2.37	2.90	2.35	2.99	3.36
Water Purification	6.71E-04	1.10E-03	1.34E-03	1.09E-03	1.39E-03	1.56E-03
Cooking	0.46	0.75	0.91	0.74	0.94	1.06
Communications	6.71E-07	1.10E-06	1.34E-06	1.09E-06	1.39E-06	1.56E-06
<b>Total</b>	<b>1.91</b>	<b>3.12</b>	<b>3.81</b>	<b>3.09</b>	<b>3.94</b>	<b>4.42</b>

The previously OS calculation can be further improved by expanding Equation 8. Up to this point, the Oasis is calculated from the available energy provided by load shedding strategies. While accurate for the campus operation, it does not consider the curtailed energy produced by the microgrid. Within the HOMER simulation, this is represented as the energy sold back to the AEE grid. However, during a blackout this energy is fully curtailed within the current system design. Consequently, a larger portion of the population can be served by accounting for the curtailed energy in the Oasis distribution. The expanded version of Equation 8 is provided below as Equation 25.

Equation 25: Revised Oasis Score

$$Oasis\ Score = \sum_{i=service}^4 \frac{DRM_i \cdot E_i \cdot n_i}{n_{i,max} \cdot E_M} + \sum_{j=service}^4 \frac{DRM_j \cdot E_j \cdot n_j}{n_{j,max} \cdot E_C}$$

Capturing and utilization of the curtailed energy during a blackout has significant benefits to the Oasis. On average, the amount of energy sold to the AEE grid from the microgrid (62,781.9 kWh/day) is roughly equal to the campus load served by the microgrid (61,800.1 kWh/day). This amount of energy allows for significantly more people to receive aid through the Oasis services. The right-most column of Table 39 shows the number of people served by only the curtailed energy, which is added to each of the scenario values.

Table 39: Maximum people served in each service per scenario compared to only using only the curtailed energy of the microgrid.

	Maximum Number of People Served						
	P4	P3	P2	P4 PR100	P3 PR100	P2 PR100	Curtailed
<b>Medical</b>	1,556	2,122	2,447	2,111	2,507	2,735	<b>662</b>
<b>Water</b>	1,946	2,652	3,059	2,639	3,134	3,419	<b>828</b>
<b>Cafeteria</b>	1,946	2,652	3,059	2,639	3,134	3,419	<b>828</b>
<b>Telecom</b>	2,594	3,536	4,079	3,519	4,178	4,558	<b>1,104</b>

Incorporating this quantity enhances each scenario's OS (Table 40) by 4.79 points. The increase is uniform throughout scenarios since the amount of load shedding performed within the campus does not impact the average amount of energy that is sold to the grid on a given day.

Table 40: Adjusted Oasis Score results with the inclusion of the curtailed energy in each scenario.

Service	P4	P3	P2	P4 PR100	P3 PR100	P2 PR100
Medical Services	2.53	3.44	3.97	3.43	4.07	4.44
Water Purification	1.17E-03	1.59E-03	1.84E-03	1.59E-03	1.88E-03	2.05E-03
Cooking	0.79	1.08	1.25	1.08	1.28	1.40
Communications	1.17E-06	1.59E-06	1.84E-06	1.59E-06	1.88E-06	2.05E-06
<b>Total</b>	<b>3.32</b>	<b>4.53</b>	<b>5.22</b>	<b>4.51</b>	<b>5.35</b>	<b>5.84</b>

### 5.3.1 Land

This work considers the limited availability of land within the campus. In doing so, it aims to make use of the least number of green spaces for energy generation, distribution, and storage purposes. In addition, it provides a preliminary estimate for the potential land use impact of the Oasis services.

Most of the area to be taken up by the generation systems is the rooftops and proposed covered parking for the PV system. A total area of 143,483 m<sup>2</sup> is utilized by the panels: 69,209 m<sup>2</sup> from repurposed rooftops and 74,274 m<sup>2</sup> in space from existing parking lots. In the case of the parking lots, the PV panels would provide shading for the lots and not require new lots to be constructed.

The wind turbines require the designation of some green areas, as per general requirements outlined in the PR100 One-year progress report [16]. Specifically, a total of 9,000 m<sup>2</sup> is necessary for both turbines, as outlined in Section 4.1.2.1. Half of this area is proposed to come from uncontrolled vegetation, while the other half comes from existing agricultural land.

Battery energy storage systems are anticipated to be installed, ideally, within the basements of nearby buildings or, if this is not possible, in any of the many unused areas near parking lots throughout the campus. Many of these, like the areas around the biology building’s parking lot or behind the Department of Buildings and Grounds, are currently dirt lots that are not significantly used by the campus or by local flora. The VRFBs require a total footprint of 12.2 m by 7.4 m, each. For all three in the Forced Battery system, a combined total area of 270.84 m<sup>2</sup> is required.

Should a H<sub>2</sub> storage systems be included, all components that utilize or produce H<sub>2</sub> (electrolyzer, tank, and fuel cell) must be sited at a minimum of 15.24 m (50 ft) from any surrounding structures as per the Occupational Safety and Health Administration’s (OSHA) Hydrogen safety standard [31], [148]. Due to the minimal impact of an H<sub>2</sub> system in any of the proposed systems, the area estimate for the components has been calculated.

When operated as an Oasis, land access will be granted to members of the community who have lost essential services following the natural disaster. Most members of the community are expected to visit the campus to receive aid and then return to their homes once their area has been restored to pre-disaster condition. Medical, cooking, and water will be staged at a specific location as specified by the UPRM. Temporary camps could be made available for those displaced from their homes by the SWE, although this would require coordination with FEMA efforts.

Providing medical access to people within the UPRM geographical boundary could prove to be somewhat challenging based on the mobile emergency response units that are available [149]. These facilities-on-wheels require approximately 102m<sup>2</sup> of real estate, which results in 204m<sup>2</sup> of parking space that can accommodate 2 vehicles supporting a daily average of 10 people as per the Oasis P4 scenario. At the other extreme, 306 m<sup>2</sup> would be required to accommodate 3 vehicles to support a daily average of 17 people per the Oasis PR100 P2 scenario. This represents 0.3% and 0.4% of the total estimated parking lot area of 74,275 m<sup>2</sup>. Given the high in-patient waiting times in Puerto Rico [150], it is likely that less people per day will be receiving the medical treatment they require, thus more facilities-on-wheels will be needed.

Water treatment is considered as a treatment-plant-on-wheels [133] and uses a shipping container footprint of approximately 18m<sup>2</sup>. Following a similar approach to the medical service, 18m<sup>2</sup> would be required to provide a daily average of 14 people with access to clean drinking water with a single water purification unit

as per the Oasis P4 scenario. The same amount of land would be required in Oasis PR100 P2 scenario, which serves 21 people on average per day.

The external cafeteria is calculated by using the EIA commercial cafeteria specific consumption of 468.23 kWh/m<sup>2</sup> [151]. When using the daily average energy supply for the cafeteria service for each scenario, this results in a range between 0.189m<sup>2</sup> and 0.306m<sup>2</sup> from the Oasis P4 to the Oasis PR100 P2 respectively. These values equate to an insignificant amount of area that can be used to prepare food; however, a larger amount of area will be required for cooking and logistical purposes, which necessitates a more detailed analysis in a future study.

### 5.3.2 Energy

The overall objective of this work is to provide a microgrid with 100% renewable energy supply. Solar PV panels, hurricane-resistant wind turbines, VRF batteries, hydrogen storage systems, and other technologies will require importing from the mainland USA. This will not only contribute to GHG emissions associated with importation but can also result in bottlenecks should parts not be available. Although outside the scope of this study, it is important to note that a separate LCA study would provide more clarity on the ramifications related to these importations.

On the other hand, the implementation of a microgrid system will inherently curb GHG emissions from the energy no longer purchased from the grid. In the recommended Forced Battery system, this equates to a reduction of 22.56 GWh of electricity purchased from the grid every year. This is estimated to cut 22,560 tonnes of CO<sub>2</sub> emission each year, assuming 1 kg of CO<sub>2</sub> per kWh produced by the AEE grid [152].

Some of the technologies to reduce energy consumption, as well as materials for parts of the microgrid and oasis systems, can be sourced locally, such as second-life vehicle batteries, LPG tanks, and refurbished diesel engines. This will result in a reduced strain on supply chain lines, which in turn will result in a lesser consumption of energy to source equipment. Moreover, as the campus moves to meet the PR100 goals the implementation of energy efficiency measures and load shedding capabilities will provide significant gains in energy management practices thereby reducing the overall consumption from the University. The capability to strategically load shed and the improved consumption monitoring strategies are expected to have large positive impacts on the campus's ability to improve energy efficiency. Additionally, the creation of the microgrid provides a local generation source that can produce energy and provide a continuous flow of electricity to the neighboring community immediately after extreme weather events that knock out the AEE grid. This access to reliable sources of electricity is expected to save lives and enhance the quality-of-life following periods of grid collapse.

### 5.3.3 Food

The implementation of a microgrid system is not expected to have a large impact on food access. The microgrid biomass resource, should a biomass system be included, is sourced from residual urban waste and non-edible agricultural waste from the campus. These feedstocks are not expected to impart any strains on the food supply chain as they already exist and are currently disposed of with no second life. Should future projects increase the demand and generation capacities of the biomass system, the sourcing of additional biomass may have an impact on food available. This would be a point of focus for the future work to consider. Large-scale wind turbines are planned to be installed on existing agricultural land on the campus. However, since the campus does not produce crops for general consumption, the crop's primary function is educational, this reallocation of land use is not anticipated to have a large impact on food resources for the region.

As the microgrid will not induce an increased consumption of food resources when operated and therefore there is no expected additional food consumption in Oasis mode for energy generation, specifically. However, there is expected to be a higher food consumption on campus due to the added functionality of providing meals for the members of the community who have been displaced completely or have lost access to cooking appliances because of the natural disaster. In this respect, while the UPRM campus food consumption will increase, the overall food consumption of the Mayagüez community will remain unaffected (or possibly reduced due to rationing and other restrictions that may be deemed necessary) from pre-disaster levels.

### 5.3.4 Water

The proposed microgrid system is not anticipated to have an impact on water use or availability. There is expected to be an increased consumption for the PV system as the panels will require periodic cleaning to



prevent efficiency losses because of dust buildup. However, the exact quantity of water consumed for this general maintenance is outside the scope of the study and assumed to be negligible. In the event an H<sub>2</sub> system is included, existing hydrogen storage technologies, specifically for PEM fuel cells, require ultra-pure water to operate. The equipment necessary to achieve the filtration requirements of this high-purity water could be used for producing potable water during the Oasis operation. Additionally, the ability to produce ultrapure water on campus could reduce the need to purchase and import ultrapure water for laboratory experiments.

It is important to comment on how the design of such a system could impact water consumption in the surrounding region. A closed-loop system would require periodic refilling and replacement of the water, resulting in a lower impact on water access to the region. In contrast, an open-loop system would have a constant water input requirement, thereby affecting local water access more than the close-loop alternative.

The water purification system does not provide any value for feedwater supply. However, assuming a 90% rejection rate [153] and the same daily average of people served provides a range between 53.6L and 86.7L of brackish water per day for the Oasis P4 and Oasis PR100 P2 scenarios respectively. This feedwater may not be available from the tap following the assumption that there is a blackout in the grid preventing pumping. Thus, the feedwater will need to be sourced from collected rain or seawater imports to the campus boundary. Furthermore, special care must be taken when handling the brine during discharge to prevent contaminating other sources.

### 5.3.5 Social

Energy communities centered around microgrids are often setup without an interest in market participation which can result in scale up issues as described by Warneryd & Karltorp [154]. In the UPRM case, the microgrid participates in the energy market for most of the year, with the key exception being following severe weather incidents. This allows for a good return on investment for the microgrid itself, while also providing aid to the community without a need to create unnecessary burdens on the surrounding populous. As a result, the primary social impact of the microgrid results from its operation as an energy oasis during periods of AEE grid outages.

Additionally, certain secondary benefits, or benefits that may not be largely tangible or may require long periods of time before they come to fruition, may result from the implementation of such a largescale renewable microgrid. For instance, the educational benefits provided by having access to the microgrid for studying engineers at the UPRM campus will result in immeasurable positive impacts and changes they have on the island and across the world through their future work. In addition, an improved infrastructure for residential, commercial, and large-scale microgrid installation on the islands due to the successful implementation of such a large-scale design.

## 6 Conclusion

The results of this study provide promising potential for the UPRM campus. With numerous microgrid designs all yielding high performance, increased energy independence, and fast ROIs compared to the existing system, the University has a large selection of configurations to choose from that meet their needs and financial capabilities.

The HOMER Pro system optimization yielded three configurations capable of meeting the UPRM energy demands and achieving the requirements outlined in this study: the Minimum LCOE (Figure 28), Forced Hydrogen (Figure 31), and Forced Battery (Figure 32). The systems all rely heavily upon solar energy generation, due to its high availability at the project site and lower cost per kWh compared to other resources but also include a small portion of wind energy generation from turbines. The design recommended based on the criteria of the study, the Forced Battery system, is the only one of the three systems that includes an effective storage system, a component that is critical for the active utilization of the microgrid during blackout events in the region.

Each configuration boasts a Renewable Fraction above 88% and an LCOE below 0.06\$/kWh, which is approximately 20% of the current electricity cost from the AEE. From a financial standpoint, all three configurations result in positive returns when compared to the current BAU system, regardless of changes in component or grid electricity costs. The findings suggest a considerable increase in the value provided by the microgrid in terms of LCOE, NPV, and IRR with increasing grid electricity costs and worsening storms.

The renewable energy-based Oasis system provides a solution to the adverse effects caused when the Puerto Rican electrical grid is disabled, and fossil fuel resources are no longer available for backup generators. Through the study there is evidence to suggest a portion of the population can receive a continuation of services, and there is potential for increased disaster relief capacity made available through the system. These benefits are observed even at the lowest potential of load shedding where it is estimated that 683 people can be accommodated within the medical services each day, 853 people can be provided three meals and enough water for the day, and 1,138 telecommunication devices can be provided connection to cellular services each day. When existing energy produced by the microgrid and sold to the AEE grid is considered for the Oasis, these values increase to 2,767 for medical services, 3,288 people for food and water, and 4,611 telecommunication devices.

This type of end-use also reduces the overall dependency on government-driven relief activities, as they are made available immediately in the event of a natural disaster. This allows for the government-driven resources to be allocated to other affected areas, providing more relief across the island than before. Moreover, the model is not limited to the UPRM campus as it can be easily adapted to any microgrid system. However, the load shedding potential for different case studies must be adapted for each individual system. Lastly, the work provides an evaluation scheme to determine the performance of similar Oasis systems for comparison between systems regardless of individual designs. In the case of the PRREO within the UPRM campus, the Oasis receives a score of 1.91 to 4.42, depending on the priority level. When the energy originally sold to the grid is included, these values increase to 3.32 to 5.84, indicating that larger energy pools provided to the Oasis increase the score using this approach.

## 7 The Road Ahead

The successful execution of a project this size requires a significant amount of coordination and foresight to achieve. This section outlines a few of the key recommendations, critical limitations of the study, and potential future work that have been identified throughout the study.

### 7.1 Recommendations & Limitations

Throughout the completion of the study, the largest limitation that has directly impacted the results is the available data. The lack of digital energy meters throughout the campus results in the only reliable source of energy data for the campus consumption being the monthly electrical utility bills for the entire campus. As such, all load data for the campus as a whole and individual buildings is extrapolated from these data points, in addition to small scale studies into energy consumption of specific buildings [41]. This limitation of data access extends into knowledge about existing electrical generators and thermal loads throughout the campus. These have been excluded from the scope of the study to this point. With these in mind, investments into consistent data tracking throughout the campus and knowledge of the different technologies currently available would provide significant insights into the specific consumptions of buildings and loads and greatly improve the accuracy of system designs and estimated costs. The benefits would further extend to the Oasis by enabling more accurate load shedding estimates and microgrid operation.

Should additional generation capacity be required, due to development of the campus or to accommodate a larger load than originally estimated or for some other unforeseen reason, it is recommended to expand the PV system. Given the weather patterns and solar GHI of the site, it provides the largest generation capacity increase per price compared to the other systems analyzed in this study. Additional PV capacity can be found from:

1. **Walkways** – Similar to the parking area, PV panels would provide a shaded structure above walking paths across the campus. This is considered separate from parking due to the added complexity of such a design creating a web-like structure across the campus.
2. **Miscellaneous** – Light posts that are not intrinsically part of the previous 3 categories or art installations similar to those found in Babcock Ranch [155] could provide a small amount of additional capacity to the system.

Regarding the microgrid, site specific installation costs have not been included to simplify the study. However, should a microgrid system be studied in further depth or financed for actual installation in PR, it is important to note that all component costs are anticipated to be higher than industry standards within the US market. This is due to the added import costs required to deliver the components from manufacturers abroad or in the US to the island. This will also likely incur a longer project installation time than normal. Along with these added barriers, an agreement between the UPRM microgrid managers and the electric utility company (LUMA/PREPA) must be made before initiating the detailed electrical design and construction of this proposed microgrid in accordance with IEEE Std. 1547-2018 [63]. The nameplate capacity cannot exceed 500kVA or it cannot have an annual average load demand greater than 10% of the aggregate DER nameplate rating at the point of connection (PoC) or the point of common coupling (PCC). More details surrounding this design constraint can be found in the standard [63].

As a result of the process of estimating the building loads for the Oasis, a document showcasing the hours of utilization of each building, represented as a percentage of total available time, has been obtained for the UPRM campus. Most of the rooms available to students have been found to be underutilized (with some cases of overutilization for Laboratories). While load shedding will allow the Oasis to provide disaster relief, it may come at the expense of student's ability to attend lectures in their chosen degree path due to limited availability. Two potential solutions to this problem are proposed here, although others may be available given the specifics of the campus:

1. Offer a re-worked school schedule where there are enough time slots throughout the day for students of different fields, years, and tracks to attend their courses in the available rooms (ex. Instead of school hours ranging from 7:30-18:00, the school hours can extend to 22:00).
2. Another alternative (and one that might result in more class participation overall) is to host all-online courses, where students can join a classroom with interdisciplinary participation. To this end, students from different backgrounds can participate in lectures using the same classrooms and campus internet to maximize the utilization of the rooms.

In addition to the Oasis scenarios already discussed in this study, another option is available to the campus that would allow increased demand control without the full investment into a microgrid. The Baratex

scenario introduces demand side management capabilities to the campus by adding in the load shedding capabilities outlined in Section 4.2.1, thereby enabling an overall reduction in energy demand based on the intended operating strategy (Table 41). This can be done during natural disasters to reduce the overall strain on the electrical grid when production is low and island-wide scheduled blackouts are mandated. Furthermore, it allows the campus to reduce the operating costs when the grid prices are at their highest by load-shedding specific buildings based on the priority levels in Section 3.2.1.2. The total campus demand for this scenario is the same as the PR100 scenario, 19,152 MWh per year and suffers equally from a disruption to the grid, resulting in an annual supply of 8,562 MWh.

*Table 41: Input considerations for each scenario including Baratex; Y includes the variable whereas N excludes the variable.*

Variable	Scenarios								
	BAU	PR100	Baratex	P4	PR100 P4	P3	PR100 P3	P2	PR100 P2
30% Energy Efficiency Improvement	N	Y	Y	N	Y	N	Y	N	Y
100% RE from Grid	N	Y	Y	N	Y	N	Y	N	Y
Demand Side Management	N	N	Y	Y	Y	Y	Y	Y	Y
Energy Storage	N	N	N	Y	Y	Y	Y	Y	Y
Solar	N	N	N	Y	Y	Y	Y	Y	Y
Wind	N	N	N	Y	Y	Y	Y	Y	Y
Biogas	N	N	N	Y	Y	Y	Y	Y	Y
Load-Shedding P4	N	N	Y	Y	Y	Y	Y	Y	Y
Load-Shedding P3	N	N	Y	N	N	Y	Y	Y	Y
Load-Shedding P2	N	N	Y	N	N	N	N	Y	Y
Oasis Services	N	N	N	Y	Y	Y	Y	Y	Y

## 7.2 Future Work

To fully understand the environmental impacts of the proposed microgrid, an LCA (cradle-to-grave) is recommended. The execution of an LCA, including the unique transportation requirements of construction on an island, and analyzing the results will provide a more accurate understanding of the emissions incurred by the components and their installation as well as those abated by the avoidance of electricity generated by the island's fossil fuel-heavy grid.

The Energy Oasis and microgrid have both been analyzed solely on a long-term, energy-oriented basis. Further studies are required to understand what components may be required for voltage- and frequency-control during operation. These studies will benefit greatly from more refined consumption data across the campus, as recommended above. Additionally, operation of the energy storage system from the recommended microgrid has not been manipulated or optimized for the purposes of the Energy Oasis. As such, subsequent analysis is required to understand what, if any, benefits may be obtained by improved battery management in the unique situation of an Energy Oasis. Other energy efficiency improvements, such as those outlined in the PR100 and the electrification of the campus transportation system, and their impacts on a microgrid design and/or Energy Oasis would also benefit from future, more detailed studies.

In analyzing the Oasis Score and adjusting its methodology another limitation has been identified. In its current state, the formulas used (both Equation 8 and Equation 25) only consider the flow going to the services in proportion to the total energy provided by the microgrid. It does not take into consideration the efficiency of the Oasis services. Further study and manipulation of the score calculation method is required to include efficiency measures, both for the efficiency of energy distribution as well as the efficiency of energy conversion into the services. Without this adjustment, utilization of the OS outlined in this study as a baseline for Oasis performance and optimization would result in the maximization of energy towards medical and cooking services, as they provided the largest impact towards the OS. Refining the OS would provide a greater value added to the energy cooperatives under development [30], [156] should they pursue a disaster relief component.

## Bibliography

- [1] “Puerto Rico Profile.” <https://www.eia.gov/state/print.php?sid=RQ> (accessed Mar. 28, 2023).
- [2] “For desperate Puerto Ricans, fuel a precious commodity,” *Reuters*, Sep. 27, 2017. Accessed: Mar. 28, 2023. [Online]. Available: <https://www.reuters.com/article/us-usa-puertorico-fuel-idUSKCN1C216B>
- [3] FEMA, “Hurricane Maria Update,” *FEMA*, Nov. 06, 2017. Accessed: Mar. 31, 2023. [Online]. Available: <https://www.fema.gov/press-release/20210318/hurricane-maria-update-0>
- [4] “Why Puerto Rico Has Struggled to Stabilize Its Electricity Grid,” *Bloomberg Government*, Sep. 30, 2022. <https://about.bgov.com/news/why-puerto-rico-has-struggled-to-stabilize-its-electricity-grid/> (accessed Mar. 28, 2023).
- [5] “How Texas failed to protect its power grid against extreme weather | The Texas Tribune.” <https://www.texastribune.org/2021/02/22/texas-power-grid-extreme-weather/> (accessed Mar. 28, 2023).
- [6] “Sistema de Energía Solar,” *Casa Pueblo • Puerto Rico*. <https://casapueblo.org/proyectos/sistema-de-energia-solar/> (accessed Mar. 28, 2023).
- [7] “Puerto Ricans are powering their own rooftop solar boom,” *Canary Media*, Jun. 08, 2022. <https://www.canarymedia.com/articles/solar/puerto-ricans-are-powering-their-own-rooftop-solar-boom> (accessed Mar. 28, 2023).
- [8] A. A. Irizarry-Rivera, J. A. Colucci-Ríos, and E. O’Neill-Carrillo, “Achievable Renewable Energy Targets for Puerto Rico’s Renewable Energy Portfolio Standard,” Puerto Rico’s Energy Affairs Administration, Puerto Rico, Nov. 2009. Accessed: Mar. 31, 2023. [Online]. Available: <https://www.uprm.edu/aret/>
- [9] A. A. Irizarry-Rivera, J. A. Colucci-Ríos, and E. O’Neill-Carrillo, “Achievable Renewable Energy Targets for Puerto Rico’s Renewable Energy Portfolio Standard Chapter 1,” Puerto Rico’s Energy Affairs Administration, Puerto Rico, Nov. 2009. [Online]. Available: <https://www.uprm.edu/aret/>
- [10] LUMA Energy, “Electric Energy Generation (Jan 2023).” *Nuestro Banco*, Jan. 2023. Accessed: Mar. 17, 2023. [Online]. Available: <https://www.bde.pr.gov/BDE/PRED.html>
- [11] S. Martinuzzi, W. A. Gould, and O. M. Ramos González, “Land development, land use, and urban sprawl in Puerto Rico integrating remote sensing and population census data,” *Landscape and Urban Planning*, vol. 79, no. 3, pp. 288–297, Mar. 2007, doi: 10.1016/j.landurbplan.2006.02.014.
- [12] M. M. McMahon, “Disasters and Poverty,” *Disaster Management & Response*, vol. 5, no. 4, pp. 95–97, Oct. 2007, doi: 10.1016/j.dmr.2007.09.001.
- [13] M. Simon, “Puerto Rico’s Path Toward Renewable Energy Development,” *Kleinman Center for Energy Policy*, May 18, 2022. <https://kleinmanenergy.upenn.edu/news-insights/puerto-ricos-path-toward-renewable-energy-development/> (accessed Mar. 03, 2023).
- [14] “DOE Launches Study To Consider Equitable Pathways To Power Puerto Rico With 100% Renewable Energy.” <https://www.nrel.gov/news/program/2022/doe-launches-study-to-consider-equitable-pathways-to-power-puerto-rico-with-100-renewable-energy.html> (accessed Mar. 28, 2023).
- [15] “Puerto Rico Grid Resilience and Transitions to 100% Renewable Energy Study (PR100),” *Energy.gov*. <https://www.energy.gov/gdo/puerto-rico-grid-resilience-and-transitions-100-renewable-energy-study-pr100> (accessed Mar. 30, 2023).
- [16] N. Blair *et al.*, “PR100 One-Year Progress Summary Report: Preliminary Modeling Results and High-Resolution Solar and Wind Data Sets,” NREL/TP-7A40-85018, 1922399, MainId:85791, Jan. 2023. doi: 10.2172/1922399.
- [17] “‘Puerto Rico Energy Public Policy Act’ [17-2019],” no. 17, 2021.
- [18] H. Ritchie, M. Roser, and P. Rosado, “Energy,” *Our World in Data*, Oct. 2022, Accessed: Jun. 15, 2023. [Online]. Available: <https://ourworldindata.org/energy-access>
- [19] “Is U.S. Energy Use Distributed as Unequally as Our Wealth?,” *Environment*, Mar. 12, 2013. <https://www.nationalgeographic.com/environment/article/is-energy-use-distributed-as-unequally-as-our-wealth> (accessed Mar. 31, 2023).

- [20] D. Trimble and A. Massol-Deyá, “Press Release: Casa Pueblo and ACESA are transforming Adjuntas into the first ‘Pueblo Solar,’” *Honnold Foundation*, Oct. 20, 2020. <https://www.honnoldfoundation.org/news/press-release-casa-pueblo-and-small-business-owners-advance-their-vision-of-transforming-the-town-of-adjuntas-into-the-first-pueblo-solar> (accessed Mar. 22, 2023).
- [21] “Microgrids.” <https://www.nrel.gov/grid/microgrids.html> (accessed Feb. 08, 2023).
- [22] M. Gandiglio, P. Marocco, I. Bianco, D. Lovera, G. A. Blengini, and M. Santarelli, “Life cycle assessment of a renewable energy system with hydrogen-battery storage for a remote off-grid community,” *International Journal of Hydrogen Energy*, vol. 47, no. 77, pp. 32822–32834, Sep. 2022, doi: 10.1016/j.ijhydene.2022.07.199.
- [23] M. Li, X. Zhang, G. Li, and C. Jiang, “A feasibility study of microgrids for reducing energy use and GHG emissions in an industrial application,” *Applied Energy*, vol. 176, pp. 138–148, Aug. 2016, doi: 10.1016/j.apenergy.2016.05.070.
- [24] A. Monforti Ferrario *et al.*, “A model-based parametric and optimal sizing of a battery/hydrogen storage of a real hybrid microgrid supplying a residential load: Towards island operation,” *Advances in Applied Energy*, vol. 3, p. 100048, Aug. 2021, doi: 10.1016/j.adapen.2021.100048.
- [25] B. Jenkins *et al.*, “Techno-Economic Analysis of Low Carbon Hydrogen Production from Offshore Wind Using Battolyser Technology,” *Energies*, vol. 15, no. 16, Art. no. 16, Jan. 2022, doi: 10.3390/en15165796.
- [26] P. Marocco, D. Ferrero, A. Lanzini, and M. Santarelli, “The role of hydrogen in the optimal design of off-grid hybrid renewable energy systems,” *Journal of Energy Storage*, vol. 46, p. 103893, Feb. 2022, doi: 10.1016/j.est.2021.103893.
- [27] P. Marocco *et al.*, “A study of the techno-economic feasibility of H<sub>2</sub>-based energy storage systems in remote areas,” *Energy Conversion and Management*, vol. 211, p. 112768, May 2020, doi: 10.1016/j.enconman.2020.112768.
- [28] Z. Shahid, M. Santarelli, P. Marocco, D. Ferrero, and U. Zahid, “Techno-economic feasibility analysis of Renewable-fed Power-to-Power (P2P) systems for small French islands,” *Energy Conversion and Management*, vol. 255, p. 115368, Mar. 2022, doi: 10.1016/j.enconman.2022.115368.
- [29] ISO, “ISO 50001 - Energy management systems.” International Organization for Standardization, Oct. 20, 2021. Accessed: Mar. 28, 2023. [Online]. Available: <https://www.iso.org/publication/PUB100400.html>
- [30] “Public Utility Regulatory Policies Act of 1978 (PURPA),” *Energy.gov*. <https://www.energy.gov/oe/public-utility-regulatory-policies-act-1978-purpa> (accessed Mar. 31, 2023).
- [31] “Hydrogen Standard 1910.103,” *Occupational Safety and Health Administration*. <https://www.osha.gov/laws-regs/regulations/standardnumber/1910/1910.103> (accessed Mar. 31, 2023).
- [32] E. O’Neill-Carrillo, I. Jordan, A. Irizarry-Rivera, and R. Cintron, “The Long Road to Community Microgrids: Adapting to the Necessary Changes for Renewable Energy Implementation,” *IEEE Electrification Magazine*, vol. 6, no. 4, pp. 6–17, Dec. 2018, doi: 10.1109/MELE.2018.2871239.
- [33] M. Lave, J. Kleissl, A. Ellis, and F. Mejia, “Simulated PV power plant variability: Impact of utility-imposed ramp limitations in Puerto Rico,” in *2013 IEEE 39th Photovoltaic Specialists Conference (PVSC)*, Jun. 2013, pp. 1817–1821. doi: 10.1109/PVSC.2013.6744495.
- [34] A. Paspatis, K. Fiorentzis, Y. Katsigiannis, and E. Karapidakis, “Smart Campus Microgrids towards a Sustainable Energy Transition—The Case Study of the Hellenic Mediterranean University in Crete,” *Mathematics*, vol. 10, no. 7, p. 1065, Mar. 2022, doi: 10.3390/math10071065.
- [35] Carmen, “FPL Babcock Ranch Solar Energy Center, US,” *Power Technology*, Dec. 16, 2021. <https://www.power-technology.com/marketdata/fpl-babcock-ranch-solar-energy-center-us/> (accessed Mar. 22, 2023).
- [36] “Babcock Ranch - Current Coastal Realty.” <https://currentcoastalrealty.com/neighborhoods/babcock-ranch> (accessed Mar. 22, 2023).



- [37] C. M. Marcos and E. P. Rodriguez, "Solar Power Offers Puerto Ricans a Lifeline but Remains an Elusive Goal," *The New York Times*, May 09, 2022. Accessed: Mar. 22, 2023. [Online]. Available: <https://www.nytimes.com/2022/05/09/business/energy-environment/puerto-rico-solar-power.html>
- [38] M. Husein and I.-Y. Chung, "Optimal design and financial feasibility of a university campus microgrid considering renewable energy incentives," *Applied Energy*, vol. 225, pp. 273–289, Sep. 2018, doi: 10.1016/j.apenergy.2018.05.036.
- [39] R. Jing, X. Wang, Y. Zhao, Y. Zhou, J. Wu, and J. Lin, "Planning urban energy systems adapting to extreme weather," *Advances in Applied Energy*, vol. 3, p. 100053, Aug. 2021, doi: 10.1016/j.adapen.2021.100053.
- [40] D. Cordero, M. Farhat, B. Fickes, J. Pruitt, and S. Sardag, "Biomass Residue-Fueled Micro-Grid for a Rural Community in Puerto Rico," Project, University of Michigan, 2019. Accessed: Feb. 25, 2023. [Online]. Available: <https://hdl.handle.net/2027.42/148833>
- [41] Y. V. Garcia, O. Garzon, F. Andrade, A. Irizarry, and O. F. Rodriguez-Martinez, "Methodology to Implement a Microgrid in a University Campus," *Applied Sciences*, vol. 12, no. 9, Art. no. 9, Jan. 2022, doi: 10.3390/app12094563.
- [42] G. A. Carrión, R. A. Cintrón, M. A. Rodríguez, W. E. Sanabria, R. Reyes, and E. O'Neill-Carrillo, "Community Microgrids to Increase Local Resiliency," in *2018 IEEE International Symposium on Technology and Society (ISTAS)*, Nov. 2018, pp. 1–7. doi: 10.1109/ISTAS.2018.8638269.
- [43] F. L. Inca, "Essential adaptive protection for potential UPRM microgrid system," Thesis, 2021. Accessed: Mar. 30, 2023. [Online]. Available: <https://scholar.uprm.edu/handle/20.500.11801/2798>
- [44] "Preparing Solar Photovoltaic Systems Against Storms", [Online]. Available: <https://www.nrel.gov/docs/fy22osti/83117.pdf>
- [45] Q. Jin and V. C. Li, "Structural and durability assessment of ECC/concrete dual-layer system for tall wind turbine towers," *Engineering Structures*, vol. 196, p. 109338, Oct. 2019, doi: 10.1016/j.engstruct.2019.109338.
- [46] J. Montesano, H. Chu, and C. V. Singh, "Development of a physics-based multi-scale progressive damage model for assessing the durability of wind turbine blades," *Composite Structures*, vol. 141, pp. 50–62, May 2016, doi: 10.1016/j.compstruct.2016.01.011.
- [47] A. Malave, J. Montanez, and M. Nunez, *Optimization of Hurricane Resistance Wind Turbine Blades*. 2019. doi: 10.18687/LACCEI2019.1.1.344.
- [48] H. Xie *et al.*, "A membrane-based seawater electrolyser for hydrogen generation," *Nature*, vol. 612, no. 7941, Art. no. 7941, Dec. 2022, doi: 10.1038/s41586-022-05379-5.
- [49] P. Patel, "Seawater-to-Hydrogen Tech Makes a New, Blue H2 - IEEE Spectrum," Dec. 14, 2022. Accessed: Mar. 31, 2023. [Online]. Available: <https://spectrum.ieee.org/electrolysis-of-seawater>
- [50] E. O'Neill-Carrillo and A. Irizarry-Rivera, "How to Harden Puerto Rico's grid against hurricanes," *IEEE Spectrum*, vol. 56, no. 11, pp. 42–48, Nov. 2019, doi: 10.1109/MSPEC.2019.8889972.
- [51] E. Rothschild, "Solar survives the storms in Puerto Rico," *pv magazine USA*, Nov. 07, 2017. <https://pv-magazine-usa.com/2017/11/07/solar-survives-the-storms-in-puerto-rico/> (accessed Mar. 03, 2023).
- [52] J. A. Bennett *et al.*, "Extending energy system modelling to include extreme weather risks and application to hurricane events in Puerto Rico," *Nat Energy*, vol. 6, no. 3, Art. no. 3, Mar. 2021, doi: 10.1038/s41560-020-00758-6.
- [53] N. Nhede, "Disaster preparedness - Microgrids and their benefits during a disaster," *Smart Energy International*, Mar. 31, 2020. <https://www.smart-energy.com/industry-sectors/energy-grid-management/the-big-benefits-of-microgrids-in-disaster/> (accessed Mar. 31, 2023).
- [54] L. Flanagan, "Disaster Response DERs Are a Logical Choice for Companies and Government," *Microgrid Knowledge*, Oct. 19, 2021. <https://www.microgridknowledge.com/resources/microgrid-perspectives/article/11427664/disaster-response-ders-are-a-logical-choice-for-companies-and-government> (accessed Mar. 31, 2023).

- [55] M. Ilic, R. S. Ulerio, E. Corbett, E. Austin, M. Shatz, and E. Limpaecher, “A Framework for Evaluating Electric Power Grid Improvements in Puerto Rico”.
- [56] FEMA, “National Disaster Recovery Framework, Second Edition.” Department of Homeland Security, Jun. 2016.
- [57] Vizzuality, “Puerto Rico Deforestation Rates & Statistics | GFW.” <https://www.globalforestwatch.org/dashboards/country/PRI?category=fires> (accessed Mar. 23, 2023).
- [58] J. P. Kossin, K. R. Knapp, T. L. Olander, and C. S. Velden, “Global increase in major tropical cyclone exceedance probability over the past four decades,” *Proceedings of the National Academy of Sciences*, vol. 117, no. 22, pp. 11975–11980, Jun. 2020, doi: 10.1073/pnas.1920849117.
- [59] “Hurricane Season in Puerto Rico (What to Know, By a Local) - Travel Lemming,” Jan. 06, 2022. <https://travellemming.com/hurricane-season-in-puerto-rico/> (accessed Feb. 08, 2023).
- [60] A. Wachtel, D. Melander, and O. Hart, “ReNCAT: The Resilient Node Cluster Analysis Tool,” SAND2022-10888R, 1880920, 709019, Aug. 2022. doi: 10.2172/1880920.
- [61] “Resiliency Scorecard and Microgrid Stabilization.” Accessed: Mar. 30, 2023. [Online]. Available: <https://www.cpuc.ca.gov/-/media/cpuc-website/divisions/energy-division/documents/resiliency-and-microgrids/resiliency-and-microgrids-events-and-materials/20210617vorpillar3resilscorerencatpresentation.pdf>
- [62] “CommunityLifelinesToolkit2.0v2.pdf.” Accessed: Mar. 30, 2023. [Online]. Available: <https://www.fema.gov/sites/default/files/2020-05/CommunityLifelinesToolkit2.0v2.pdf>
- [63] “IEEE Standard for Interconnection and Interoperability of Distributed Energy Resources with Associated Electric Power Systems Interfaces,” *IEEE Std 1547-2018 (Revision of IEEE Std 1547-2003)*, pp. 1–138, Apr. 2018, doi: 10.1109/IEEESTD.2018.8332112.
- [64] V. M. Maestre, A. Ortiz, and I. Ortiz, “Transition to a low-carbon building stock. Techno-economic and spatial optimization of renewables-hydrogen strategies in Spain,” *Journal of Energy Storage*, vol. 56, p. 105889, Dec. 2022, doi: 10.1016/j.est.2022.105889.
- [65] M. Rezaeimozafar, R. F. D. Monaghan, E. Barrett, and M. Duffy, “A review of behind-the-meter energy storage systems in smart grids,” *Renewable and Sustainable Energy Reviews*, vol. 164, p. 112573, Aug. 2022, doi: 10.1016/j.rser.2022.112573.
- [66] “How Long Does It Take to Install Solar Panels? | Boston Solar | MA.” <https://www.bostonsolar.us/solar-blog-resource-center/blog/how-long-does-it-take-to-install-solar-panels/> (accessed Mar. 31, 2023).
- [67] S. Ghose and M. J. Franchetti, “Chapter 11 - Economic Aspects of Food Waste-to-Energy System Deployment,” in *Sustainable Food Waste-To-energy Systems*, T. A. Trabold and C. W. Babbitt, Eds., Academic Press, 2018, pp. 203–229. doi: 10.1016/B978-0-12-811157-4.00011-5.
- [68] NREL, “Annual Technology Baseline: Definitions,” *Annual Technology Baseline*. <https://public.tableau.com/views/2022FinancialsLCOE/LandingDetail?embed=y&:showVizHome=n&:bootstrapWhenNotified=y&:apiID=handler0> (accessed May 31, 2023).
- [69] “HOMER Pro - Microgrid Software for Designing Optimized Hybrid Microgrids.” <https://www.homerenergy.com/products/pro/index.html> (accessed Mar. 03, 2023).
- [70] M. Kottek, J. Grieser, C. Beck, B. Rudolf, and F. Rubel, “World Map of the Köppen-Geiger climate classification updated,” *metz*, vol. 15, no. 3, pp. 259–263, Jul. 2006, doi: 10.1127/0941-2948/2006/0130.
- [71] Google, “Google Earth.” <https://earth.google.com/web/> (accessed Mar. 03, 2023).
- [72] “Mayagüez Climate, Weather By Month, Average Temperature (Puerto Rico) - Weather Spark.” <https://weatherspark.com/y/27582/Average-Weather-in-Mayag%C3%BCez-Puerto-Rico-Year-Round#Sections-Clouds> (accessed Mar. 04, 2023).
- [73] “NSRDB.” Accessed: Mar. 28, 2023. [Online]. Available: <https://nsrdb.nrel.gov/>
- [74] NASA, “POWER | Data Access Viewer.” <https://power.larc.nasa.gov/data-access-viewer/> (accessed Jun. 01, 2023).

- [75] A. Aslam, N. Ahmed, S. A. Qureshi, M. Assadi, and N. Ahmed, “Advances in Solar PV Systems; A Comprehensive Review of PV Performance, Influencing Factors, and Mitigation Techniques,” *Energies*, vol. 15, no. 20, Art. no. 20, Jan. 2022, doi: 10.3390/en15207595.
- [76] Jinko Solar, “Jinko Solar Tiger Pro 72H Module Datasheet.” Jinko Solar, 2022. Accessed: Mar. 03, 2023. [Online]. Available: [https://jinkosolarcdn.shwebspace.com/uploads/63da19e2/JKM540-560M-72HL4-\(V\)-F3-EN.pdf](https://jinkosolarcdn.shwebspace.com/uploads/63da19e2/JKM540-560M-72HL4-(V)-F3-EN.pdf)
- [77] LA Solar, “LA Solar Half Cell Module Datasheet.” LA Solar Inc. Accessed: Apr. 06, 2023. [Online]. Available: <https://lasolarfactory.com/files/1b62cae8fc624f8d4b4cad94de192d83.pdf>
- [78] Phono Solar, “Phono Solar TwinPlus Series Module Datasheet.” Phono Solar Inc. Accessed: Apr. 06, 2023. [Online]. Available: <http://www.phonosolar.com/static/upload/file/20221226/1671989481485434.pdf>
- [79] R. G. Ross, Jr., “Design Tech for Flat-Plate Photovoltaic Arrays,” presented at the The 15th Photovoltaic Specialists Conference, Orlando, Florida, May 1981, p. 7. Accessed: Apr. 10, 2023. [Online]. Available: [https://www2.jpl.nasa.gov/adv\\_tech/photovol/ppr\\_81-85/Design%20Tech%20for%20FP%20PV%20Arrays\\_PVSC1981.pdf](https://www2.jpl.nasa.gov/adv_tech/photovol/ppr_81-85/Design%20Tech%20for%20FP%20PV%20Arrays_PVSC1981.pdf)
- [80] Sollega Inc., “Sollega FastRack 510-6 Datasheet\_UL3741\_230109.” Sollega, Inc. Accessed: Feb. 08, 2023. [Online]. Available: [https://sollega.com/downloads/fr510/Sollega%20FastRack%20510-6%20Datasheet\\_UL3741\\_230109.pdf](https://sollega.com/downloads/fr510/Sollega%20FastRack%20510-6%20Datasheet_UL3741_230109.pdf)
- [81] Sollega Inc., “Solar racking solutions made simple - Sollega,” *Sollega*. <https://sollega.com/> (accessed Apr. 07, 2023).
- [82] V. Ramasamy *et al.*, “U.S. Solar Photovoltaic System and Energy Storage Cost Benchmarks, With Minimum Sustainable Price Analysis: Q1 2022,” NREL/TP-7A40-83586, 1891204, MainId:84359, Sep. 2022. doi: 10.2172/1891204.
- [83] LA Solar Group, “Solar Warranty | 25 Year Warranty Solar Panels,” *LA Solar Group*. <https://lasolargroup.com/solar-warranty/> (accessed Apr. 11, 2023).
- [84] “2022 Cost Components,” *Tableau Software*. <https://public.tableau.com/views/2022CostComponents/CostComponents?:embed=y&:toolbar=no&Technology=CommPV&:embed=y&:showVizHome=n&:bootstrapWhenNotified=y&:apiID=handler2> (accessed Apr. 12, 2023).
- [85] Google, “Project Sunroof,” *Google Project Sunroof*. <https://sunroof.withgoogle.com/> (accessed Apr. 15, 2023).
- [86] S. Asgeirsson, “IceWind RW600 Performance,” Feb. 07, 2023.
- [87] IceWind, “IceWind RW500 Datasheet Rev. 2.” Accessed: May 05, 2023. [Online]. Available: <https://icewind.is/wp-content/uploads/2020/08/rw-500-Icewind-wind-turbine.-Mil.pdf>
- [88] IceWind, “Industrial – ICEWIND.” <https://icewind.is/industrial/> (accessed May 05, 2023).
- [89] T. Stehly and P. Duffy, “2021 Cost of Wind Energy Review,” Dec. 2022. [Online]. Available: <https://www.nrel.gov/docs/fy23osti/84774.pdf>
- [90] NREL, “Annual Technology Baseline: Distributed Wind,” *Tableau Software*, Jul. 21, 2022. <https://public.tableau.com/views/2022CMTS/TechSummary?:embed=y&:toolbar=no&Technology=DistributedWind&:embed=y&:showVizHome=n&:bootstrapWhenNotified=y&:apiID=handler0> (accessed May 16, 2023).
- [91] P. Denholm, M. Hand, M. Jackson, and S. Ong, “Land Use Requirements of Modern Wind Power Plants in the United States,” NREL/TP-6A2-45834, 964608, Aug. 2009. doi: 10.2172/964608.
- [92] R. C. Bansal, T. S. Bhatti, and D. P. Kothari, “On some of the design aspects of wind energy conversion systems,” *Energy Conversion and Management*, vol. 43, no. 16, pp. 2175–2187, Nov. 2002, doi: 10.1016/S0196-8904(01)00166-2.
- [93] Danish Wind Industry Association, “Park Effect,” *Danish Wind Industry Association*, Jun. 01, 2003. <http://www.xn--drmsttre-64ad.dk/wp-content/wind/miller/windpower%20web/en/tour/wres/park.htm> (accessed May 16, 2023).

- [94] Environmental Quality Board, *Regulation of the Environmental Quality Board for the Control of Noise Pollution Ammended Version*. 1970. Accessed: May 16, 2023. [Online]. Available: <http://app.estado.gobierno.pr/ReglamentosOnLine/Reglamentos/2809ING.pdf>
- [95] V. Katinas, M. Marciukaitis, and M. Tamašauskienė, “Analysis of the wind turbine noise emissions and impact on the environment,” *Renewable and Sustainable Energy Reviews*, vol. 58, pp. 825–831, May 2016, doi: 10.1016/j.rser.2015.12.140.
- [96] Jagdish, “Mango Farming, Cultivation (Aam) Guide for Beginners | Agri Farming,” *Agri Farming*, Jun. 21, 2019. <https://www.agrifarming.in/mango-farming> (accessed May 26, 2023).
- [97] “2008 Ford F-450 Specs, Trims & Colors,” *Cars.com*. [https://www.cars.com/research/ford-f\\_450-2008/specs](https://www.cars.com/research/ford-f_450-2008/specs) (accessed May 26, 2023).
- [98] EPA Office of Resource Conservation and Recovery, “Volume-To-Weight Conversion Factors,” U.S. Environmental Protection Agency, Apr. 2016. Accessed: May 26, 2023. [Online]. Available: [https://www.epa.gov/sites/default/files/2016-04/documents/volume\\_to\\_weight\\_conversion\\_factors\\_memorandum\\_04192016\\_508fnl.pdf](https://www.epa.gov/sites/default/files/2016-04/documents/volume_to_weight_conversion_factors_memorandum_04192016_508fnl.pdf)
- [99] S. Anderson *et al.*, “Generacion Circular: Hacia una economia circular,” Puerto Rico, Version 1.0, Jun. 2021. Accessed: May 26, 2023. [Online]. Available: [https://www.generacioncircular.org/wp-content/uploads/2021/06/GenC\\_Gui%CC%81a-de-Manejo\\_FINAL\\_06042021.pdf](https://www.generacioncircular.org/wp-content/uploads/2021/06/GenC_Gui%CC%81a-de-Manejo_FINAL_06042021.pdf)
- [100] L. Mu, L. Zhang, K. Zhu, J. Ma, M. Ifran, and A. Li, “Anaerobic co-digestion of sewage sludge, food waste and yard waste: Synergistic enhancement on process stability and biogas production,” *Science of The Total Environment*, vol. 704, p. 135429, Feb. 2020, doi: 10.1016/j.scitotenv.2019.135429.
- [101] S. Sukarni, “Exploring the potential of municipal solid waste (MSW) as solid fuel for energy generation: Case study in the Malang City, Indonesia,” presented at the PROCEEDINGS OF THE INTERNATIONAL MECHANICAL ENGINEERING AND ENGINEERING EDUCATION CONFERENCES (IMEEEEC 2016), East Java, Indonesia, 2016, p. 020003. doi: 10.1063/1.4965733.
- [102] M. Taylor, P. Ralon, and S. Al-Zoghoul, “Renewable power generation costs in 2021,” IRENA, Abu Dhabi, 2022. [Online]. Available: [https://www.irena.org/-/media/Files/IRENA/Agency/Publication/2022/Jul/IRENA\\_Power\\_Generation\\_Costs\\_2021.pdf?rev=34c22a4b244d434da0accde7de7c73d8](https://www.irena.org/-/media/Files/IRENA/Agency/Publication/2022/Jul/IRENA_Power_Generation_Costs_2021.pdf?rev=34c22a4b244d434da0accde7de7c73d8)
- [103] IRENA, “Renewable Power Generation Costs in 2021.” 2022.
- [104] A. A. Irizarry-Rivera, J. A. Colucci-Ríos, and E. O’Neill-Carrillo, “Achievable Renewable Energy Targets for Puerto Rico Chapter 3 Ocean,” Puerto Rico’s Energy Affairs Administration, Puerto Rico, Nov. 2009. Accessed: Apr. 15, 2023. [Online]. Available: [https://www.uprm.edu/aret/docs/Ch\\_3\\_Ocean.pdf](https://www.uprm.edu/aret/docs/Ch_3_Ocean.pdf)
- [105] M. F. Canals Silander and C. G. García Moreno, “On the spatial distribution of the wave energy resource in Puerto Rico and the United States Virgin Islands,” *Renewable Energy*, vol. 136, pp. 442–451, Jun. 2019, doi: 10.1016/j.renene.2018.12.120.
- [106] L. Kilcher, M. Fogarty, and M. Lawson, “Marine Energy in the United States: An Overview of Opportunities,” National Renewable Energy Lab. (NREL), Golden, CO (United States), NREL/TP-5700-78773, Feb. 2021. doi: 10.2172/1766861.
- [107] R. Shirley and D. Kammen, “Renewable energy sector development in the Caribbean: Current trends and lessons from history,” *Energy Policy*, vol. 57, pp. 244–252, Jun. 2013, doi: 10.1016/j.enpol.2013.01.049.
- [108] R. N. Anderson and D. K. Larue, “Wellbore heat flow from the Toa Baja Scientific Drillhole, Puerto Rico,” *Geophysical Research Letters*, vol. 18, no. 3, pp. 537–540, 1991, doi: 10.1029/91GL00391.
- [109] B. Rohena, “Developing geothermal power in Puerto Rico: Cost benefit analysis and barriers for development,” Master’s Thesis, Utrecht University, Utrecht, Netherlands, 2014. [Online]. Available: <https://studenttheses.uu.nl/handle/20.500.12932/33177>
- [110] N. US Department of Commerce, “PR and USVI Normals.” [https://www.weather.gov/sju/climo\\_pr\\_usvi\\_normals](https://www.weather.gov/sju/climo_pr_usvi_normals) (accessed Apr. 15, 2023).
- [111] A. A. Irizarry-Rivera, J. A. Colucci-Ríos, and E. O’Neill-Carrillo, “Achievable Renewable Energy Targets for Puerto Rico’s Renewable Energy Portfolio Standard Chapter 8 Micro Hydro,” Puerto

- Rico's Energy Affairs Administration, Puerto Rico, Nov. 2009. [Online]. Available: [https://www.uprm.edu/aret/docs/Ch\\_8\\_Micro\\_hydro.pdf](https://www.uprm.edu/aret/docs/Ch_8_Micro_hydro.pdf)
- [112] USGS, "USGS | National Water Dashboard." <https://dashboard.waterdata.usgs.gov> (accessed Apr. 15, 2023).
- [113] J. Salasovich and G. Mosey, "Feasibility Study of Economics and Performance of Solar Photovoltaics in the Commonwealth of Puerto Rico," NREL/TP-6A20-49237, 1013267, Mar. 2011. doi: 10.2172/1013267.
- [114] A. A. Kebede, T. Kalogiannis, J. Van Mierlo, and M. Berecibar, "A comprehensive review of stationary energy storage devices for large scale renewable energy sources grid integration," *Renewable and Sustainable Energy Reviews*, vol. 159, p. 112213, May 2022, doi: 10.1016/j.rser.2022.112213.
- [115] W. Waag and D. U. Sauer, "SECONDARY BATTERIES – LEAD– ACID SYSTEMS | State-of-Charge/Health," in *Encyclopedia of Electrochemical Power Sources*, J. Garche, Ed., Amsterdam: Elsevier, 2009, pp. 793–804. doi: 10.1016/B978-044452745-5.00149-0.
- [116] SCU Power, "High Power Lithium Battery, High Energy Density Lithium Batteries | SCU," <https://www.scupower.com/>. <https://www.scupower.com/lithium-ion-battery/high-energy-density-lithium-batteries/> (accessed May 28, 2023).
- [117] Energetech Solar, "Energy Storage System - 1MWh 500V-800V," *Energetech Solar*. <https://energetechsolar.com/1mwh-500v-800v-battery-energy-storage-system> (accessed May 28, 2023).
- [118] Intilion, "intilion Scalecube Product Sheet v.2." Intilion. Accessed: May 28, 2023. [Online]. Available: <https://intilion.com/documents/general/Product-Sheet-INTILION-scalecube.pdf>
- [119] K. Mongird *et al.*, "Energy Storage Technology and Cost Characterization Report," HydroWIRES, Jul. 2019.
- [120] X. Luo, J. Wang, M. Dooner, and J. Clarke, "Overview of current development in electrical energy storage technologies and the application potential in power system operation," *Applied Energy*, vol. 137, pp. 511–536, Jan. 2015, doi: 10.1016/j.apenergy.2014.09.081.
- [121] R. Wittman, "Side by Side Comparison of Redox Flow and Li-ion Batteries," Jun. 01, 2021. Accessed: May 28, 2023. [Online]. Available: <https://www.osti.gov/servlets/purl/1876722/>
- [122] CellCube, "The CellCube system," *Cellcube*. <https://www.cellcube.com/the-cellcube-system/> (accessed May 27, 2023).
- [123] P. Bocek, "Datasheet CellCube Rel.4.0 Family\_V2.0." CellCube, 2022. [Online]. Available: [https://www.cellcube.com/wp-content/uploads/2022/09/Datasheet-CellCube-Rel.4.0-Family\\_V2.0.pdf](https://www.cellcube.com/wp-content/uploads/2022/09/Datasheet-CellCube-Rel.4.0-Family_V2.0.pdf)
- [124] K. Hu *et al.*, "Comparative study of alkaline water electrolysis, proton exchange membrane water electrolysis and solid oxide electrolysis through multiphysics modeling," *Applied Energy*, vol. 312, p. 118788, Apr. 2022, doi: 10.1016/j.apenergy.2022.118788.
- [125] T. B. Nur and M. M. Harahap, "Prediction of the monthly cost of energy usage by PEMFC at housing in North Sumatra Province, Indonesia," *IOP Conf. Ser.: Earth Environ. Sci.*, vol. 927, no. 1, p. 012035, Dec. 2021, doi: 10.1088/1755-1315/927/1/012035.
- [126] IEA, "Global Hydrogen Review 2022," International Energy Agency, 2022. [Online]. Available: <https://iea.blob.core.windows.net/assets/c5bc75b1-9e4d-460d-9056-6e8e626a11c4/GlobalHydrogenReview2022.pdf>
- [127] L. Tribioli and R. Cozzolino, "Techno-economic analysis of a stand-alone microgrid for a commercial building in eight different climate zones," *Energy Conversion and Management*, vol. 179, pp. 58–71, Jan. 2019, doi: 10.1016/j.enconman.2018.10.061.
- [128] S. Hirodantis, S. Ioannou, and M. Raspopoulos, *LOAD SHEDDING SCHEMES FOR ISLANDING DISTRIBUTION NETWORK OPERATION*. 2020. doi: 10.1049/icp.2021.1268.
- [129] B. Kroposki, T. Basso, and R. DeBlasio, "Microgrid standards and technologies," in *2008 IEEE Power and Energy Society General Meeting - Conversion and Delivery of Electrical Energy in the 21st Century*, Jul. 2008, pp. 1–4. doi: 10.1109/PES.2008.4596703.

- [130] Texas Electrical Code, “Texas Electrical Code 2020: Chapter 7 Article 705,” *UpCodes*, Jan. 11, 2020. <https://up.codes/s/interconnected-electric-power-production-sources> (accessed Jul. 02, 2023).
- [131] K. Bawaneh, F. Ghazi Nezami, M. Rasheduzzaman, and B. Deken, “Energy Consumption Analysis and Characterization of Healthcare Facilities in the United States,” *Energies*, vol. 12, no. 19, Art. no. 19, Jan. 2019, doi: 10.3390/en12193775.
- [132] “Required Space per Person,” *Engineering Toolbox*. [https://www.engineeringtoolbox.com/number-persons-buildings-d\\_118.html](https://www.engineeringtoolbox.com/number-persons-buildings-d_118.html) (accessed Jun. 20, 2023).
- [133] “Solutions: Solar Powered Desalination Plug & Play - Sustainable Water,” *Elemental Water Makers*. <https://www.elementalwatermakers.com/solutions/plug-play-solar-desalination/> (accessed Jun. 21, 2023).
- [134] M. N. Sawka, S. N. Chevront, and R. Carter Iii, “Human Water Needs,” *Nutrition Reviews*, vol. 63, no. suppl\_1, pp. S30–S39, Jun. 2005, doi: 10.1111/j.1753-4887.2005.tb00152.x.
- [135] “How much water should I drink each day?,” Jul. 09, 2018. <https://www.medicalnewstoday.com/articles/306638> (accessed Jun. 21, 2023).
- [136] “Fuels - Higher and Lower Calorific Values.” [https://www.engineeringtoolbox.com/fuels-higher-calorific-values-d\\_169.html](https://www.engineeringtoolbox.com/fuels-higher-calorific-values-d_169.html) (accessed Jun. 21, 2023).
- [137] “Energy Star Guide for Cafes, Restaurants, and Institutional Kitchens.” [https://www.energystar.gov/sites/default/files/asset/document/CR%20ES%20Restaurant%20Guide%202015%20v8\\_0.pdf](https://www.energystar.gov/sites/default/files/asset/document/CR%20ES%20Restaurant%20Guide%202015%20v8_0.pdf) (accessed Jun. 21, 2023).
- [138] RDT, “Restaurant Energy Consumption Statistics and the High Cost of Energy.” <https://solutions.rdtonline.com/blog/restaurant-energy-consumption-statistics> (accessed Jun. 21, 2023).
- [139] “About the Commercial Buildings Energy Consumption Survey (CBECS),” *Energy Information Administration*. <https://www.eia.gov/consumption/commercial/data/2012/c&e/cfm/pba4.php> (accessed Jun. 21, 2023).
- [140] H. Vella, “5G vs 4G: what is the real difference between them?,” *Raconteur*, Feb. 17, 2022. <https://www.raconteur.net/technology/4g-vs-5g-mobile-technology/> (accessed Jun. 21, 2023).
- [141] S. Tombaz, P. Frenger, M. Olsson, and A. Nilsson, “Energy performance of 5G-NX radio access at country level,” in *2016 IEEE 12th International Conference on Wireless and Mobile Computing, Networking and Communications (WiMob)*, Oct. 2016, pp. 1–6. doi: 10.1109/WiMOB.2016.7763183.
- [142] “Upgrading cell towers could save enough energy to power entire cities | Computerworld.” <https://www.computerworld.com/article/3668168/upgrading-cell-towers-could-save-enough-energy-to-power-entire-cities.html> (accessed Jun. 21, 2023).
- [143] L. Williams, B. K. Sovacool, and T. J. Foxon, “The energy use implications of 5G: Reviewing whole network operational energy, embodied energy, and indirect effects,” *Renewable and Sustainable Energy Reviews*, vol. 157, p. 112033, Apr. 2022, doi: 10.1016/j.rser.2021.112033.
- [144] “Iem, cell on wheels with 12m telescopic mast» MOBISTAT» Calzavara,” *Calzavara*. <https://calzavara.it/cow-cell-on-wheels-cell-towers/cow-cell-on-wheels-lem/> (accessed Jun. 21, 2023).
- [145] “Emergency Communications Systems Value Analysis Guide,” 2020.
- [146] “Government Emergency Telecommunications Service (GETS) | CISA.” <https://www.cisa.gov/resources-tools/services/government-emergency-telecommunications-service-gets> (accessed Jun. 21, 2023).
- [147] N. Kishore *et al.*, “Mortality in Puerto Rico after Hurricane Maria,” *New England Journal of Medicine*, vol. 379, no. 2, pp. 162–170, Jul. 2018, doi: 10.1056/NEJMsa1803972.
- [148] “Hydrogen Safety, Codes and Standards,” *Energy.gov*. <https://www.energy.gov/eere/fuelcells/safety-codes-and-standards> (accessed Mar. 31, 2023).
- [149] F. Dittberner, “Mobile Emergency Room Facilities,” *Mobile Healthcare Facilities LLC*. <https://mhcfac.com/facilities/mobile-emergency-room-facilities/> (accessed Jul. 04, 2023).



- [150] v2aweb, “The disparity in hospital quality metrics between Puerto Rico and the US,” *V2A*, Dec. 02, 2019. <https://v2aconsulting.com/the-disparity-in-hospital-quality-metrics-between-puerto-rico-and-the-us/> (accessed Jul. 04, 2023).
- [151] “About the Commercial Buildings Energy Consumption Survey (CBECS).” <https://www.eia.gov/consumption/commercial/data/2012/c&e/cfm/pba4.php> (accessed Jul. 04, 2023).
- [152] EIA, “Puerto Rico: Territory Energy Profile Data,” *Puerto Rico: Territory Profile and Energy Estimates*, Jun. 15, 2023. <https://www.eia.gov/state/data.php?sid=RQ> (accessed Jun. 17, 2023).
- [153] Y. Liu, Z. Zhang, W. Li, R. Liu, J. Qiu, and S. Wang, “Water purification performance and energy consumption of gradient nanocomposite membranes,” *Composites Part B: Engineering*, vol. 202, p. 108426, Dec. 2020, doi: 10.1016/j.compositesb.2020.108426.
- [154] M. Warneryd and K. Karltorp, “Microgrid communities: disclosing the path to future system-active communities,” *Sustainable Futures*, vol. 4, p. 100079, Jan. 2022, doi: 10.1016/j.sftr.2022.100079.
- [155] Babcock Ranch, “Technology At Babcock Ranch | America’s First Solar Powered Town,” *Babcock Ranch*, Aug. 30, 2021. <https://babcockranch.com/lifestyle/technology/> (accessed Apr. 10, 2023).
- [156] L. Jaramillo, C. Ortiz, L. Orama, M. Perez, J. Castillo, and P. Sepulveda, “Estado de Situacion Energetica De Puerto Rico,” Oficina Estatal de Politica Publica Energetica, Hato Rey, Puerto Rico, Informe Anual 2017, 2018. Accessed: Mar. 31, 2023. [Online]. Available: <https://static1.squarespace.com/static/5b6c67d071069910870c6820/t/5cbd046be5e5f0648a778456/1555891502310/%282018%29+Oeppe%2C+Estado+de+situacio%CC%81n+energe%CC%81tica+de+Puerto+Rico+%282017%29.pdf>

## Appendix A. UPRM Electricity Consumption Data

Mes	Lectura Anterior	Lectura Actual	KW. Cons	Consumo (KW)	Costo X KW	Total
Jul-20	6830.00	7017.00	187	2,468,400	\$0.17	\$417,914.00
Aug-20	7017.00	7182.20	165	2,180,640	\$0.17	\$377,597.79
Sep-20	7182.20	7366.00	184	2,426,160	\$0.17	\$414,482.64
Oct-20	7366.00	7556.00	190	2,508,000	\$0.17	\$424,556.28
Nov-20	7556.00	7734.00	178	2,349,600	\$0.17	\$399,626.87
Dec-20	7734.00	7912.00	178	2,349,600	\$0.17	\$399,626.87
Jan-21	7912.00	8054.00	142	1,874,400	\$0.18	\$339,130.87
Feb-21	8054.00	8214.00	160	2,112,000	\$0.18	\$375,358.51
Mar-21	8214.00	8377.00	163	2,151,600	\$0.18	\$383,227.95
Apr-21	8377.00	8540.00	163	2,151,600	\$0.19	\$415,561.16
May-21	8540.00	8701.00	161	2,125,200	\$0.19	\$412,195.03
Jun-21	8701.00	8867.55	167	2,198,460	\$0.19	\$424,796.12
Jul-21	8867.55	9062.56	195	2,574,132	\$0.21	\$528,266.93
Aug-21	9062.56	9244.00	181	2,715,240	\$0.20	\$555,368.70
Sep-21	9244.00	9435.00	191	2,521,200	\$0.21	\$528,920.98
Oct-21	9435.00	9614.06	179	2,363,592	\$0.22	\$515,027.37
Nov-21	9614.06	9776.97	163	2,150,412	\$0.22	\$466,854.56
Dec-21	9776.97	9950.83	174	2,294,952	\$0.22	\$497,058.81
1-Jan	49.17	112.12	161	2,129,028	\$0.26	\$547,865.87
Feb-22	112.12	249.20	137	1,809,456	\$0.25	\$459,323.62
Mar-22	249.20	416.20	167	2,204,400	\$0.25	\$555,519.61
Apr-22	416.20	586.90	171	2,204,400	\$ -	\$ -
May-22	586.90	747.10	160	2,253,240	\$0.27	\$604,543.58
Jun-22	747.10	937.70	191	2,114,640	\$0.34	\$713,933.08

# Appendix B. ReNCAT

Mitigation Measure Characteristic	Metric
Start-up or islanding crossover transition time (intermittent downtime before specified backup is available)	Time – minutes, hrs
Notification time/Advanced notice needed for backup available at specified load/duration	Time – minutes, hrs
Duration of backup – with no other inputs	Time – minutes, hrs
Load Capacity (which loads are backed up and how much load (Critical, Priority, Discretionary))	kWh, MWh or % of load
Fuel Type/Fuel Availability	Unit of fuel, availability before/during islanding
Emissions level – GHG and particulates	MMCO2, PPM
Geographic boundary	Location on geographic map, sq ft, sq mi
Blue Sky participation	kWh, kW

## Resiliency Valuation Methodology III. Resiliency Scorecard (draft)

Resiliency Scorecard: Mitigation Measure Characteristics	Points	Score
Duration of backup – with no other inputs		
4 hrs	1	
6 hrs	2	
24 hrs	3	
48 hrs (2 days)	4	
96 hrs (4 days)	5	
Indefinite	6	
Load Capacity (which loads are backed up and how much load (Critical, Priority, Discretionary))		
Critical		
90 - 100%	9	
50 - 90%	8	
0 - 50%	7	
Priority		
90 - 100%	6	
50 - 90%	5	
0 - 50%	4	
Discretionary		
90 - 100%	3	
50 - 90%	2	
0 - 50%	1	

Resiliency Scorecard: Mitigation Measure Characteristics	Points	Score
Fuel Availability		
Onsite, intermittent	2	
Onsite, produced	3	
Piped infrastructure	2	
Wires infrastructure	2	
Transport	1	
Emissions level – GHG and particulates		
Non-GHG emitting	4	
Meets CARB emission standards	3	
GHG emissions < xxx	2	
Cap n Trade	1	

Resiliency Scorecard: Mitigation Measure Characteristics	Points	Score
Start-up/ islanding /isolation/ crossover transition time (intermittent downtime before specified backup is available)		
0 - 1 min	5	
2 - 5 min	4	
5 - 30 min	3	
30 - 120 min	2	
< 120 min	1	
Notification time/Advanced notice needed for backup available at specified load/duration		
0 - 1 min	5	
2 - 5 min	4	
5 - 30 min	3	
30 - 120 min	2	
< 120 min	1	
Blue Sky Services		
Demand Response	2	
Voltage/Frequency	1	
Wholesale participation	1	
NEM participation	1	

California Public Utilities Commission

### Hypothetical Example: County

	Critical	Priority	Discretionary
<b>Resiliency Targets</b>	100%/24 hrs	60%/24 hrs	50%/24hrs
<b>Current system performance against Hazards:</b>			
<b>Hazard #1</b> Wildfire	0%	0%	0%
<b>Hazard #2</b> High Winds	70%/Indefinite	75%/Indefinite	80%/Indefinite
<b>Hazard #3</b> High heat events	50%/Indefinite	30%/Indefinite	30%/Indefinite

Mitigation Measure	Option 1: Covered Conductors, undergrounding, new feeders and reclosers, sectionalizers			Resiliency Scorecard
	Critical	Priority	Discretionary	
<b>Hazard #1</b> Wildfire	75%/Indefinite	20%/Indefinite	0%/Indefinite	31
<b>Hazard #2</b> High Winds	60%/Indefinite	20%/Indefinite	40%/Indefinite	31
<b>Hazard #3</b> High heat events	50%/Indefinite	20%/Indefinite	20%/Indefinite	30

	Option 1	Option 2	Option 3
Mitigation Measure	Covered Conductors, undergrounding, new feeders and reclosers, sectionalizers	IFOM MGs with dispatchable BTM DERs	IFOM MG, PV, Batt
<b>Hazard 3: High Heat Events</b>	<b>Option 1</b>	<b>Option 2</b>	<b>Option 3</b>
Effect of Mitigation on Target	50% CL; 20% PL; 20% DL	100% CL, 50% PL, 30% DL	50% CL; 20% PL; 20% DL
Resilience Enhancement cost	\$5.65M	\$4.1M	\$ 2.5M
<b>Resiliency Scorecard</b>	<b>30</b>	<b>31</b>	<b>30</b>

Hazard 1: Wildfire	Option 1	Option 2	Option 3
Mitigation Measure	Covered Conductors, undergrounding, new feeders and reclosers, sectionalizers	IFOM MGs with dispatchable BTM DERs	IFOM MG, PV, Batt
Effect of Mitigation on Target	75% CL; 20% PL; 0% DL	60% CL; 35% PL; 30% DL	50% CL; 20% PL; 0% DL
<b>Resiliency Scorecard</b>	<b>31</b>	<b>36</b>	<b>34</b>
Hazard 2: High Winds	Option 1	Option 2	Option 3
Effect of Mitigation on Target	60% CL; 20% PL; 40% DL	100% CL, 40% PL, 10% DL	50% CL; 20% PL; 20% DL
<b>Resiliency Scorecard</b>	<b>31</b>	<b>37</b>	<b>34</b>
Hazard 3: High Heat Events	Option 1	Option 2	Option 3
Effect of Mitigation on Target	50% CL; 20% PL; 20% DL	100% CL, 50% PL, 30% DL	50% CL; 20% PL; 20% DL
Resilience Enhancement cost	\$5.65M	\$4.1M	\$ 2.5M
<b>Resiliency Scorecard</b>	<b>30</b>	<b>31</b>	<b>30</b>

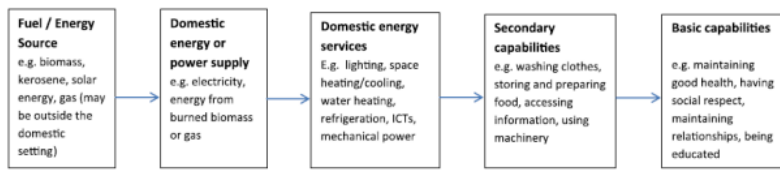


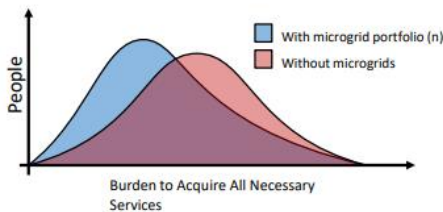
Fig. 1. Conceptualising the relationship between energy, services and outcomes.



- We are utilizing this theory, but advancing/extending in two ways:
- **Chronic vs. Acute:** we are applying the capabilities framework to acute, post disaster scenarios, whereas previous literature focuses on chronic "blue sky" capabilities
  - **Rigorous Quantification:** we are the first to apply a mathematical formulation to the theory

## 11 Performance Based Metric: Social Burden

The **social burden metric** calculates how hard society is working to achieve their basic human needs.



### Effort

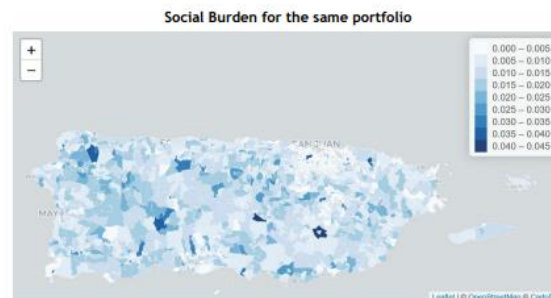
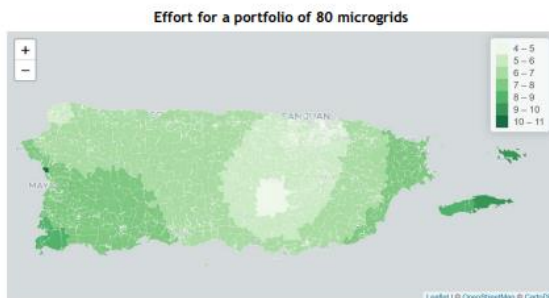
Time + money spent to achieve basic level of human needs

### Burden

$$B_C = \sum_{inf} \sum_{pop} \frac{E_{inf, pop}}{A_{pop}}$$

### Ability

Median household income  
Additional predictors



# LASOLAR

## HALF CELL

LS530BL-LS550BL

### 144 CELL

MONOCRYSTALLINE MODULE

### 530W-550W

POWER OUTPUT RANGE

### 21.28%

MAXIMUM EFFICIENCY

### 0 to +3%

POSITIVE POWER TOLERANCE



## 25 YEAR WARRANTY

### Main Characteristics



Mismatch loss reduction for maximum efficiency



Reduced power loss by minimizing the effect of shadow shading



Competitive low light performance



Two EL tests to ensure the best quality

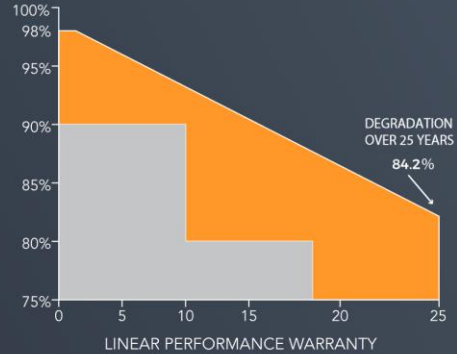


BOS's reduced and increased ROI is ideal for commercial and industrial scale projects



Proven reliability through PVEL's rigorous weatherproofing tests:

- Dust, acid and alkali resistance, hail test
- 2400pa wind pressure and 5400pa snow pressure
- Anti PID



### QUALIFICATIONS AND CERTIFICATES



Intertek  
5020665



UL/IEC61215, UL/IEC61730  
ANTI-PID IEC TS 62804-1:2015  
ISO9001, ISO14001, ISO45001



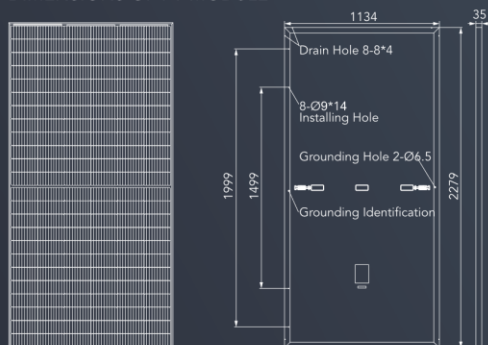


## Electrical Characteristics

Component Model	LS530BL	LS535BL	LS540BL	LS545BL	LS550BL
Maximum Power (PMP)	530	535	540	545	550
Open Circuit Voltage (VOC)	49.3	49.4	49.5	49.6	49.7
Short Circuit Current (ISC)	13.6	13.70	13.81	13.92	14.02
Maximum Power Voltage (VMP)	41.03	41.29	41.55	41.81	42.07
Maximum Power Current (IMP)	12.92	12.96	13.00	13.04	13.08
Component Efficiency ( $\eta_c$ )	20.56	20.76	20.95	21.14	21.28
Power Tolerance	(0, +3%)				
Maximum System Voltage	1500V DC				
Maximum Rated Fuse Current	35 A				

STC: Irradiance 1000 W/m<sup>2</sup> module temperature 25 °C AM=1.5

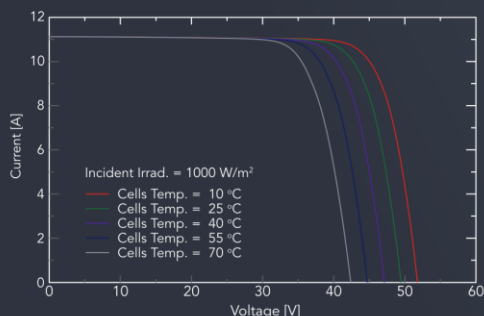
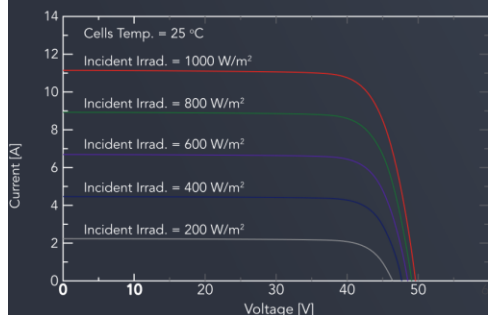
### DIMENSIONS OF PV MODULE



## Temperature Characteristics

Maximum Power Temperature Coefficient	-0.35 % / °C
Temperature Coefficient Of Open Circuit Voltage	-0.27 % / °C
Temperature Coefficient Of Short Circuit Current	+0.05 % / °C
Working Temperature	-40 ~ +85 °C
Nominal Operating Cell Temperature (NOCT)	45 ± 2 °C

## I-V Curve



## Structural Characteristics

Module Size	2279x1134x35mm
Weight	26.5kg
Battery	single crystal PERC182x91mm (144pieces)
Glass	3.2mm tempered coated glass, low iron
Frame	anodized aluminum alloy
Junction Box	IP68, 3 diodes
Output Lead	4.0mm 2250mm(+) / 350mm(-) or customized
Mechanical Load	front 5400pa / back 2400pa

## Packing Method

Module Size	2279x1134x35mm
Container	40' HQ
Quantity Per Pallet	31
Number Of Pallets Per Container	20
Quantity Per Container	620





**ICEWIND**  
EXTREME WIND ENERGY

**RW500** Wind Turbines

**EXTREMELY DURABLE  
NO NEED TO FACE WIND  
PRODUCTION IN LOW AND HIGH WIND  
SILENT OPERATION  
EASY TO INSTALL**

[www.icewind.is](http://www.icewind.is)  
[info@icewind.is](mailto:info@icewind.is)  
+354 861-2011

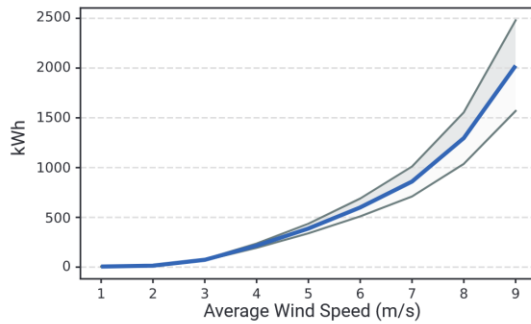
**IceWind** designs and manufactures robust micro vertical-axis wind turbines and other hybrid energy solutions to power telecom towers, weather and seismic stations, and on-grid and off-grid lodgings. All products are designed and tested in Iceland, one of the windiest places on earth.

RW series vertical-axis wind turbines are built to be mounted directly on commercial or military telecom towers, communication depots, relay station, and radar outposts, reducing operational costs, and increasing backup power time. RW turbines are designed to deliver long lasting performance, with little or no maintenance for over 20 years. They are able to withstand wind speeds up to 135 mph (Category 4 Hurricane wind speeds) and will consistently deliver power, even in the harshest conditions such as snow, ice and sand storms.

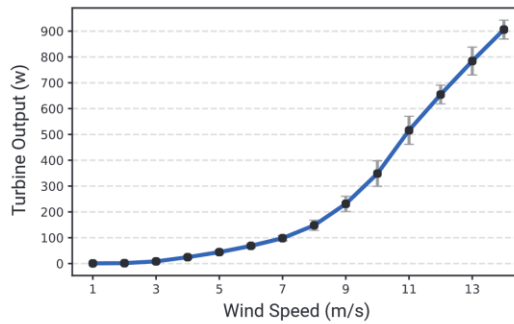
## RW500

Survival speed	135 mph	60 m/s
Startup wind speed	4.5 mph	2 m/s
Cut in wind speed	5.5 mph	2.5 m/s
Rated power	500 W	
Max power	3000 W	
Rated wind speed	22 mph	10 m/s
Noise level	< 30 dB	
Height	86 inch	2.2 m
Diameter	51 inch	1.3 m
Weight	187 lbs	85 kg
Generator	2 x 500 W AFPMG	
Number of blades	3 Inner, 3 Outer	

Annual RW500 Output



RW500 Power Curve



All rights reserved.

Trademarks mentioned in this document are the property of Icewind, its affiliates, or their respective owners.

Subject to changes and errors.

The information given in this document only contains general descriptions and/or performance features, which may not always specifically reflect those described, or which may undergo modification in the course of further development of the products. The requested performance features are binding only when they are expressly agreed upon in the concluded contract.

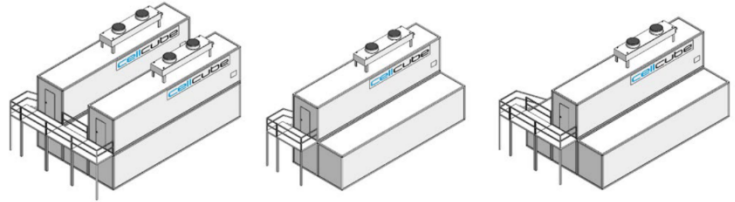
[www.icewind.is](http://www.icewind.is)  
[info@icewind.is](mailto:info@icewind.is)  
 +354 861-2011

**ICEWIND** 

# Appendix E. Redox Flow Battery Datasheet [123]



## DC Data Sheet - CellCube FB 250 / FB 500 Series Release 4.0



### Technical Data

	FB 500-2000	FB 250-1000	FB 250-2000
<b>Battery technology</b>			
Vanadium Redox Flow Battery			
<b>Battery performance DC<sup>1)</sup></b>			
Rated charge/discharge DC power	470 / 530 kW	235 / 265 kW	
Max. charge / discharge DC power	940 / 800 kW	470 / 400 kW	
<b>Usable energy at DC POC<sup>2)</sup></b>			
<b>@ 100% constant rated DC power</b>			
Auxiliary energy not deducted	2,470 kWh	1,235 kWh	2,470 kWh
Auxiliary energy deducted <sup>3)</sup>	2,400 kWh	1,200 kWh	2,400 kWh
<b>Maximum usable energy at DC POC</b>			
<b>@ 50% constant rated DC power</b>			
Auxiliary energy not deducted <sup>4)</sup>	2,960 kWh	1,480 kWh	2,960 kWh
Auxiliary energy deducted	2,800 kWh	1,400 kWh	2,800 kWh
Cycle life	> 20,000 @ 100% DOD		
<b>Battery interface</b>			
DC connection	530 ... 910 V, IT-Grid		
Max. DC current	2x 762 A	762 A	
Protection DC side	Fuses, insulation monitoring, surge protection device, main switch		
AC connection	400 V, 50 Hz / 60 Hz, 3P+N+PE, TN-S-grid		
Auxiliary power (max. / average) <sup>5)</sup>	40 kW / 16 kW	20 kW / 8 kW	
Communication	MODBUS TCP/IP		
<b>General</b>			
Design lifetime	25 years		
Electrolyte solution	Water based vanadium electrolyte, non-flammable, re-usable		
Noise emission <sup>6)</sup>	< 45 dB(A)		
Standards and directives complied with <sup>7)</sup>	CE		
Ambient temperature range	-15 °C ... + 45 °C		
Temperature management <sup>8)</sup>	Max. 24 hrs ambient average temperature: 27 °C @ 2 cycles per day 30 °C @ 1 cycle per day		

<sup>1)</sup> All data measured at an average electrolyte temperature of 35 °C

<sup>2)</sup> POC = Point of connection

<sup>3)</sup> Refers to "rated energy"

<sup>4)</sup> Refers to "name plate energy"

<sup>5)</sup> Depending on SOC, power, temperature

<sup>6)</sup> Sound pressure level at a distance of 10 m

<sup>7)</sup> Other compliances or Field Evaluations available on request

<sup>8)</sup> Other temperature management options available on request. One cycle is equivalent to the turnover of rated energy

**Technical Data**

FB 500-2000	FB 250-1000	FB 250-2000
-------------	-------------	-------------

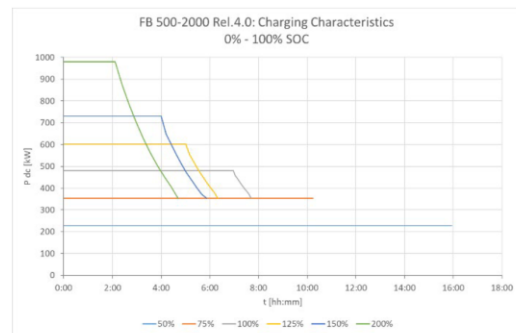
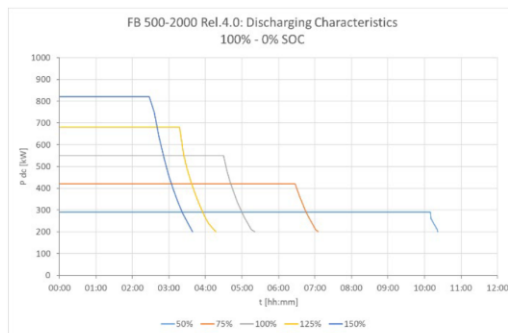
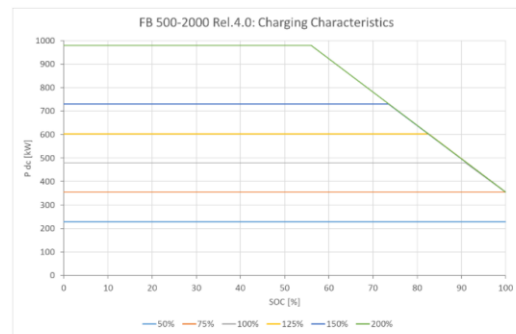
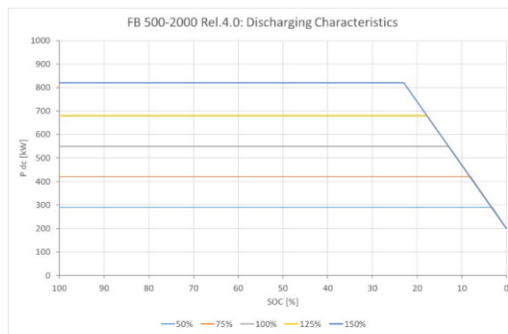
**Mechanical data**

Enclosure type<sup>9)</sup>  
Footprint (w/o stairs) L x W  
Height with cooling system  
Total weight in operation  
Degree of protection

Thermally isolated 40' ISO HC-containers with C3 coating		
12.2 m x 7.4 m	12.2 m x 4.9 m	12.2 m x 7.4 m
7.5 m		
265 t	135 t	245 t
IP 54		

**Characteristics**

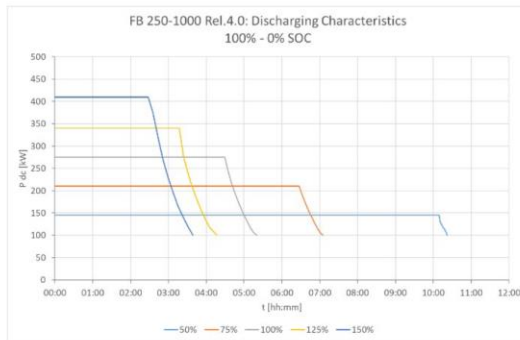
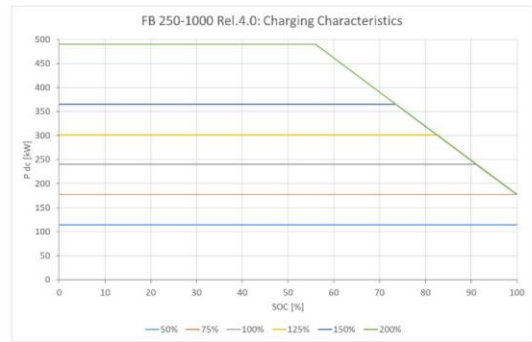
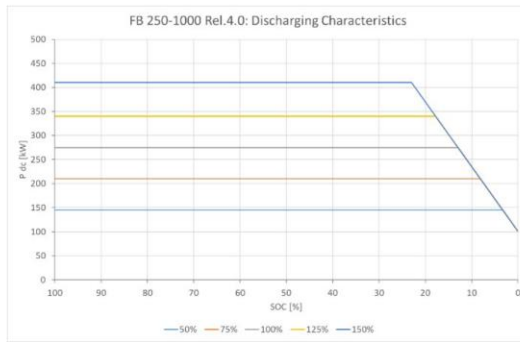
FB 500-2000



<sup>9)</sup> other coating options available on request

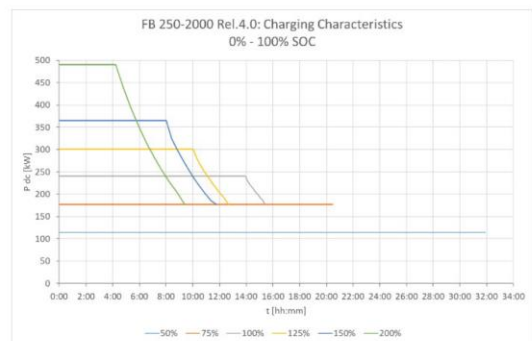
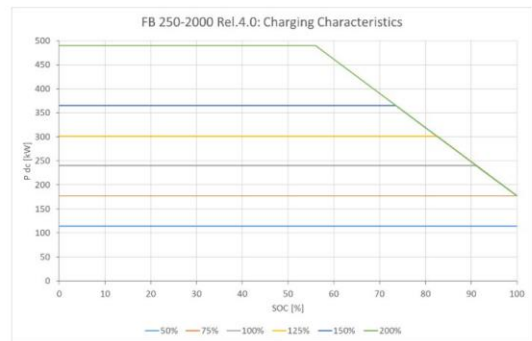
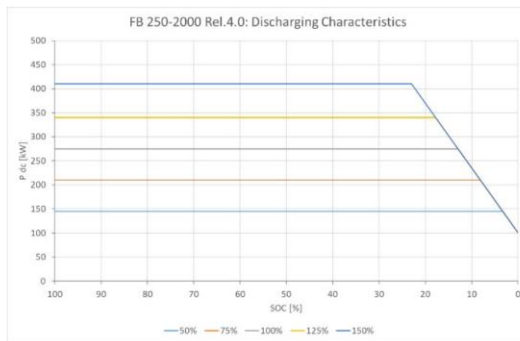
**Characteristics**

**FB 250-1000**



**Characteristics**

**FB 250-2000**



## Appendix F. Hydrogen Tank Costs

Tank	Advanced			Moderate			Conservative		
	CAPEX	Replace	OPEX	CAPEX	Replace	OPEX	CAPEX	Replace	OPEX
<i>kg</i>	<i>\$ USD</i>	<i>\$ USD</i>	<i>\$ USD/yr</i>	<i>\$ USD</i>	<i>\$ USD</i>	<i>\$ USD/yr</i>	<i>\$ USD</i>	<i>\$ USD</i>	<i>\$ USD/yr</i>
0	\$ 600.00	\$ 510.00	\$ 6.00	\$ 750.00	\$ 637.50	\$ 7.50	\$ 900.00	\$ 765.00	\$ 9.00
100	\$ 10,600.00	\$ 9,010.00	\$ 106.00	\$ 12,250.00	\$ 10,412.50	\$ 122.50	\$ 13,900.00	\$ 11,815.00	\$ 139.00
200	\$ 20,600.00	\$ 17,510.00	\$ 206.00	\$ 23,750.00	\$ 20,187.50	\$ 237.50	\$ 26,900.00	\$ 22,865.00	\$ 269.00
300	\$ 30,600.00	\$ 26,010.00	\$ 306.00	\$ 35,250.00	\$ 29,962.50	\$ 352.50	\$ 39,900.00	\$ 33,915.00	\$ 399.00
400	\$ 40,600.00	\$ 34,510.00	\$ 406.00	\$ 46,750.00	\$ 39,737.50	\$ 467.50	\$ 52,900.00	\$ 44,965.00	\$ 529.00
500	\$ 50,600.00	\$ 43,010.00	\$ 506.00	\$ 58,250.00	\$ 49,512.50	\$ 582.50	\$ 65,900.00	\$ 56,015.00	\$ 659.00
600	\$ 60,600.00	\$ 51,510.00	\$ 606.00	\$ 69,750.00	\$ 59,287.50	\$ 697.50	\$ 78,900.00	\$ 67,065.00	\$ 789.00
700	\$ 70,600.00	\$ 60,010.00	\$ 706.00	\$ 81,250.00	\$ 69,062.50	\$ 812.50	\$ 91,900.00	\$ 78,115.00	\$ 919.00
800	\$ 80,600.00	\$ 68,510.00	\$ 806.00	\$ 92,750.00	\$ 78,837.50	\$ 927.50	\$ 104,900.00	\$ 89,165.00	\$ 1,049.00
900	\$ 90,600.00	\$ 77,010.00	\$ 906.00	\$ 104,250.00	\$ 88,612.50	\$ 1,042.50	\$ 117,900.00	\$ 100,215.00	\$ 1,179.00
1000	\$ 100,600.00	\$ 85,510.00	\$ 1,006.00	\$ 115,750.00	\$ 98,387.50	\$ 1,157.50	\$ 130,900.00	\$ 111,265.00	\$ 1,309.00



## Appendix G. HOMER Inputs

The microgrid system is optimized using HOMER with all resources and components included to ensure all possible scenarios are captured. Figure 46 provides the detailed schematic for the entire system.

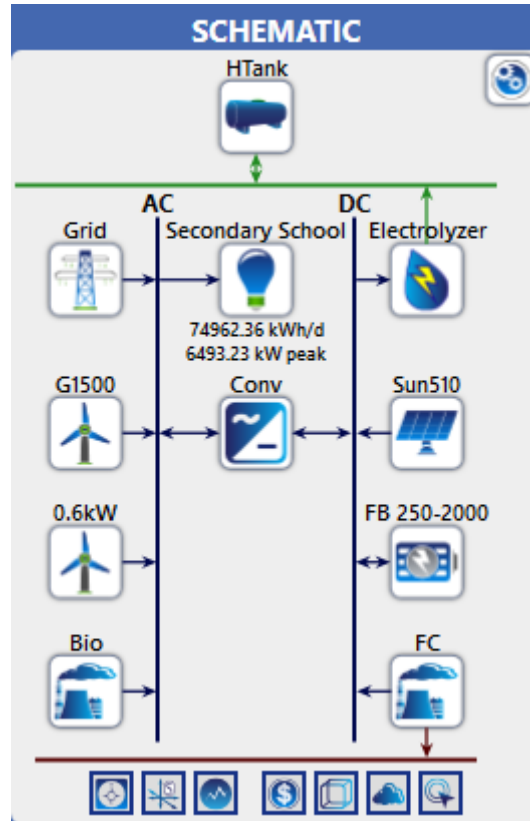


Figure 46: Overall schematic of the microgrid in HOMER.

The system load values for the campus as well as hourly, monthly, and annual profiles are simulated as in Figure 47.



Figure 47: System load inputs and profile.

Resource availability within the campus for solar (Figure 48), wind (Figure 49), and biomass (Figure 50) as defined in HOMER. Figure 51 profiles the temperature of the region as well, given its impact on the performance of some system components.

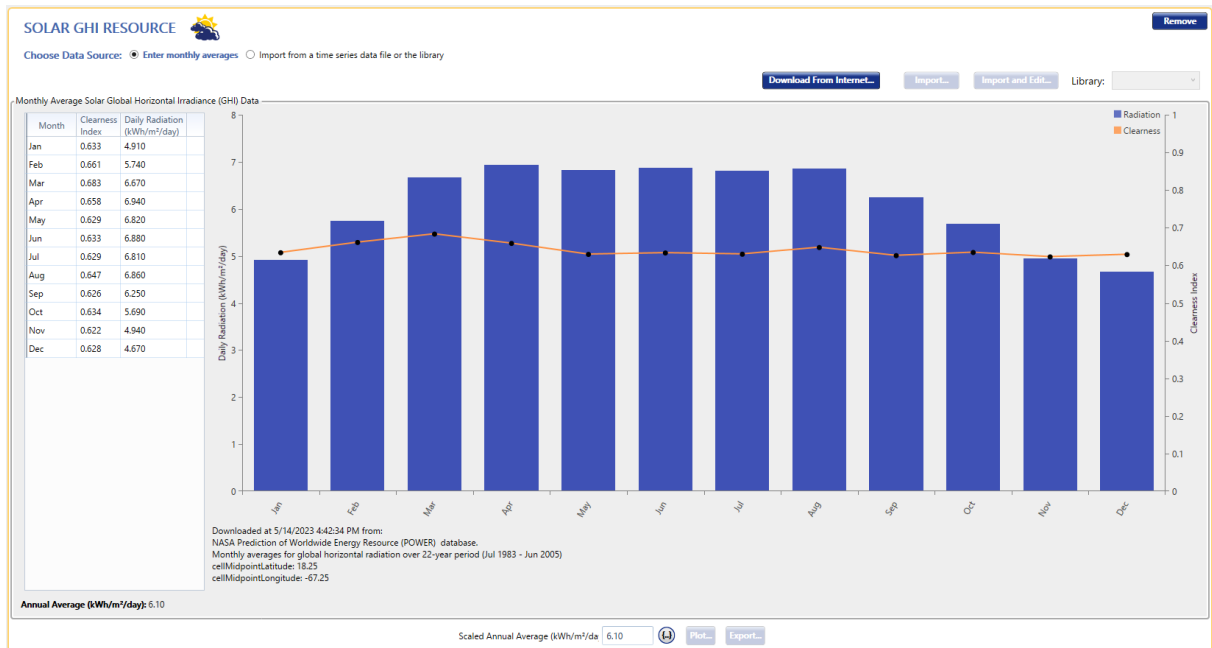


Figure 48: Solar GHI profile for the UPRM campus.

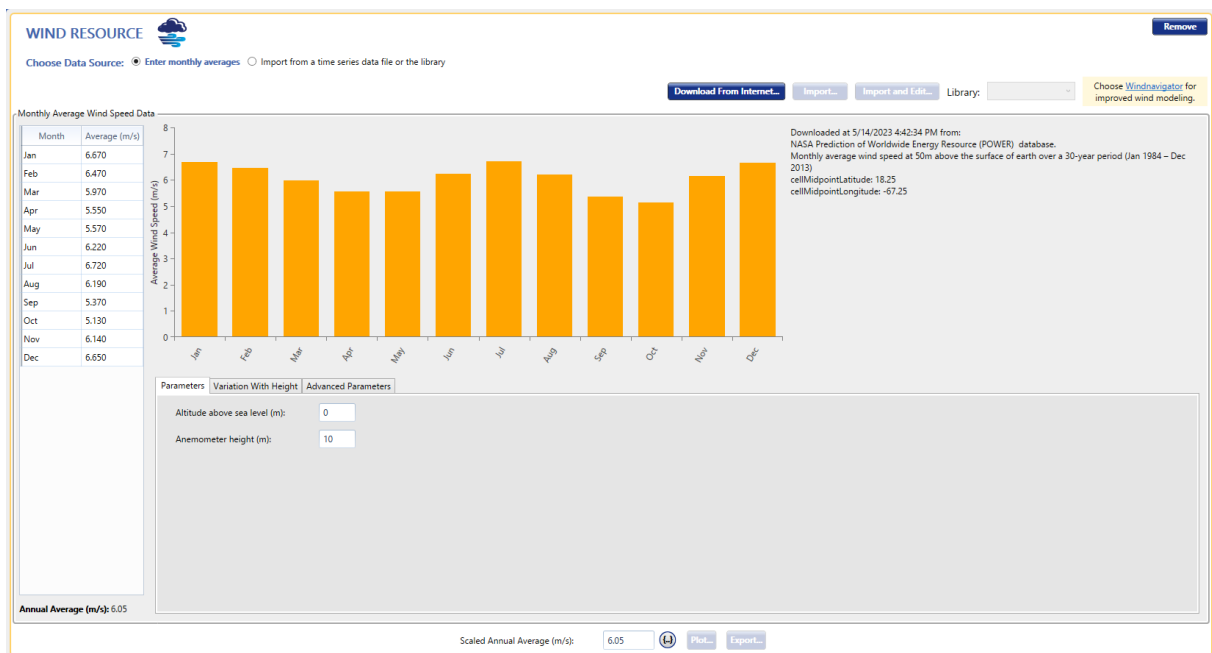


Figure 49: Wind availability at 50m above ground for UPRM.

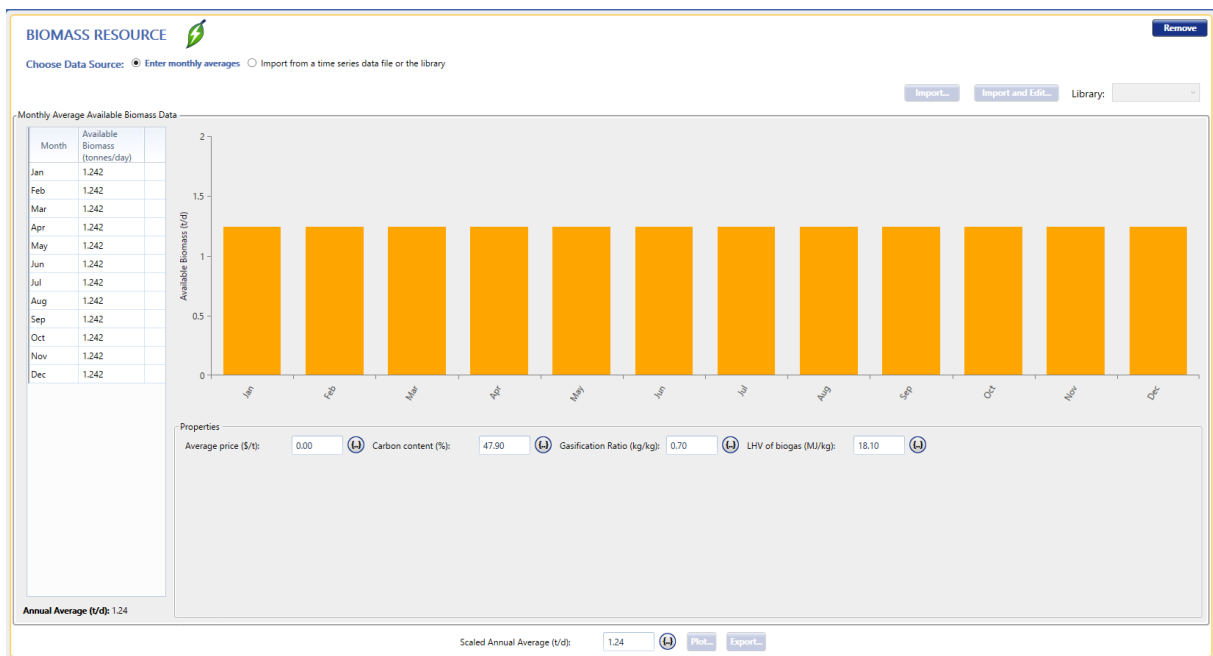


Figure 50: Biomass production capabilities within the campus grounds.



Figure 51: Temperature profile for the region.

The input values for the cost structures and size limitations of all components are displayed in Figure 52- Figure 60 below.

Generic large, free converter | Name: Generic large, free convert | Remove | Copy To Library

**CONVERTER** Complete Catalog

**Properties**  
 Name: Generic large, free converter  
 Abbreviation: Conv  
 homerenergy.com  
 Notes:  
 This converter allows you to size the battery system without having to size the converter when using the LF and CC controllers.  
 It accounts for the efficiency losses of converting from the AC to DC bus (i.e. rectifier efficiency) and for losses from the DC to AC bus (i.e. inverter efficiency). However, it is intended to be as large as necessary to avoid bottlenecks converting between the AC & DC bus. Under this approach, costs for any AC/DC conversion must be allocated in the battery costs.  
 For more information, see the HOMER Knowledgebase article "Modeling an AC coupled battery in HOMER" by clicking the homerenergy.com link.

**Costs**

Capacity (kW)	Capital (\$)	Replacement (\$)	O&M (\$/year)
1	\$0.0	\$0.0	\$0.0

Click here to add new item

Multiplier: [ ] [ ] [ ]

**Capacity Optimization**  
 HOMER Optimizer™  
 Search Space  
 Size (kW)  
 0  
 9999999

**Generic**  
 homerenergy.com

**HOMER Energy**

**Inverter Input**  
 Lifetime (years): 15.00 [ ]  
 Efficiency (%): 95.00 [ ]  
 Parallel with AC generator?

**Rectifier Input**  
 Relative Capacity (%): 100.00 [ ]  
 Efficiency (%): 95.00 [ ]

**Need help learning HOMER?**  
 Learn more about online courses

Figure 52: Large generic converter input values.

Add/Remove Sunpreme510SNPM-GxB-510

PV | Name: Sunpreme510SNPM-GxB-510 | Abbreviation: Sun510 | Remove | Copy To Library

**Properties**  
 Name: Sunpreme510SNPM-GxB-510  
 Abbreviation: Sun510  
 Panel Type: Flat plate  
 Rated Capacity (kW): 23652  
 Temperature Coefficient: -0.350  
 Operating Temperature (°C): 45  
 Efficiency (%): 21.28  
 Manufacturer: Sunpreme  
 CEC PV Modules  
 Notes:  
 This component comes from the CEC module database, which was most recently updated in August 2017. The name plate power is: 510W. The nameplate voltage is: 74.70 V. The nameplate current is: 9.40A. The family and technology and type associated with this module is: Thin Film , Thin Film and Flat Plate. The date which CEC attributes to this module and the date this module was last updated are: . . . Notes from CEC are as follows.

**Cost**

Capacity (kW)	Capital (\$)	Replacement (\$)	O&M (\$/year)
1	1,740.00	186.00	21.70

Lifetime: time (years): 25.00 [ ] More...

**Site Specific Input**  
 Derating Factor (%): 85.00 [ ]


**Electrical Bus**  
 AC  DC

**Sizing**  
 HOMER Optimizer™  
 Search Space  
 kW  
 0  
 23652

Advanced...

Figure 53: Solar PV cost structure and size constraint input values.

Add/Remove Generic 1.5 MW Icewind RW600

**WIND TURBINE**  Name: Generic 1.5 MW Abbreviation: G1500

Remove  
Copy To Library

**Properties**  
Name: **Generic 1.5 MW**  
Abbreviation: **G1500**  
Rated Capacity (kW): **1500**  
Manufacturer: **Generic**  
[homerenergy.com](http://homerenergy.com)  
Notes:

Quantity	Capital (\$)	Replacement (\$)	O&M (\$/year)
1	\$5,310,000.00	\$3,883,500.00	\$49,875.00

Click here to add new item

Multiplier:

**Site Specific Input**  
Lifetime (years):   Hub Height (m):    Consider ambient temperature effects?

**Quantity Optimization**  
HOMER Optimizer™  
Search Space

Quantity


0  
1  
2

Electrical Bus  AC  DC

Advanced...

Figure 54: Generic 1.5-MW wind turbine cost structure and size constraint inputs.

Add/Remove Generic 1.5 MW Icewind RW600

**WIND TURBINE**  Name: Icewind RW600 Abbreviation: 0.6kW

Remove  
Copy To Library

**Properties**  
Name: **Icewind RW600**  
Abbreviation: **0.6kW**  
Rated Capacity (kW): **1**  
Manufacturer: **Generic**  
[homerenergy.com](http://homerenergy.com)  
Notes:

Quantity	Capital (\$)	Replacement (\$)	O&M (\$/year)
1	\$10,500.00	\$8,000.00	\$19.95

Click here to add new item

Multiplier:

**Site Specific Input**  
Lifetime (years):   Hub Height (m):    Consider ambient temperature effects?

**Quantity Optimization**  
HOMER Optimizer™  
Search Space

Quantity

0  
1  
20  
60  
126

Electrical Bus  AC  DC

Advanced...

Figure 55: IceWind RW600 turbine cost structure and size constraints.

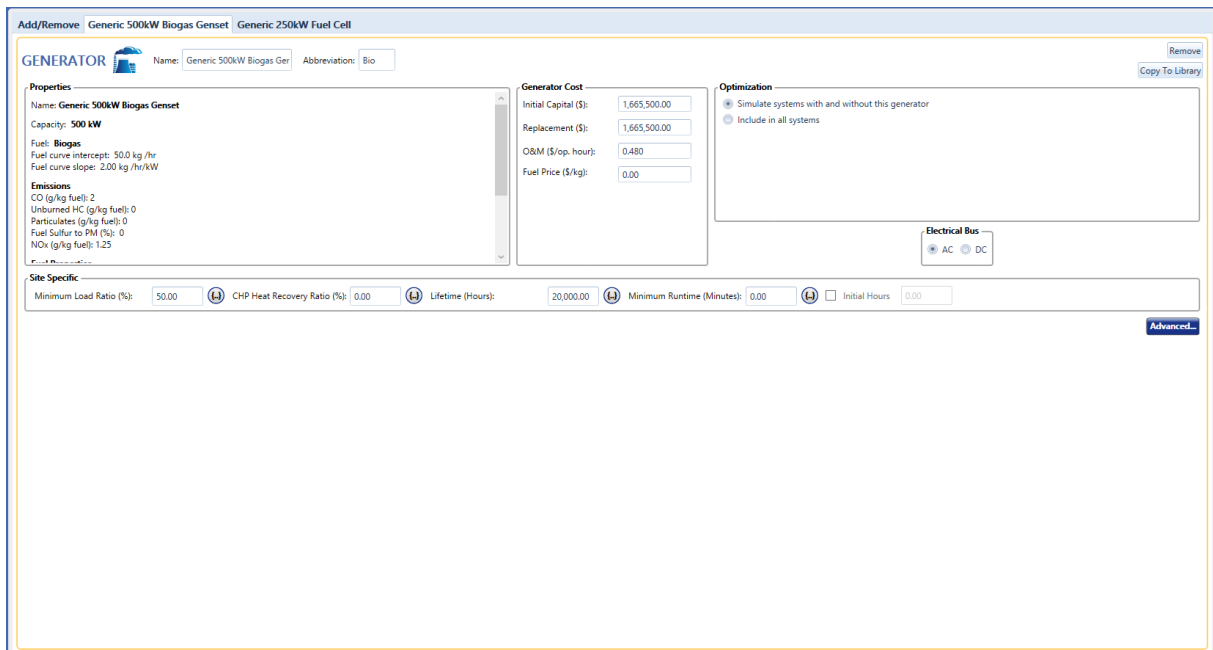


Figure 56: Biogas genset cost and efficiency inputs.

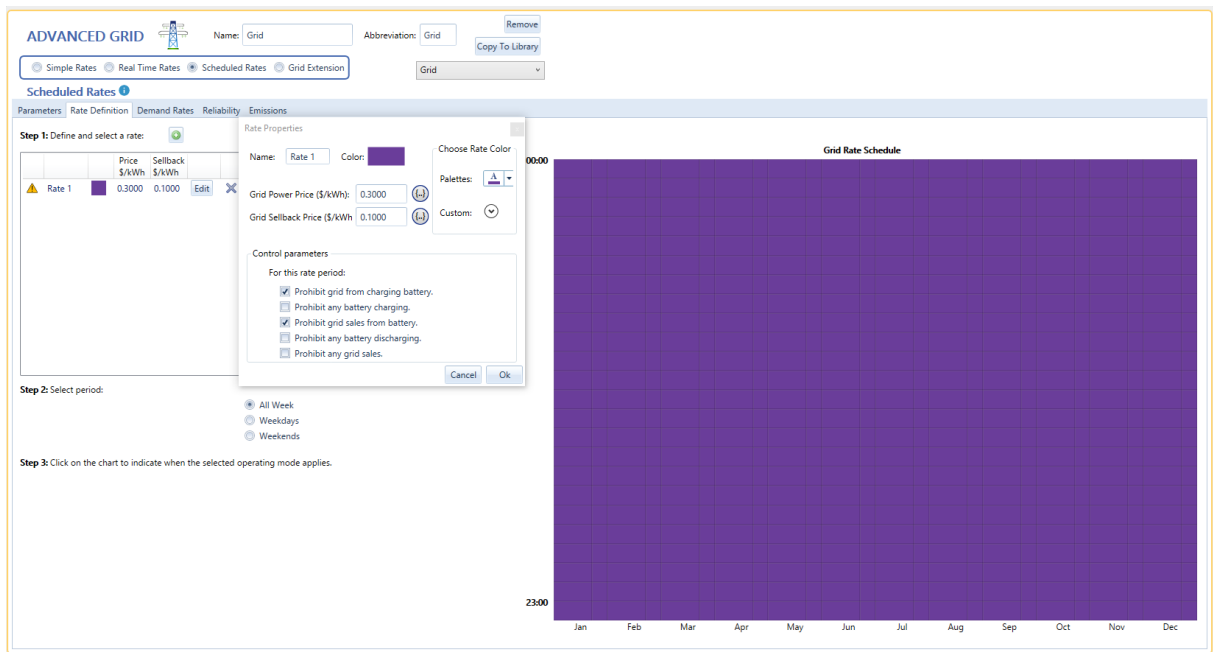


Figure 57: Grid energy purchase and buyback rates used. Specific constraint criteria are displayed on the pop-out. No information is behind the pop-out.



ELECTROLYZER

Name:  Abbreviation:

**Properties**

Name: **Generic Electrolyzer**

Abbreviation: **Electrolyzer**

Manufacturer: **Generic**

[www.homerenergy.com](http://www.homerenergy.com)

Notes:  
**This is a generic electrolyzer.**

**Costs**

Capacity (kW)	Capital (\$)	Replacement (\$)	O&M (\$/year)
1	\$1,585.00	\$475.50	\$31.70

[Click here to add new item](#)

**Capacity Optimization**

Size (kW)
0
100
250
500
750
1000

Lifetime (years):

Efficiency (%):

Minimum load ratio (%):

Electrical Bus:  AC  DC

**Electrolyzer Schedule**

Step 1: Select a mode:  Forced On  Optimize

Step 2: Select a time period:  
 All Week  
 Weekdays  
 Weekends

Step 3: Click on the chart when the selected operating applies.

23:00

Figure 58: Electrolyzer cost, size and conversion efficiency input values.

HYDROGEN TANK

Name:  Abbreviation:

**Properties**

Name: **Hydrogen Tank**

Abbreviation: **HTank**

Manufacturer: **Generic**

[www.homerenergy.com](http://www.homerenergy.com)

Notes:  
**This is a generic hydrogen tank.**

**Costs**

Size (kg)	Capital (\$)	Replacement (\$)	O&M (\$/year)
100	\$12,250.00	\$10,412.50	\$122.50
200	\$23,750.00	\$20,187.50	\$237.50
300	\$32,250.00	\$29,962.50	\$352.50
400	\$46,750.00	\$39,737.50	\$467.50
500	\$58,250.00	\$49,512.50	\$582.50
1000	\$115,750.00	\$98,387.50	\$1,157.50

[Click here to add new item](#)

**Capacity Optimization**

Size (kg)
0
100
200
300
400
500
1000

**Initial Tank Level**

Relative to tank size (%):

Absolute amount (kg):

Require year-end tank level to equal or exceed initial tank level.

Lifetime (years):

Figure 59: Hydrogen tank price scaling (as defined in Appendix F) and initial size options.

Add/Remove Generic 500kW Biogas Genset Generic 250kW Fuel Cell

**GENERATOR** Name: Generic 250kW Fuel Cell Abbreviation: FC Remove  
Copy To Library

Properties	Generator Cost	Optimization
Name: <b>Generic 250kW Fuel Cell</b> Capacity: <b>250 kW</b> Fuel: <b>Stored Hydrogen</b> Fuel curve intercept: 0 kg /hr Fuel curve slope: 0.0500 kg /hr/kW <b>Emissions</b> CO (g/kg fuel): 0.2 Unburned HC (g/kg fuel): 0 Particulates (g/kg fuel): 0 Fuel Sulfur to PM (%): 0 NOx (g/kg fuel): 0.02	Initial Capital (\$): 396,250.00 Replacement (\$): 158,500.00 O&M (\$/op. hour): 0.010 Fuel Price (\$/kg): 0	<input checked="" type="checkbox"/> Simulate systems with and without this generator <input checked="" type="checkbox"/> Include in all systems
<b>Electrical Bus</b> <input checked="" type="radio"/> AC <input type="radio"/> DC		
<b>Site Specific</b> Minimum Load Ratio (%): 0.00 <input type="checkbox"/> CHP Heat Recovery Ratio (%): 60.00 <input type="checkbox"/> Lifetime (Hours): 50,000.00 <input type="checkbox"/> Minimum Runtime (Minutes): 0.00 <input type="checkbox"/> Initial Hours: 0.00		

**Advanced**

Figure 60: Hydrogen fuel cell cost inputs.

## Appendix H. Measured Energy Loads

Consumos 2018	Gabinete	Trafo	Enero [kWh]	Febrero	Marzo	Abril	Mayo	Junio	Julio	Agosto	Septiembre	Octubre	Noviembre	Diciembre	Class #	Total [kWh/year]	Specific Consumption [kWh/m2]	Class Description
MuSA	Anexo Pinero	150	0.0	0.0	0.0	0.0	28099.0	0.0	0.0	0.0	0.0	0.0	0.0	0.0	1	28099.0	10.622677	Storage
Coliseo	Planta Fisica	750	23411.0	22111.0	26519.0	27954.0	36320.0	64913.0	33978.0	41599.0	46429.0	59186.9	45025.0	43190.0	2	470635.9	42.485865	AC and Lighting
ADEM	ADEM	1500	91793.0	74320.0	92373.0	87097.0	97059.0	105070.0	106948.0	97045.0	105539.0	107932.2	96554.0	83318.0	3	1145048.2	57.886557	Lectures
Ingeniería Civil	Edificio Enfermo	750	23411.0	22111.0	26519.0	27954.0	36320.0	64913.0	33978.0	41599.0	46429.0	59186.9	45025.0	43190.0	4	470635.9	62.147545	Engineering Lectures and Labs
Servicios Médicos	Frente Pinero	225	25501.0	22528.0	9954.0	5027.0	3342.0	3284.0	15228.0	22739.0	18568.0	19881.0	28991.0	29906.0	5	204949.0	117.856479	Medical Services
Biología	Biología	2500/2800	258123.0	201157.0	199694.0	199069.0	454153.0	468730.0	447713.0	456370.0	449357.0	467918.8	335934.0	411293.9	6	4349512.7	133.412123	Labs & Classes high
Natatorio	Imprensa Nuevo	1500	83568.0	72041.0	84679.0	80609.0	79843.0	79882.0	69971.0	73065.0	72261.0	72548.9	75859.0	79184.0	7	923510.9	141.292579	Water Pumping, AC, and lighting
		<b>Total</b>	164116.0	141070.0	155365.0	148032.0	201140.0	238180.0	190132.0	202982.0	216965.0	246187.0	215595.0	199604.0		2,319,368.00		

# Appendix I. Building Load Estimates and Categories

Identifier on Map					Rooftop Area (Google Earth Estimate)	Building Total Area Estimate	Percentage of total	Annual Energy Consumption for 2018	Annual Energy Consumption for 2022		
Name/Function	Translation	MID #	Priority (1 is High Priority, 4 is Darkzone)	[m <sup>2</sup> ]	# of Floor	[m <sup>2</sup> ]	Area	Usage Class	[kWh/year]	Contribution Percentag	[kWh/year]
1	Taller de Arte en Remodelacion	Art Workshop under Remodelling	3	4	809.3	1	809.322	0.20%	2	34385.17896	27,377.922
2	Administracion de Empresas	Business Administration	1	3	3956.2	5	19780.9	4.83%	3	1145048.2	911,702.121
3	Almacen del CID	Research and Development Warehouse	1	4	119.8	1	119.8425	0.03%	1	1273.048215	1,013.617
4	Almacen Obras de MuSA	MuSA Artwork Warehouse	3	4	404.5	2	808.974	0.20%	1	8593.469817	6,842.231
5	Antiguo Centro Nuclear	Old Nuclear Center	1	2	1740.0	4	6960.028	1.70%	6	928552.1101	739,325.146
6	Antigua Pista Atletica	Old Athletic Track	3	4	0.0	1	0	0.00%	1	0	0.000%
7	Banda y Orquesta	Band and Orchestra	3	4	531.2	1	531.1925	0.13%	2	22568.17309	17,969.070
8	Biblioteca General	General Library	3	1	4297.8	5	21488.85	5.25%	5	2532600.209	2,016,488.897
9	Edificio de Biologia	Biology Building	1	1	5433.7	6	32602.08	7.96%	6	4349512.7	3,463,138.018
10	Centro de Cuido Diurno	Daycare Center	2	3	628.1	1	628.0551	0.15%	3	36355.94749	28,947.074
11	Centro de Estudiantes	Student Center	3	2	2579.6	5	12897.8	3.15%	7	1822363.419	1,450,989.220
12	Central Telefonica	Telecommunications Center	2	1	261.2	1	261.2498	0.06%	4	16236.03368	12,927.339
13	CISA	CISA	1	2	344.8	1	344.7811	0.08%	2	14648.32343	11,663.184
14	Coliseo Rafael A. Mangual	Rafael E. Mangual Coliseum	2	4	3692.5	3	11077.47	2.71%	2	470635.9	1,370%
15	Complejo de Tennis 2010	Tennis Complex 2010	2	4	7081.4	1	7081.4257	1.73%	2	300860.4995	239,549.004
16	Cuarto Limpio (CID)	Clean Room, Research and Development	1	3	511.0	2	1021.904	0.25%	6	136334.3819	108,551.190
17	Naturatorio 2010	Naturatorio 2010	2	4	2178.4	3	6536.16	1.60%	7	923510.9	735,311.270
18	a Economica / Calidad de Vida / Dept de	Financial Aid, Quality of Life, Counseling De	3	2	616.2	1	616.2196	0.15%	3	35670.83114	28,401.575
19	Departamento de Edificios y Terrenos	Facilities Department	2	1	5039.5	1	5039.4854	1.23%	3	291718.46	232,699.994
20	Sanchez Hidalgo (DECEP / PpMES / Econ	Sanchez Hidalgo Building, DECEP, PpMES, Econ	2	3	1346.6	5	6733.05	1.64%	3	389753.0842	310,326.424
21	Edificio A (Dormitorio de Atletas)	Building A, Athlete Dormitories	2	2	706.7	7	4946.7432	1.21%	5	583005.7385	464,196.676
22	io B (Adm. Pequeños Negocios / Ofic. Aoiding	B. Small Business Admin, Admin Offic	2	3	668.6	3	2005.761	0.49%	3	116106.5989	92,445.569
23	Edificio C (Oficina de Extension Agricola)	Building C, Agricultural Branch Office	2	3	667.8	3	2003.4495	0.49%	3	115972.7941	92,339.032
24	Edificio D (Red Sismica)	Building D, Seismic Network	2	2	521.3	1	521.3243	0.13%	4	32399.02535	25,796.521
25	Edificio Chardon (Estudios Generales)	Chardon Building, General Studies	3	4	2934.2	5	14671.15	3.58%	2	623316.505	496,292.627
26	Edificio Jesus T. Piñero	Jesus T. Piñero Building	3	2	2399.4	3	7198.14	1.76%	3	416675.5431	331,762.433
27	Edificio Jose de Diego	Jose de Diego Building	3	2	656.6	2	1313.1024	0.32%	3	76010.97723	60,520.919
28	- Celis 101 / Registro / Decanato de Arte,	Admissions, Registry, Dean of Arts and Sci	3	1	1296.1	4	7184.32	1.75%	4	446487.8409	355,489.375
29	Edificio Luis Monzon	Luis Monzon Building	3	4	1591.4	6	9548.16	2.33%	3	552710.1103	440,074.907
30	Edificio Luis Stefani	Luis Stefani Building	3	3	7813.9	3	23441.64	5.72%	6	3127398.954	2,490,075.317
31	Edificio Oficinas de Facultad	Faculty Offices Building	2	3	730.7	4	2922.7644	0.71%	4	181642.6318	144,626.202
32	Edificio Ramirez de Arellano y Rossello	Ramirez de Arellano y Rossello Building	2	2	621.4	2	1242.727	0.30%	6	165794.8471	132,007.992
33	Edificio Josefina Torres Torres (Enfermeri	Josefina Torres Torres Building, Nursing	2	4	2066.6	2	4133.2	1.01%	3	239256.7184	190,499.280
34	Canchas de Racquetball 2010	Racquetball Courts 2010	2	4	717.5	1	717.47	0.18%	2	30482.33889	24,270.427
35	Edificio Terrats (Finanzas y Pagaduria)	Terrats Building, Finances and Payments	3	3	1514.4	2	3028.76	0.74%	3	175324.4891	139,595.616
36	Finca Alzamora	Alzamora Farm	2	2	2517.8	1	2517.7573	0.61%	2	106969.0979	85,170.173
37	Fisica, Geologia y Ciencias Marinas	Physics, Geology, Marine Sciences	2	4	39048.4	3	117145.2	2.86%	4	7280286.58	5,796,657.918
38	Gimnasio Angel F. Espada	Angel F. Espada Gym	3	4	1802.7	2	3605.48	0.88%	1	38299.85087	30,494.834
39	ic. En Remodelacion Guardia Universita	Campus Police Offices, Under Remodelin	3	1	0.0	1	0	0.00%	3	0	0.000%
40	Imprenta y Artes Plasticas	Printing and Fine Arts	1	4	1963.2	2	3926.48	0.96%	4	244021.0922	194,292.736
41	Edificio de Ingenieria Civil	Civil Engineering Building	1	3	3786.4	2	7572.88	1.85%	4	470635.9	374,726.364
42	Edificio de Ingenieria Industrial	Industrial Engineering Building	3	3	547.4	3	1642.2	0.40%	5	193543.9106	154,102.154
43	ificio Antonio Luchetti (Ingenieria Mecan	Antonio Luchetti Building, Mechanical Engineer	3	3	1913.5	2	3827.04	0.93%	6	510573.5304	406,525.219
44	Edificio de Ingenieria Quimica	Chemical Engineering Building	1	1	3071.2	3	9213.69	2.25%	5	1085893.067	864,602.042
45	Museo de Vehiculos Solares	Solar Vehicle Museum	1	4	648.5	1	648.4901	0.16%	2	27551.66314	21,936.989
46	Laboratorio de Ingenieria Agricola	Agricultural Engineering Laboratory	2	3	1439.8	2	2879.64	0.70%	4	178962.5563	142,492.292
47	Laboratorio de Vehiculos Solares	Solar Vehicle Laboratory	1	4	472.0	1	472.0494	0.12%	7	66697.07691	53,105.071
48	ntro Interdisciplinario de Estudios del Lito	Interdisciplinary Literary Studies Center	1	4	106.1	1	106.1496	0.03%	2	4509.857624	3,590.807
49	MuSA (Museo y Senado Academico)	MuSA Museum and Academic Senate	3	3	881.7	3	2645.19	0.65%	1	28099	22,372.786
50	Nueva Pista Atletica	New Athletic Track	3	4	0.0	1	0	0.00%	2	0	0.000%
51	CID (Oficina Administrativa)	earch and Development, Administrative OF	1	2	626.1	2	1252.2528	0.31%	3	72488.60338	57,716.359
52	Ofic. Campus Verde (Casa Solar 2005)	Green Campus Office, Solar House 2005	1	4	108.7	1	107.956	0.03%	3	6249.201173	4,975.694
53	Programa de Rehabilitacion Vocacional	Career Rehabilitation Program	2	4	221.4	1	221.3937	0.05%	3	12815.71909	10,204.041
54	OMCA	ce of Continuous Improvement and Assessn	2	4	289.0	1	288.982	0.07%	3	16728.17308	13,319.187
55	Edificio de Quimica	Chemistry Building	1	1	4582.7	5	22913.45	5.60%	6	3056932.005	2,433,968.624
56	Red Sismica (UPRM Residence #2)	UPRM Residence #2	2	1	223.3	1	223.3116	0.05%	5	26318.71901	20,955.303
57	Residencia del Rector	Director's Residence	3	2	583.7	1	583.7342	0.14%	5	68796.85777	54,776.944
58	R.O.T.C	R.O.T.C.	3	4	1110.8	3	3332.4	0.81%	3	192901.1633	153,590.390
59	Sendero de los Ejercicios	Exercise Trail	3	4	0.0	1	0	0.00%	1	0	0.000%
60	Servicios Medicos y Sala de Emergencia	Medical Services and Emergency Room	3	1	579.7	3	1738.971	0.42%	5	204949	163,183.033
61	Taller de Artes Graficas	Graphic Arts Workshop	3	4	254.0	1	253.9746	0.06%	5	29932.55224	23,832.684
62	alaciones Temporeras Guardia Universit	Campus Police Offices, Temporary Installat	3	1	487.2	1	487.2028	0.12%	3	28202.49277	22,455.188
63	Salon Mezzanine	Mezzanine Hall	2	4	808.4	2	1616.8172	0.39%	2	68691.87802	54,693.358
NOM1	Alumbrado	Street Lighting Not On Map	2	4				#DIV/0!	1	0	0.000%
NOM2	Areas Sin Nombres	Unnamed Areas, Not On Map	4	4	57,435.12			#DIV/0!	1	0	0.000%
UPRM	Total Area				135,051.63		409,440.20	100%		34,364,255.53	27,361,262.74

\*Orange highlight is for known Areas (1 is West, 2 is Central/North, 3 is East) Yellow highlight is for uncertainty. Red Highlight means the value is unused (existing solar).

## Appendix J. Building Loads Based on MID and Priority Level

Building Identifier	Building Name	MID 1				MID 2				MID 3			
		Priority				Priority				Priority			
		1	2	3	4	1	2	3	4	1	2	3	4
1	Art Workshop under Remodeling	0.0	0.0	0.0	0.0	0.0	0.0	0.0	0.0	0.0	0.0	0.0	27377.9
2	Business Administration	0.0	0.0	911702.1	0.0	0.0	0.0	0.0	0.0	0.0	0.0	0.0	0.0
3	R&D Warehouse	0.0	0.0	0.0	1013.6	0.0	0.0	0.0	0.0	0.0	0.0	0.0	0.0
4	MuSA Artwork Warehouse	0.0	0.0	0.0	0.0	0.0	0.0	0.0	0.0	0.0	0.0	0.0	6842.2
5	Old Nuclear Center	0.0	739325.1	0.0	0.0	0.0	0.0	0.0	0.0	0.0	0.0	0.0	0.0
6	Old Athletic Track	0.0	0.0	0.0	0.0	0.0	0.0	0.0	0.0	0.0	0.0	0.0	0.0
7	Band and Orchestra	0.0	0.0	0.0	0.0	0.0	0.0	0.0	0.0	0.0	0.0	0.0	17969.1
8	General Library	0.0	0.0	0.0	0.0	0.0	0.0	0.0	0.0	2016488.9	0.0	0.0	0.0
9	Biology Building	3463138.0	0.0	0.0	0.0	0.0	0.0	0.0	0.0	0.0	0.0	0.0	0.0
10	Daycare Center	0.0	0.0	0.0	0.0	0.0	0.0	28947.1	0.0	0.0	0.0	0.0	0.0
11	Student Center	0.0	0.0	0.0	0.0	0.0	0.0	0.0	0.0	0.0	1450989.2	0.0	0.0
12	Telecommunications Center	0.0	0.0	0.0	0.0	12927.3	0.0	0.0	0.0	0.0	0.0	0.0	0.0
13	CISA	0.0	11663.2	0.0	0.0	0.0	0.0	0.0	0.0	0.0	0.0	0.0	0.0
14	Rafael E. Mangual Coliseum	0.0	0.0	0.0	0.0	0.0	0.0	0.0	374726.4	0.0	0.0	0.0	0.0
15	Tennis Complex 2010	0.0	0.0	0.0	0.0	0.0	0.0	0.0	239549.0	0.0	0.0	0.0	0.0
16	Clean Room (R&D)	0.0	0.0	108551.2	0.0	0.0	0.0	0.0	0.0	0.0	0.0	0.0	0.0
17	Natorium 2010	0.0	0.0	0.0	0.0	0.0	0.0	0.0	735311.3	0.0	0.0	0.0	0.0
18	Dean of Student Affairs (Financial Aid / Quality of Life / Counseling Dept. and Psychology Services)	0.0	0.0	0.0	0.0	0.0	0.0	0.0	0.0	0.0	28401.6	0.0	0.0
19	Building and Grounds Dept.	0.0	0.0	0.0	0.0	232270.0	0.0	0.0	0.0	0.0	0.0	0.0	0.0
20	Sanchez Hidalgo Building (DECEP / PpMES / Economy)	0.0	0.0	0.0	0.0	0.0	0.0	310326.4	0.0	0.0	0.0	0.0	0.0

21	Building A (Athlete Dormitories)	0.0	0.0	0.0	0.0	0.0	464196.7	0.0	0.0	0.0	0.0	0.0	0.0
22	Building B (Small Business Administration / Admin. Office)	0.0	0.0	0.0	0.0	0.0	0.0	92445.6	0.0	0.0	0.0	0.0	0.0
23	Building C (Agricultural Branch Office)	0.0	0.0	0.0	0.0	0.0	0.0	92339.0	0.0	0.0	0.0	0.0	0.0
24	Building D (Seismic Network)	0.0	0.0	0.0	0.0	0.0	25796.5	0.0	0.0	0.0	0.0	0.0	0.0
25	Chardon Building (General Studies)	0.0	0.0	0.0	0.0	0.0	0.0	0.0	0.0	0.0	0.0	0.0	496292.6
26	Jesus T. Piñero Building	0.0	0.0	0.0	0.0	0.0	0.0	0.0	0.0	0.0	331762.4	0.0	0.0
27	Jose de Diego Building	0.0	0.0	0.0	0.0	0.0	0.0	0.0	0.0	0.0	60520.9	0.0	0.0
28	Luis de Celis Building (IT/Admissions - Celis 101 / Registry / Dean of Arts and Sciences / Graduate Studies)	0.0	0.0	0.0	0.0	0.0	0.0	0.0	0.0	355499.4	0.0	0.0	0.0
29	Luis Monzon Building	0.0	0.0	0.0	0.0	0.0	0.0	0.0	0.0	0.0	0.0	0.0	440074.9
30	Luis Stefani Building	0.0	0.0	0.0	0.0	0.0	0.0	0.0	0.0	0.0	0.0	2490075.3	0.0
31	Faculty Offices Building	0.0	0.0	0.0	0.0	0.0	0.0	144626.2	0.0	0.0	0.0	0.0	0.0
32	Ramirez de Arellano y Rossell Building	0.0	0.0	0.0	0.0	0.0	0.0	132008.0	0.0	0.0	0.0	0.0	0.0
33	Josefina Torres Torres Building (Nursing)	0.0	0.0	0.0	0.0	0.0	0.0	0.0	190499.3	0.0	0.0	0.0	0.0
34	Racquetball Courts 2010	0.0	0.0	0.0	0.0	0.0	0.0	0.0	24270.4	0.0	0.0	0.0	0.0
35	Terrats Building (Finances and Payments)	0.0	0.0	0.0	0.0	0.0	0.0	0.0	0.0	0.0	0.0	139595.6	0.0
36	Alzamora Farm	0.0	0.0	0.0	0.0	0.0	0.0	85170.2	0.0	0.0	0.0	0.0	0.0
37	Physics, Geology, and Marine Sciences	0.0	0.0	0.0	0.0	0.0	0.0	0.0	5796657.9	0.0	0.0	0.0	0.0
38	Angel F. Espada Gym	0.0	0.0	0.0	0.0	0.0	0.0	0.0	0.0	0.0	0.0	0.0	30494.8
39	Campus Police Office under Remodeling	0.0	0.0	0.0	0.0	0.0	0.0	0.0	0.0	0.0	0.0	0.0	0.0
40	Printing and Fine Arts	0.0	0.0	0.0	194292.7	0.0	0.0	0.0	0.0	0.0	0.0	0.0	0.0
41	Civil Engineering Building	0.0	0.0	374726.4	0.0	0.0	0.0	0.0	0.0	0.0	0.0	0.0	0.0
42	Industrial Engineering Building	0.0	0.0	0.0	0.0	0.0	0.0	0.0	0.0	0.0	154102.2	0.0	0.0



43	Antonio Luchetti Building (Mechanical Engineering)	0.0	0.0	0.0	0.0	0.0	0.0	0.0	0.0	0.0	0.0	406525. 2	0.0
44	Chemical Engineering Building	864602.0	0.0	0.0	0.0	0.0	0.0	0.0	0.0	0.0	0.0	0.0	0.0
45	Solar Vehicle Museum	0.0	0.0	0.0	21937.0	0.0	0.0	0.0	0.0	0.0	0.0	0.0	0.0
46	Agricultural Engineering Laboratory	0.0	0.0	0.0	0.0	0.0	0.0	142492 .3	0.0	0.0	0.0	0.0	0.0
47	Solar Vehicle Laboratory	0.0	0.0	0.0	53105.1	0.0	0.0	0.0	0.0	0.0	0.0	0.0	0.0
48	Interdisciplinary Literary Studies Center	0.0	0.0	0.0	3590.8	0.0	0.0	0.0	0.0	0.0	0.0	0.0	0.0
49	MuSA (Museum and Academic Senate)	0.0	0.0	0.0	0.0	0.0	0.0	0.0	0.0	0.0	0.0	22372.8	0.0
50	New Athletic Track	0.0	0.0	0.0	0.0	0.0	0.0	0.0	0.0	0.0	0.0	0.0	0.0
51	R&D (Administrative Office)	0.0	57716.4	0.0	0.0	0.0	0.0	0.0	0.0	0.0	0.0	0.0	0.0
52	Green Campus Office (Solar House 2005)	0.0	0.0	0.0	4975.7	0.0	0.0	0.0	0.0	0.0	0.0	0.0	0.0
53	Career Rehabilitation Program	0.0	0.0	0.0	0.0	0.0	0.0	0.0	10204.0	0.0	0.0	0.0	0.0
54	Office of Continuous Improvement and Assessment	0.0	0.0	0.0	0.0	0.0	0.0	0.0	13319.2	0.0	0.0	0.0	0.0
55	Chemistry Building	2433968.6	0.0	0.0	0.0	0.0	0.0	0.0	0.0	0.0	0.0	0.0	0.0
56	UPRM Residence #2	0.0	0.0	0.0	0.0	0.0	20955. 3	0.0	0.0	0.0	0.0	0.0	0.0
57	Director Residence	0.0	0.0	0.0	0.0	0.0	0.0	0.0	0.0	0.0	54776.9	0.0	0.0
58	R.O.T.C.	0.0	0.0	0.0	0.0	0.0	0.0	0.0	0.0	0.0	0.0	0.0	153590 .4
59	Exercise Trail	0.0	0.0	0.0	0.0	0.0	0.0	0.0	0.0	0.0	0.0	0.0	0.0
60	Medical Services and Emergency Room	0.0	0.0	0.0	0.0	0.0	0.0	0.0	0.0	16318 3.0	0.0	0.0	0.0
61	Graphic Arts Workshop	0.0	0.0	0.0	0.0	0.0	0.0	0.0	0.0	0.0	0.0	0.0	23832. 7
62	New Campus Police Offices_Temporary Installations	0.0	0.0	0.0	0.0	0.0	0.0	0.0	0.0	22455. 2	0.0	0.0	0.0
63	Mezzanine Hall	0.0	0.0	0.0	0.0	0.0	0.0	0.0	54693.4	0.0	0.0	0.0	0.0
64	Street Lighting Not On Map	0.0	0.0	0.0	0.0	0.0	0.0	0.0	0.0	0.0	0.0	0.0	0.0
65	Unnamed Areas_Not On Map	0.0	0.0	0.0	0.0	0.0	0.0	0.0	0.0	0.0	0.0	0.0	0.0
	Sum Annual Energy [MWh/year]	6761.7	808.7	1395.0	278.9	245.2	510.9	1028.4	7439.2	2557.6	1926.5	3212.7	1196.5
	Percent of Total per Priority	73.14%	8.75%	15.09%	3.02%	2.66%	5.54%	11.15%	80.65%	28.76 %	21.66%	36.12%	13.45%
		MID 1 9244.3				MID 2 9223.7				MID 3 8893.2			

## Appendix K. Current Accounts Settings and Inputs

Transformation Settings	UPRM Microgrid Electricity Generation	Module Settings		Output Fuels		Processes				
		Capacities	ON	Shortfall Rule	RequirementsRemainUnmet	Variables	UPRM Solar	UPRM Wind	UPRM Biogas	
		System Load Curve	ON	Surplus Rule	SurplusAvailable	Dispatch Rule	PercentShare	PercentShare	PercentShare	
				Usage Rule	DomesticPriority	Interest Rate	DiscountRate	DiscountRate	DiscountRate	
		YearlyShape	YearlyShape(Microgrid_OFF)	Import Target	0	Lifetime	30	30	30	
		Peak Load Ratio	100	Export Target	0	Exogenous Capacity	0	0	0	
				Has Regional Imports	No	Maximum Availability	100	100	100	
				Output Fuel	Electricity	Minimum Utilization	0	0	0	
						Capacity Credit	100	100	100	
						Addition Size	0	0	0	
						Dispatchable	No	No	No	
						Merit Order	1	1	1	
						First Simulation Year	2022	2022	2022	
						Full Load Hours	0	0	0	
						Process Share	0	0	0	
						Process Efficiency	100	100	100	
						Feedstock Fuels	UPRM Solar	UPRM Wind	UPRM Biogas	
						Feedstock Fuel Share	100	100	100	
		UPRM Biogas Production	Module Settings		Output Fuels		Processes			
			Capacities	ON	Shortfall Rule	RequirementsRemainUnmet	Variables	Agricultural Scraps	Food Scraps	
System Load Curve	OFF		Surplus Rule	SurplusAvailable	Dispatch Rule	PercentShare	PercentShare			
			Usage Rule	DomesticPriority	Interest Rate	DiscountRate	DiscountRate			
YearlyShape	NA		Import Target	0	Lifetime	30	30			
Peak Load Ratio	NA		Export Target	0	Exogenous Capacity	0	0			
			Has Regional Imports	No	Maximum Availability	100	100			
			Output Fuel	UPRM Biogas	Minimum Utilization	0	0			

			Capacity Credit	100	100
			Addition Size	0	0
			Dispatchable	No	No
			Merit Order	1	1
			First Simulation Year	2022	2022
			Full Load Hours	0	0
			Process Share	0	0
			Process Efficiency	100	100
			Feedstock Fuels	Bagasse	Vegetal Wastes
			Feedstock Fuel Share	100	100

AEE Electricity Generation	Module Settings		Output Fuels		Processes									
	Capacities	ON	Shortfall Rule	RequirementsRemainUnmet	Variables	Residual Fuel Oil	Diesel	Natural Gas	Gasoline	Coal Unspecified	Renewables			
	System Load Curve	ON	Surplus Rule	SurplusWasted	Dispatch Rule	PercentShare	PercentShare	PercentShare	PercentShare	PercentShare	PercentShare			
			Usage Rule	DomesticPriority	Interest Rate	DiscountRate	DiscountRate	DiscountRate	DiscountRate	DiscountRate	DiscountRate			
	YearlyShape	YearlyShape(AC_Load_Served, AC_Load_Oasis)	Import Target	0	Lifetime	30	30	30	30	30	30			
	Peak Load Ratio	100	Export Target	0	Exogenous Capacity	1045.84	338.36	830.52	0	738.24	123.04			
			Has Regional Imports	No	Maximum Availability	100	100	100	100	100	100			
			Output Fuel	Electricity	Minimum Utilization	0	0	0	0	0	0			
					Capacity Credit	100	100	100	100	100	100			
					Addition Size	0	0	0	0	0	0			
					Dispatchable	Yes	Yes	Yes	Yes	Yes	No			
					Merit Order	1	1	1	1	1	1			
					First Simulation Year	BaseYear	BaseYear	BaseYear	BaseYear	BaseYear	BaseYear			
					Process Share	34	11	27		24	4			
					Process Efficiency	100	100	100	100	100	100			
					Feedstock Fuels	Residual Fuel Oil	Diesel	Natural Gas	Gasoline	Coal Unspecified	Hydro	Solar	Wind	Biogas
					Feedstock Fuel Share	100	100	100	100	100	2.08	87.5	8.33	Remainder(100)

Resources	Primary	Additions to Reserves	Resource Imports	Base Year Reserves	Resource Exports	Yield	Units	Unmet Requirements	
		UPRM Wind	NA	0	NA	0	0	Gigawatt-Hour	RequirementsUnmet
		UPRM Solar	NA	0	NA	0	0	Gigawatt-Hour	RequirementsUnmet
		Hydro	NA	0	NA	0	0.022801051	Gigawatt-Hour	RequirementsUnmet
		Vegetal Wastes	NA	0	NA	0	0	Metric Tonne	RequirementsUnmet
		Bagasse	NA	0	NA	0	0	Metric Tonne	RequirementsUnmet
		Solar	NA	0	NA	0	0.15893	Gigawatt-Hour	RequirementsUnmet
		Wind	NA	0	NA	0	0.01514	Gigawatt-Hour	RequirementsUnmet
		Coal Unspecified	0	0	0	0	NA	NA	MeetWithImports
		Natural Gas	0	0	0	0	NA	NA	MeetWithImports
Secondary	Biogas	NA	0	NA	0	NA	NA	RequirementsUnmet	
	UPRM Biogas	NA	0	NA	0	NA	NA	RequirementsUnmet	
	Gasoline	NA	0	NA	0	NA	NA	RequirementsUnmet	
	Diesel	NA	0	NA	0	NA	NA	MeetWithImports	
	Residual Fuel Oil	NA	0	NA	0	NA	NA	MeetWithImports	
	Electricity	NA	0	NA	0	NA	NA	RequirementsUnmet	

## Appendix L. Microgrid Component Cost Sensitivity Results

		Summary	Load (kWh/yr)	Grid Sales (kWh/yr)	PV (kW)	1.5 MW Wind	0.6kW Wind	Biogen (kW)
<b>Advanced</b>	Baseline	<i>Grid</i>	27,361,261	0	0	0	0	0
	Min LCOE	<i>PV+W+Grid</i>	27,361,261	27,244,892	23,652	2	0	0
	Forced H2	<i>PV+W+H2+Grid</i>		27,332,859	23,652	2	0	0
	Forced Battery	<i>PV+W+Batt+Grid</i>		24,936,432	23,652	2	0	0
	Highest Ren Frac	<i>PV+W+Bio+Batt+Grid</i>		25,016,875	23,652	2	0	500
	Full Diversification	<i>PV+W+Bio+Batt+H2+Grid</i>		25,291,074	23,652	2	0	500
<b>Moderate</b>	Min LCOE	<i>PV+W+Grid</i>	27,361,261	27,244,892	23,652	2	0	0
	Forced H2	<i>PV+W+H2+Grid</i>		27,066,639	23,652	2	0	0
	Forced Battery	<i>PV+W+Batt+Grid</i>		24,936,432	23,652	2	0	0
	Highest Ren Frac	<i>PV+W+Bio+Batt+Grid</i>		24,948,900	23,652	2	0	500
	Full Diversification	<i>PV+W+Bio+Batt+H2+Grid</i>		25,288,121	23,652	2	0	500
<b>Conservative*</b>	Min LCOE	<i>PV+W+Grid</i>	27,361,261	27,244,892	23,652	2	0	0
	Forced H2	<i>PV+W+H2+Grid</i>		27,066,662	23,652	2	0	0
	Forced Battery	<i>PV+W+Batt+Grid</i>		24,936,432	23,652	2	0	0
	Highest Ren Frac	<i>PV+W+Bio+Batt+Grid</i>		24,936,432	23,652	2	0	500
	Full Diversification	<i>PV+W+Bio+Batt+H2+Grid</i>		25,296,496	23,652	2	0	500
<b>Conservative</b>	Min LCOE	<i>PV+Grid</i>	27,361,261	21,319,856	23,652	0	0	0
	Forced H2	<i>PV+H2+Grid</i>		21,103,425	23,652	0	0	0
	Forced Battery	<i>PV+Batt+Grid</i>		19,132,215	23,652	0	0	0
	Highest Ren Frac	<i>PV+W+Batt+Grid</i>		19,132,622	23,652	0	1	0
	Full Diversification	<i>PV+W+Bio+Batt+H2+Grid</i>		19,549,329	23,652	0	1	500

\*Conservative market scenario with microgrid system forced to match the moderate and advanced systems.

		Summary	250kW Batt	EC (kW)	FC (kW)	H2 Tank (kg)	Grid Purchase (kWh/yr)	LCOE (\$/kWh)	Ren Frac (%)	NPV (\$)
	Baseline	<i>Grid</i>	0	0	0	0		\$ 0.30000	0.0%	\$ 106,113,948
Advanced	Min LCOE	<i>PV+W+Grid</i>	0	0	0	0	6,388,603	\$ 0.03523	88.3%	\$ 24,871,570
	Forced H2	<i>PV+W+H2+Grid</i>	0	100	250	100	6,337,297	\$ 0.03560	88.4%	\$ 25,168,370
	Forced Battery	<i>PV+W+Batt+Grid</i>	3	0	0	0	4,804,224	\$ 0.04118	90.8%	\$ 27,843,390
	Highest Ren Frac	<i>PV+W+Bio+Batt+Grid</i>	3	0	0	0	4,739,521	\$ 0.04125	91.0%	\$ 27,928,170
	Full Diversification	<i>PV+W+Bio+Batt+H2+Grid</i>	3	100	250	100	5,109,074	\$ 0.04225	90.3%	\$ 28,755,880
Moderate	Min LCOE	<i>PV+W+Grid</i>	0	0	0	0	6,388,603	\$ 0.04637	88.3%	\$ 32,737,030
	Forced H2	<i>PV+W+H2+Grid</i>	0	100	250	100	6,343,887	\$ 0.04801	88.3%	\$ 33,861,630
	Forced Battery	<i>PV+W+Batt+Grid</i>	3	0	0	0	4,804,224	\$ 0.05326	90.8%	\$ 36,011,150
	Highest Ren Frac	<i>PV+W+Bio+Batt+Grid</i>	3	0	0	0	4,664,094	\$ 0.05511	91.1%	\$ 37,267,720
	Full Diversification	<i>PV+W+Bio+Batt+H2+Grid</i>	3	100	250	100	5,078,976	\$ 0.05606	90.4%	\$ 38,158,590
Conservative*	Min LCOE	<i>PV+W+Grid</i>	0	0	0	0	6,388,603	\$ 0.05950	88.3%	\$ 42,000,740
	Forced H2	<i>PV+W+H2+Grid</i>	0	100	250	100	6,343,900	\$ 0.06148	88.3%	\$ 43,137,120
	Forced Battery	<i>PV+W+Batt+Grid</i>	3	0	0	0	4,804,224	\$ 0.06746	90.8%	\$ 45,606,250
	Highest Ren Frac	<i>PV+W+Bio+Batt+Grid</i>	3	0	0	0	4,804,224	\$ 0.07086	90.8%	\$ 47,904,390
	Full Diversification	<i>PV+W+Bio+Batt+H2+Grid</i>	3	100	250	100	4,977,169	\$ 0.07199	90.5%	\$ 48,903,140
Conservative	Min LCOE	<i>PV+Grid</i>	0	0	0	0	10,010,197	\$ 0.05719	79.4%	\$ 35,992,770
	Forced H2	<i>PV+H2+Grid</i>	0	100	250	100	9,992,950	\$ 0.05897	79.4%	\$ 36,944,720
	Forced Battery	<i>PV+Batt+Grid</i>	3	0	0	0	8,474,570	\$ 0.06573	81.8%	\$ 39,505,120
	Highest Ren Frac	<i>PV+W+Batt+Grid</i>	3	0	0	0	8,474,136	\$ 0.06576	81.8%	\$ 39,522,500
	Full Diversification	<i>PV+W+Bio+Batt+H2+Grid</i>	3	100	250	100	8,745,255	\$ 0.07045	81.4%	\$ 42,720,550

\*Conservative market scenario with microgrid system forced to match the moderate and advanced systems.

		Summary	CAPEX (\$)	OPEX (\$/yr)	ROI (%)	IRR (%)	Simple Payback (yr)	Disc. Payback (yr)
	Baseline	Grid	\$ -	\$ 8,208,378.00				
Advanced	Min LCOE	PV+W+Grid	\$ 44,924,760	\$ (1,551,202.00)	17.7%	21.6%	4.60	5.53
	Forced H2	PV+W+H2+Grid	\$ 45,371,360	\$ (1,562,790.00)	17.5%	21.4%	4.64	5.59
	Forced Battery	PV+W+Batt+Grid	\$ 46,873,260	\$ (1,472,044.00)	16.7%	20.5%	4.84	5.87
	Highest Ren Frac	PV+W+Bio+Batt+Grid	\$ 47,169,260	\$ (1,488,383.00)	16.6%	20.4%	4.87	5.90
	Full Diversification	PV+W+Bio+Batt+H2+Grid	\$ 47,669,860	\$ (1,463,079.00)	16.3%	20.1%	4.92	5.98
Moderate	Min LCOE	PV+W+Grid	\$ 51,774,480	\$ (1,472,630.00)	14.7%	18.4%	5.35	6.62
	Forced H2	PV+W+H2+Grid	\$ 52,341,480	\$ (1,429,497.00)	14.4%	18.1%	5.43	6.73
	Forced Battery	PV+W+Batt+Grid	\$ 54,034,980	\$ (1,394,222.00)	13.8%	17.5%	5.63	7.03
	Highest Ren Frac	PV+W+Bio+Batt+Grid	\$ 55,700,480	\$ (1,425,854.00)	13.3%	16.9%	5.79	7.29
	Full Diversification	PV+W+Bio+Batt+H2+Grid	\$ 56,267,480	\$ (1,400,802.00)	13.1%	16.7%	5.86	7.40
Conservative*	Min LCOE	PV+W+Grid	\$ 60,511,680	\$ (1,431,902.00)	11.9%	15.5%	6.28	8.06
	Forced H2	PV+W+H2+Grid	\$ 61,145,080	\$ (1,392,934.00)	11.7%	15.3%	6.36	8.21
	Forced Battery	PV+W+Batt+Grid	\$ 63,084,180	\$ (1,351,994.00)	11.2%	14.7%	6.60	8.60
	Highest Ren Frac	PV+W+Bio+Batt+Grid	\$ 66,082,680	\$ (1,406,170.00)	10.6%	13.9%	6.91	9.13
	Full Diversification	PV+W+Bio+Batt+H2+Grid	\$ 66,716,080	\$ 1,377,909.00	10.4%	13.8%	6.98	9.28
Conservative	Min LCOE	PV+Grid	\$ 43,519,680	\$ (582,239.40)	16.2%	20.0%	4.95	6.02
	Forced H2	PV+H2+Grid	\$ 44,153,080	\$ (557,597.00)	15.9%	19.6%	5.04	6.15
	Forced Battery	PV+Batt+Grid	\$ 46,092,180	\$ (509,538.10)	14.9%	18.7%	5.29	6.52
	Highest Ren Frac	PV+W+Batt+Grid	\$ 46,108,980	\$ (509,492.70)	14.9%	18.6%	5.29	6.53
	Full Diversification	PV+W+Bio+Batt+H2+Grid	\$ 49,740,880	\$ (543,053.10)	13.7%	17.2%	5.70	7.15

\*Conservative market scenario with microgrid system forced to match the moderate and advanced systems.